

**STRENGTHENING OF Li<sub>2</sub>O-SiO<sub>2</sub> TRANSPARENT  
GLASS-CERAMICS BY ION EXCHANGE**

**Chokchai Yatongchai**

**A Thesis Submitted in Partial Fulfillment of the Requirements for the  
Degree of Master of Engineering in Ceramic Engineering  
Suranaree University of Technology**

**ISBN 974-533-528-2**

การเพิ่มความแข็งแรงของดีเทียมซิติเกตกลาสเซรามิก

โดยการแลกเปลี่ยนไอออน

นายโชคชัย ยาทองไชย

วิทยานิพนธ์นี้เป็นส่วนหนึ่งของการศึกษาตามหลักสูตรปริญญาวิศวกรรมศาสตรมหาบัณฑิต

สาขาวิชาวิศวกรรมเซรามิก

มหาวิทยาลัยเทคโนโลยีสุรนารี

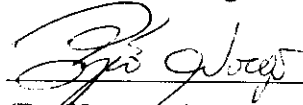
ปีการศึกษา 2548

ISBN 974-533-528-2


**STRENGTHENING OF Li<sub>2</sub>O-SiO<sub>2</sub> TRANSPARENT  
GLASS-CERAMICS BY ION EXCHANGE**

Suranaree University of Technology has approved this thesis submitted in partial fulfillment of the requirements for a Master's Degree.

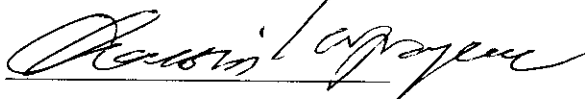
Thesis Examining Committee

  
(Dr. Veerayuth Lorprayoon)

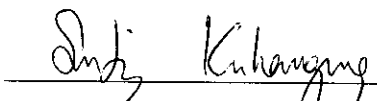
Chairperson

  
(Asst. Prof. Dr. Shigeki Morimoto)

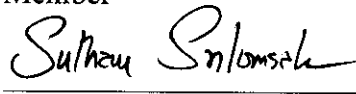
Member (Thesis Advisor)

  
(Assoc. Prof. Dr. Charussri Lorprayoon)


Member

  
(Assoc. Prof. Dr. Sutin Kuharuangrong)


Member

  
(Dr. Sutham Srilomsak)

Member

  
(Assoc. Prof. Dr. Saowanee Rattanaphani)

Vice Rector for Academic Affairs

  
(Assoc. Prof. Dr. Vorapot Khompis)

Dean of Institute of Engineering

โชคชัย ยาทองไชย : การเพิ่มความแข็งแรงของลิเทียมซิลิเกตดกลาสเซรามิกชนิดโปร่งใส  
โดยการแลกเปลี่ยนไอออน (STRENGTHENING OF  $\text{Li}_2\text{O-SiO}_2$  TRANSPARENT  
GLASS-CERAMICS BY ION EXCHANGE) อาจารย์ที่ปรึกษา : ผู้ช่วยศาสตราจารย์  
ดร.ชិเกกิ โมริโมโต, 105 หน้า. ISBN 974-533-528-2

การศึกษาการเพิ่มความแข็งแรงของลิเทียมซิลิเกตดกลาสเซรามิกชนิดโปร่งใสโดยการ  
แลกเปลี่ยนไอออน กลาสเซรามิกจะถูกทำการแลกเปลี่ยนไอออนในอ่างโซเดียมไนเตรต และ  
โปแตสเซียมไนเตรตหลอมเหลวภายใต้สภาวะต่างๆกันเพื่อหาสภาวะที่ดีที่สุดที่ทำให้กลาสเซรามิก  
มีความแข็งแรงสูงจาก การศึกษาพบว่าค่าความแข็งแรงสูงสุดของกลาสเซรามิกเท่ากับ  $487 \pm 15$   
เมกะปาสกาล โดยเกิดจากการแลกเปลี่ยนไอออนของลิเทียมกับ โปแตสเซียมที่อุณหภูมิ 500 องศา  
เซลเซียสและเวลาที่ใช้ในกระบวนการคือ 9 ชั่วโมง

นอกจากนี้ยังได้มีการศึกษาปรากฏการณ์การสลายไปของโครงสร้างผลึกในลิเทียมซิลิเกต  
กลาสเซรามิกชนิดโปร่งใส โดยการแลกเปลี่ยนไอออน การถูกทำลายและสลายไปของผลึกลิเทียมได  
ซิลิเกต ( $\text{Li}_2\text{O} \cdot 2\text{SiO}_2$ ) โดยกระบวนการแลกเปลี่ยนไอออนระหว่างไอออนของลิเทียมกับไอออนของ  
โซเดียมและ โปแตสเซียมซึ่งทำการตรวจสอบได้โดยเทคนิคเอกซเรย์ดิฟแฟรคชัน (XRD) การสลาย  
ไปของผลึกเกิดจากการแลกเปลี่ยนไอออน โดยตรงของลิเทียมที่อยู่ในผลึกลิเทียมไดซิลิเกตกับ  
ไอออนของโซเดียมหรือโปแตสเซียม การถูกแทนที่ของไอออนของลิเทียม โดยไอออนที่มีขนาดที่  
ใหญ่กว่าทำให้โครงสร้างไดซิลิเกตเกิดการเสีรูปร่างและสลายไปในที่สุด

สาขาวิชา วิศวกรรมเซรามิก  
ปีการศึกษา 2548

ลายมือชื่อนักศึกษา John Chan  
ลายมือชื่ออาจารย์ที่ปรึกษา S. Mori

CHOKCHAI YATONGCHAI : STRENGTHENING OF  $\text{Li}_2\text{O-SiO}_2$   
TRANSPARENT GLASS-CERAMICS BY ION EXCHANGE. THESIS  
ADVISOR : ASST. PROF. SHIGEKI MORIMOTO, Ph.D. 105 PP.  
ISBN 974-533-528-2

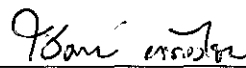
STRENGTHENING/ TRANSPARENT GLASS-CERAMICS/ ION EXCHANGE/  
AMORPHIZATION PHENOMENON

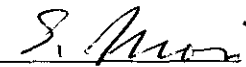
The strengthening of  $\text{Li}_2\text{O-SiO}_2$  transparent glass-ceramics by  $\text{Li}^+ \leftrightarrow \text{Na}^+$  and  $\text{Li}^+ \leftrightarrow \text{K}^+$  ion exchange was investigated. Glass-ceramics were ion exchanged in  $\text{NaNO}_3$  and  $\text{KNO}_3$  molten baths under various conditions to determine optimum condition. From the results, the maximum fracture strength of glass-ceramics of  $487 \pm 15$  MPa could be obtained from  $\text{Li}^+ \leftrightarrow \text{K}^+$  exchange at  $500^\circ\text{C}$  for 9 hours.

In addition, the Amorphization phenomenon was investigated in  $\text{Li}_2\text{O-SiO}_2$  transparent glass-ceramics by ion exchange. The destruction and disappearance of  $\text{Li}_2\text{O} \cdot 2\text{SiO}_2$  crystals by  $\text{Li}^+ \leftrightarrow \text{Na}^+$  and  $\text{Li}^+ \leftrightarrow \text{K}^+$  ion exchange was determined by X-ray diffraction (XRD). The occurrence of Amorphization was due to the ion exchange between  $\text{Na}^+$  or  $\text{K}^+$  and  $\text{Li}^+$  ion in  $\text{Li}_2\text{O} \cdot 2\text{SiO}_2$  crystals directly. The replacement of  $\text{Li}^+$  ion in  $\text{Li}_2\text{O} \cdot 2\text{SiO}_2$  crystal by larger foreign ions results in the deformation of disilicate crystal structure along with the destruction.

School of Ceramic Engineering

Academic Year 2005

Student's Signature 

Advisor's Signature 

## **ACKNOWLEDGEMENTS**

I would like to express my sincerest thanks and gratitude to my advisor, Asst. Prof. Dr. Shigeki Morimoto for his kindness to me during my study time at SUT. Without his supervision and patient help this thesis would not be successful.

I would like to express my gratitude to all the teachers of the School of Ceramic Engineering for giving me good opportunity to study. I wish to express my special thanks to Dr. Veerayuth Lorprayoon the head of the School of Ceramic Engineering, also to Assoc. Prof. Dr.Charussri Lorprayoon for their valuable discussions.

Finally, always, and most important, I appreciate the encouragement and support of family and friends throughout my studying life at SUT.

Chokchai Yatongchai

# TABLE OF CONTENTS

	<b>PAGE</b>
ABSTRACT (THAI) .....	I
ABSTRACT (ENGLISH).....	II
ACKNOWLEDGEMENTS.....	III
TABLE OF CONTENTS.....	IV
LIST OF TABLES.....	VII
LIST OF FIGURES .....	IX
<b>CHAPTER</b>	
<b>I INTRODUCTION .....</b>	<b>1</b>
1.1 General Introduction.....	1
1.2 Research Objectives .....	5
1.3 Scopes of the Research.....	5
1.4 Expected Results .....	6
<b>II LITERATURE REVIEW .....</b>	<b>7</b>
2.1 Lithium Silicate Glass-ceramics.....	7
2.2 The Strengthening of Glass and Glass-ceramics by Ion Exchange .....	11
2.3 Stress Relaxation .....	18
2.4 The Decrystallization of Glass-ceramics by Ion Exchange.....	19
2.5 The Theory of Ion Exchange.....	21

## TABLE OF CONTENTS (Continued)

	<b>PAGE</b>
<b>III EXPERIMENTAL</b> .....	30
3.1 Materials .....	30
3.2 Sample Preparation.....	30
3.2.1 Glass Melting.....	30
3.2.2 Specimen Preparation .....	31
3.3 Ion Exchange .....	31
3.4 Material Characterizations and Property Measurement .....	31
3.4.1 Strength Measurement.....	31
3.4.2 X-ray Diffraction Analysis .....	32
3.4.3 Scanning Electron Microscopy Analysis.....	33
3.4.4 Dilatometry Analysis.....	33
3.4.5 Density Measurement of Glass and Glass-ceramics.....	33
3.4.6 Differential Thermal Analysis .....	34
<b>IV RESULT AND DISCUSSION</b> .....	36
4.1 The Properties of Glass and Glass-ceramics .....	36
4.2 The Strengthening of $\text{Li}_2\text{O}\cdot 2\text{SiO}_2$ Glass by Ion Exchange.....	37
4.3 The Strengthening of $\text{Li}_2\text{O}\cdot 2\text{SiO}_2$ Transparent Glass-ceramics by Ion Exchange .....	43
4.4 The Amorphization of $\text{Li}_2\text{O}\cdot \text{SiO}_2$ Transparent Glass-ceramics by Ion Exchange.....	55



## TABLE OF CONTENTS (Continued)

	<b>PAGE</b>
<b>V CONCLUSION</b> .....	63
REFERENCES .....	65
APPENDICES	
APPENDIX A THE CALCULATION OF LATTICE CONSTANT .....	70
APPENDIX B THE CALCULATION OF CRYSTALLITE SIZE BY X-RAY DIFFRACTION TECHNIQUE.....	74
APPENDIX C THE CALIBRATION CURVE OF $\text{Li}_2\text{O}\cdot 2\text{SiO}_2$ GLASS .....	78
APPENDIX D THE CALCULATION OF DENSITY, MOLAR VOLUME AND THERMAL EXPANSION COEFFICIENT OF $\text{R}_2\text{O}\text{-SiO}_2$ GLASS .....	85
APPENDIX E THE CALCULATION OF NORMALIZED X-RAY INTENSITY .....	90
APPENDIX F X-RAY DIFFRACTION FILES .....	93
APPENDIX G CHARACTERIZATION DATA REPORT .....	99
BIOGRAPHY .....	105

## LIST OF TABLES

TABLE	PAGE
2.1 Compositions of representative glass-ceramics.....	16
2.2 Strength of ion-exchanged glass-ceramics (Abraded).....	17
3.1 Chemical composition of Li <sub>2</sub> O-SiO <sub>2</sub> glass.....	30
4.1 Summary of properties of Li <sub>2</sub> O-SiO <sub>2</sub> glass and glass-ceramics.....	37
4.2 Fracture strength of Li <sub>2</sub> O-SiO <sub>2</sub> glass before and after Li <sup>+</sup> ↔ Na <sup>+</sup> and Li <sup>+</sup> ↔ K <sup>+</sup> exchange .....	38
4.3 The calculated density, molar volume and thermal expansion coefficient of Li-, Na- and K-glasses .....	41
4.4 Fracture strength of Li <sub>2</sub> O-SiO <sub>2</sub> transparent glass-ceramics before and after Li <sup>+</sup> ↔ Na <sup>+</sup> exchange.....	44
4.5 Fracture strength of Li <sub>2</sub> O-SiO <sub>2</sub> transparent glass-ceramics before and after Li <sup>+</sup> ↔ K <sup>+</sup> exchange .....	45
4.6 Lattice constant of Li <sub>2</sub> O·2SiO <sub>2</sub> crystal before and after ion exchange.....	61
4.7 Crystal structure and lattice constant of alkali disilicate crystals.....	62
C1 The calculation of crystallinity using Ohlberg and Strickler's method.....	84
D1 Calculated density, molar volume and thermal expansion coefficient of Li <sub>2</sub> O-SiO <sub>2</sub> Glass .....	86

## LIST OF TABLES (Continued)

TABLE	PAGE
D2	Calculated density, molar volume and thermal expansion coefficient of Na <sub>2</sub> O-SiO <sub>2</sub> Glass..... 86
D3	Calculated density, molar volume and thermal expansion coefficient of K <sub>2</sub> O-SiO <sub>2</sub> Glass ..... 87
D4	Property factor of oxides in glass composition by A.A. Appen..... 88
E1	XRD pattern of Li <sub>2</sub> O-SiO <sub>2</sub> transparent glass-ceramics after Li <sup>+</sup> ↔ Na <sup>+</sup> exchange at 550°C for 4hour..... 92
F1	X-ray diffraction file of Silicon (JCPDS 027-1402) ..... 94
F2	X-ray diffraction file of lithium silicate (JCPDS 029-0828)..... 95
F3	X-ray diffraction file of cristobalite (JCPDS 039-1425)..... 96
F4	X-ray diffraction file of lithium silicate (JCPDS 027-1402)..... 97
F5	X-ray diffraction file of quartz (JCPDS 046-1045)..... 98
G1	Density and volume report of Li <sub>2</sub> O-SiO <sub>2</sub> transparent glass-ceramics (500°C-15h, 700°C-10h) by He-gas substitution method using Accupyc (Micrometrics)..... 103
G2	Density and volume report of Li <sub>2</sub> O-SiO <sub>2</sub> glass by He-gas substitution method using Accupyc (Micrometrics)..... 104

## LIST OF FIGURES

FIGURE	PAGE
2.1 Effect of temperature on the strength of potassium exchanged 1.1Na <sub>2</sub> O-1Al <sub>2</sub> O <sub>3</sub> -4SiO <sub>2</sub> glass .....	19
2.2 Weight change as a function of $t^{1/2}$ . Ag <sup>+</sup> ↔ Li <sup>+</sup> ion exchange in 11.4 mole%Li <sub>2</sub> O, 16.5 mole%Al <sub>2</sub> O <sub>3</sub> , 71.5 mole%SiO <sub>2</sub> glass.....	27
2.3 Ion-exchange isotherm at 300°C of Ag <sup>+</sup> ↔ Li <sup>+</sup> ion exchange in 11.4 mole% Li <sub>2</sub> O, 16.5 mole% Al <sub>2</sub> O <sub>3</sub> , 71.5 mole% SiO <sub>2</sub> .....	28
2.4 Test of n-type behavior for exchange system Ag <sup>+</sup> ↔ Li <sup>+</sup> at 300°C in 11.4 mole% Li <sub>2</sub> O, 16.5 mole% Al <sub>2</sub> O <sub>3</sub> , 71.5 mole% SiO <sub>2</sub> .....	29
3.1 Experimentary determined crystallinity VS calculated crystallinity for mechanical mixtures of α-quartz and parent glass .....	35
4.1 XRD patterns of transparent Li <sub>2</sub> O-SiO <sub>2</sub> glass-ceramics.....	36
4.2 The relation between fracture strength of glass and Li <sup>+</sup> ↔ Na <sup>+</sup> and Li <sup>+</sup> ↔ K <sup>+</sup> exchange time.....	39
4.3 SEM photos of the surface of Li <sub>2</sub> O-SiO <sub>2</sub> glass after ion exchange.....	39
4.4 Schematic representation of dimension change after ion exchange .....	42
4.5 The relation between fracture strength of Li <sub>2</sub> O-SiO <sub>2</sub> transparent glass-ceramics and Li <sup>+</sup> ↔ Na <sup>+</sup> exchange time .....	46

## LIST OF FIGURES (Continued)

FIGURE	PAGE
4.6 The relation between fracture strength of $\text{Li}_2\text{O-SiO}_2$ transparent glass-ceramics and $\text{Li}^+ \leftrightarrow \text{K}^+$ exchange time .....	47
4.7 The SEM photos of the surface of $\text{Li}_2\text{O-SiO}_2$ glass-ceramics after ion exchange .....	48
4.8 XRD patterns of $\text{Li}_2\text{O-SiO}_2$ transparent glass-ceramics (plate specimens) before and after $\text{Li}^+ \leftrightarrow \text{Na}^+$ exchange .....	50
4.9 XRD patterns of transparent glass-ceramics (plate specimens) before and after $\text{Li}^+ \leftrightarrow \text{K}^+$ exchange .....	51
4.10 Relation between normalized X-ray intensity of the strongest peak of $\text{Li}_2\text{O} \cdot 2\text{SiO}_2$ crystal ( $2\theta=24.8^\circ$ ) and $\text{SiO}_2$ crystal in $\text{Li}_2\text{O-SiO}_2$ transparent glass-ceramics and $\text{Li}^+ \leftrightarrow \text{Na}^+$ exchange time .....	52
4.11 Relation between normalized X-ray intensity of the strongest peak of $\text{Li}_2\text{O} \cdot 2\text{SiO}_2$ crystal ( $2\theta=24.8^\circ$ ) in $\text{Li}_2\text{O-SiO}_2$ transparent glass-ceramics and $\text{Li}^+ \leftrightarrow \text{K}^+$ exchange time .....	53
4.12 XRD patterns of $\text{Li}_2\text{O-SiO}_2$ transparent glass-ceramics before and after $\text{Li}^+ \leftrightarrow \text{Na}^+$ exchange at $650^\circ\text{C}$ .....	54
4.13 Schematic of representation of amorphization by ion exchange according to Tagantsev and Karapetyan .....	58
4.14 XRD patterns of synthesized $\text{Li}_2\text{O} \cdot 2\text{SiO}_2$ crystal before and after $\text{Li}^+ \leftrightarrow \text{Na}^+$ ion exchange .....	61

## LIST OF FIGURES (Continued)

FIGURE	PAGE
A1 XRD pattern of $\text{Li}_2\text{O}\cdot 2\text{SiO}_2$ glass-ceramics (500°C-15h, 700°C-15h) .....	71
B1 XRD pattern of $\text{Li}_2\text{O}\cdot 2\text{SiO}_2$ glass-ceramics (500°C-15h, 700°C-15h) .....	75
B2 Calibration curve of X-ray line broadening for AgCl precipitated in glass by Jone's method.....	77
C1 XRD pattern of $\text{Li}_2\text{O}\cdot \text{SiO}_2$ glass (100% Glass) .....	79
C2 XRD pattern of Quartz (100% Crystal).....	80
C3 XRD pattern of 25% $\text{Li}_2\text{O}\cdot \text{SiO}_2$ glass + 75% Quartz.....	81
C4 XRD pattern of 50% $\text{Li}_2\text{O}\cdot \text{SiO}_2$ glass + 50% Quartz.....	82
C5 XRD pattern of 75% $\text{Li}_2\text{O}\cdot \text{SiO}_2$ glass + 25% Quartz.....	83
C6 Experimentary determined crystallinity VS calculated crystallinity for mechanical mixtures of $\alpha$ -quartz and parent glass.....	84
E1 XRD pattern of $\text{Li}_2\text{O}\cdot \text{SiO}_2$ transparent glass-ceramics after $\text{Li}^+ \leftrightarrow \text{Na}^+$ at 550°C for 4hour .....	91
G1 Thermal expansion trace report of $\text{Li}_2\text{O}\cdot \text{SiO}_2$ glass using Netsch 402EP at a heating rate of 5°C/min.....	100
G2 Thermal expansion analysis trace of $\text{Li}_2\text{O}\cdot \text{SiO}_2$ transparent glass- ceramics using Netsch 402EP at a heating rate of 5°C/min .....	101
G3 Thermal analysis trace of $\text{Li}_2\text{O}\cdot \text{SiO}_2$ glass using a Perkin-Elmer DTA-7 at a heating rate of 10°C/min.....	102

# CHAPTER I

## INTRODUCTION

### 1.1 General Introduction

The development of glass-ceramics is a recent advance in the science of materials. The dramatic growth in the applications for these novel materials since the serendipitous discovery, some thirty years ago, of internal nucleation and crystal growth in lithium silicate glass (Stookey, 1954), is a testament in a wide range of application.

Glass-ceramics are polycrystalline solids prepared by the controlled crystallization of glass. They are generally well over 50% crystalline by volume and are fine-grained with crystal sizes below 10  $\mu\text{m}$ . A key feature of glass-ceramics is the maintenance of shape of previous-formed glass article. This is the most effectively achieved through internal nucleation and growth of crystals.

Glass-ceramics have significant advantages over traditional powder-processed ceramics (Beall, Karstetter and Rittler, 1967). One is the flexibility and ease of forming afforded by high speed processes such as rolling, pressing, blowing, and drawing. A total lack of internal porosity is an important characteristic of glass-ceramics. The uniformity of microstructure and reproducibility of properties which depends on structural consistency is another major advantage resulting from the homogeneous nature of the melting process. The ability to produce unique properties inherent in extremely fine-grained crystalline materials is also important. There are

manufacturing advantages in the process economy associated with high volume glass making. Also, any defects present in the glass can be observed prior to crystallization allowing simple reject inspection. Furthermore, glass-ceramics provide a wide range of thermal expansion (CTEs) from  $-75 \times 10^{-7} \text{ } ^\circ\text{C}$  to  $+200 \times 10^{-7} \text{ } ^\circ\text{C}$  that often are not readily obtained in glasses or ceramics.

Transparent glass-ceramics are composed of fine-grained crystallites, usually nano-scale size, and residual glassy phase. The transparent glass-ceramics generally have two distinctive properties: they are nanocrystalline, and they have greater thermal stability than their parent glass, frequently possessing upper use temperature of  $>800 \text{ } ^\circ\text{C}$ .

Good transparency requires glass-ceramics with low optical scattering and low ionic/atomic absorption (Beall and Pinckney, 1999). Low scattering, the more difficult to achieve, can be obtained by satisfying either of two criteria. The first criterion is satisfied when all the crystalline phases and the residual glass have closely matched indexes of refraction and when the crystals possess low birefringence.

The second criterion for low scattering is satisfied in the case where the crystal size is much smaller than the wavelength of light. Within this condition, there are two types of scattering situations. One involves independent scatters that are widely separated and obey the Rayleigh-Gans model (Kerker, 1969). In this case,  $\sigma_p$ , the total turbidity or attenuation due to scattering, is given as

$$\sigma_p \approx \left(\frac{2}{3}\right) NVk^4 a^3 (\eta \Delta \eta)^2 \quad (1.1)$$

where N is the particle number density, V is the particle volume, a is the particle radius,  $k = 2\pi/\lambda$  (where  $\lambda$  is the wavelength),  $\eta$  is the refractive index of crystal, and



$\Delta\eta$  is the index difference between the crystal and the host.

The other scattering model involves small particles that are more closely spaced. This model requires that the distance between particles be no smaller than the particle radius but can be at least up to 6 times the particle radius. Under these conditions, a quasi-continuum model developed independently by Andreev (1978) and Hopper (1985) describes interfering fields from the individual particles that produce a large compensating effect. Hopper gives the formula for turbidity as

$$\sigma_c \approx \left[ \left( \frac{2}{3} \times 10^{-3} \right) k^4 \theta^3 \right] (\eta \Delta\eta)^2 \quad (1.2)$$

where  $\theta$  is the mean phase width ( $a + W/2$ ) and  $W$  is the inter-particle spacing. In this case, improved transparency is allowed with particles sizes  $<30$  nm at larger refractive index differences, up to  $\Delta\eta = 0.3$ .

Glass-ceramics as transparent as glass can be developed and used for such applications as transparent cookware and precision optical instruments, such as ring-laser gyroscope, large telescope mirror blanks. Also, recently, active ions, such as transition metal ion and rare-earth ion, doped transparent glass-ceramics have been developed and many researches on these materials are carried out (Morimoto, 2004; Yuan et al., 1996)

$\text{Li}_2\text{O-SiO}_2$  system of glass is well known as a base glass for glass-ceramics, such as chemically machinable glass-ceramics and high strength glass-ceramics. In addition, transparent glass-ceramics based on lithium metasilicate ( $\text{Li}_2\text{O-SiO}_2$ ) and lithium disilicate ( $\text{Li}_2\text{O} \cdot 2\text{SiO}_2$ ) crystals can be obtained easily in this system (Morimoto, 2004). However, the mechanical strength of  $\text{Li}_2\text{O-SiO}_2$  transparent glass-ceramics is comparable to that of glasses (Morimoto and Emem, 2004). In some

cases, the higher mechanical strength of transparent glass-ceramics is required in special application area.

There are two methods to increase mechanical strength of glasses and glass-ceramics, thermal tempering and chemical strengthening. In thermal tempering, the shaped object is heated to just below its softening point and its surface is then chilled by means of a blast of air or an oil bath. Under these conditions the exterior of the glass cools and contracts immediately, but since glass is a poor conductor of heat the interior will not contract the glass will not crack because the interior remains plastic. When the interior starts to cool, it cannot contract because the exterior has already set, but, in attempting to contract, the interior continues to draw the exterior together. A built-in compressive stress then develops in the outer layers of the glass. When a tensile stress is applied to this glass, it is counteracted by these compressive stresses. Thus the tempered glass will not shatter until the surface compression is exceeded. The latter is called as ion exchange strengthening method, in this method, the shaped object was immersed into a molten salt bath containing larger ions (potassium ions), which replace the smaller ions (sodium ions) on the surface of the glass. The potassium ions are larger than the sodium ions and, in accommodating them, the surface of the glass becomes more crowded thus inducing compressive strains on the exterior. Glass of this type, characterized by very high strength, is useful for a great variety of applications (Kingery, Bowen and Uhlmann, 1976).

Ion exchange strengthening has many advantages over thermal strengthening, such as easy processing, available for any shapes of articles, available for thin articles, available to maintain the surface flatness and smoothness, capable of applying for low thermal expansion materials, etc (Izumitani, 1984). The  $\text{Li}^+ \leftrightarrow \text{Na}^+$  and  $\text{Li}^+ \leftrightarrow \text{K}^+$  ion

exchange are expected to increase mechanical strength of these glass-ceramics. However, the problem was reported from  $\text{Li}^+ \leftrightarrow \text{Na}^+$  ion exchange in  $\text{Li}^+$  containing glass-ceramics due to the crack generation on the surface and therefore the strengthening could not be achieved (Morimoto, 1991). Crystalline phase is destroyed and disappeared by  $\text{Li}^+ \leftrightarrow \text{Na}^+$  exchange. The reason of this phenomenon has been studying since 1969 (Beall and Duke, 1969), only a few papers on this phenomenon have been reported (Morimoto, 1991; Beall and Duke, 1969; Tagantsev and Karapetyan, 1999).

## 1.2 Research Objectives

The objective of research will be as follows;

- (i) To strengthen the  $\text{Li}_2\text{O-SiO}_2$  transparent glass-ceramics by  $\text{Li}^+ \leftrightarrow \text{Na}^+$  and  $\text{Li}^+ \leftrightarrow \text{K}^+$  ion exchanges. The optimum condition will be determined by varying temperature and time during the ion exchange.
- (ii) To investigate the “Decrystallization” or “Amorphization” by X-ray diffraction technique.

## 1.3 Scope of the Research

Investigation will be carried out as follows;

- (i) To explain the mechanism of “Decrystallization” or “Amorphization”. It was anticipated that the occurrence of decrystallization was due to the ion exchange between foreign ions ( $\text{Na}^+$ ,  $\text{K}^+$ ) and  $\text{Li}^+$  ion in  $\text{Li}_2\text{O} \cdot 2\text{SiO}_2$  crystals directly.

- (ii) To determine the optimum ion exchange condition which will increase the mechanical strength without surface crack for the  $\text{Li}_2\text{O-SiO}_2$  system transparent glass-ceramics.

## **1.4 Expected Results**

- 1.4.1 Establishment of basic technology of glass-ceramics production (composition design and process design).
- 1.4.2 Establishment of basic technology of ion exchange method.
- 1.4.3 Clarification of the mechanism of Decrystallization in glass-ceramics.

## **CHAPTER II**

### **LITERATURE REVIEW**

#### **2.1 Lithium Silicate Glass-Ceramics**

Simple silicate glass-ceramics are composed of alkali and alkali earth silicate crystals whose properties dominate that of the glass-ceramics. The most important ones were lithium silicates, both lithium metasilicate ( $\text{Li}_2\text{O}\cdot\text{SiO}_2$ ) and lithium disilicate ( $\text{Li}_2\text{O}\cdot 2\text{SiO}_2$ ).

Lithium silicate glass-ceramics consist of two composition groups. The first group, nucleated with  $\text{P}_2\text{O}_5$ , develops high expansion glass-ceramics which match the thermal expansion of several nickel based superalloys, and are used in variety of high-strength hermetic seals, connectors, and feedthroughs (Headley and Loehman, 1984). The second group, photosensitively nucleated by colloidal silver, produces a variety of chemically machined materials which are useful as fluidic devices, display screens, lens arrays, and other patterned devices (Pinkney, 2001).

The compositions of lithium silicate glass-ceramics typically comprise 70-85 weight percent  $\text{SiO}_2$ , 10-15  $\text{Li}_2\text{O}$ , 3-10  $\text{Al}_2\text{O}_3$ , 1-5  $\text{P}_2\text{O}_5$ . The glasses phase separate on heat treatment and lithium orthophosphate ( $\text{Li}_3\text{PO}_4$ ) precipitates as the first crystal phase. Lithium metasilicate ( $\text{Li}_2\text{SiO}_3$ ) and/or lithium disilicate ( $\text{Li}_2\text{SiO}_5$ ) then form, the latter predominating with further heat treatment.

There have been numerous works on the crystallization and properties of lithium silicate glass-ceramics. Lithium silicate glass is easily melted at 1350-1450 °C

and the nucleation and growth rate can be controlled and measured. Work from the early 1970s focused on the nucleation and growth behavior of lithium disilicate crystal from glasses near lithium disilicate compositions.

In 1964, Kalinina and Filipovich investigated the phases and sequence of crystallization in  $\text{Li}_2\text{O-SiO}_2$  glasses in 1964 using XRD. They concluded that homogeneous bulk crystallization of both lithium disilicate and lithium metasilicate occurred, depending on the initial glass compositions. For example, the 34.2 mol%  $\text{Li}_2\text{O}$  glass compositions crystallized into both lithium disilicate and lithium metasilicate, depending on the temperature. Heat treatment at lower temperature, e.g.,  $480^\circ\text{C}$ , led to crystallization of lithium disilicate while heat treatment at higher temperatures, e.g.,  $630^\circ\text{C}$ , led to crystallization of both lithium disilicate and lithium metasilicate. In general, the metasilicate phase has lower intensities on an X-ray diffraction pattern than the disilicate phase, so it is harder to detect. The 43.7 mol%  $\text{Li}_2\text{O}$  glass composition crystallized into lithium metasilicate after 24h at  $480^\circ\text{C}$ .

West and Glasser (1971) performed an extensive study on the crystallization of  $\text{Li}_2\text{O-SiO}_2$  glasses using X-ray diffraction. They did not detect lithium metasilicate crystallization at composition equal to or less than 36 mol%  $\text{Li}_2\text{O}$  for any heat treatment time or temperature. Difficulties arose in determining phases from the XRD patterns of materials treated at lower temperatures due to the low intensities in X-ray diffraction patterns.

Lithium metasilicate crystallization was found to precede lithium disilicate crystallization as a metastable phase in some silicate glasses. Hench, Freiman and Kinser (1971) determined that lithium metasilicate crystal forms before lithium disilicate in two glass composition of 30 and 33 mol%  $\text{Li}_2\text{O}$ , but the amount of

lithium metasilicate was extremely small and it disappeared on further heat treatment.

Jacquin and Tomazawa (1995) investigated the crystallization behavior of lithium disilicate glass powder heated in molten  $\text{LiNO}_3$  salt using X-ray diffraction techniques. Heat treatment at with  $\text{LiNO}_3$  molten salt caused a lithium metasilicate,  $\text{Li}_2\text{O}\cdot\text{SiO}_2$ , crystal phase to appear after 5-96 h. By contrast, glass powder heat-treated in air at  $500^\circ\text{C}$  remained amorphous after 5 h and turn into lithium disilicate,  $\text{Li}_2\text{O}\cdot 2\text{SiO}_2$ , crystal after 40 h. Glass powder heat treated at  $575^\circ\text{C}$  in both molten salt and in air turned into lithium disilicate crystal. Metasilicate crystallization occurs with  $\text{LiNO}_3$  molten salt at 500 and  $400^\circ\text{C}$  due to the incorporation of lithium into the sample glass powder from the melt during crystallization. An increase in lithium content in the sample after molten salt heat treatment was confirmed by chemical analysis using dc plasma emission spectroscopy.

Soares, Zanotto, Fokin and Jain (2003) studied the early crystallization of lithium disilicate glasses using TEM and XRD techniques. Three lithium silicate glasses nearby the  $\text{Li}_2\text{O}\cdot 2\text{SiO}_2$  composition were heat treated at  $\sim T_g = 454^\circ\text{C}$ , two distinct crystalline phases, stable lithium disilicate ( $\text{Li}_2\text{SiO}_5$ ) and metastable lithium metasilicate ( $\text{Li}_2\text{O}\cdot\text{SiO}_2$ ) coexist up to 120 h at  $454^\circ\text{C}$  (crystalline fraction  $<1$  vol%). For longer treatments (240-600h) only the stable phase ( $\text{Li}_2\text{O}\cdot 2\text{SiO}_2$ ) was observed.

A nucleating agent may be broadly defined as a constituent added to a glass, typically in amount of a few percent, which promote volume nucleation and enable a glass-ceramics to be produced. Examples are metallic particles, oxides and non-oxides.

$\text{P}_2\text{O}_5$  is common nucleating agent for lithium silicate glass-ceramics, which promotes heterogeneous nucleation and produces a fine grained interlocking

morphology after heat treatment (Clausbruch, Schweiger, Holand and Rheinberger, 2000). James (1982) found crystal nucleation rate of lithium disilicate in  $33.3\text{Li}_2\text{O}\cdot 65.7\text{SiO}_2\cdot 1\text{P}_2\text{O}_5$  (mol%) glass were 1000 times greater than in  $\text{Li}_2\text{O}\cdot 2\text{SiO}_2$  base glass at  $500^\circ\text{C}$ . Amorphous phase separation was observed in the glass containing  $\text{P}_2\text{O}_5$  but not in the  $\text{Li}_2\text{O}\cdot 2\text{SiO}_2$  base glass.

Headley and Loehman (1984) found that  $\text{Li}_3\text{PO}_4$  crystals were precipitated from a  $\text{Li}_2\text{O}\text{-Al}_2\text{O}_3\text{-SiO}_2$  based glass after treatment at high temperature in the range  $800\text{-}1000^\circ\text{C}$ . Lithium disilicate, lithium metasilicate and cristobalite were observed to crystallize by epitaxial growth on the  $\text{Li}_3\text{PO}_4$  crystals.

Igbal, Lee, Holland and James (1998) investigated  $\text{Li}_2\text{O}\text{-SiO}_2$  glass containing  $\text{P}_2\text{O}_5$  by XRD, TEM and NMR. They found metastable phases of lithium disilicate phase increased. No evidence was found for the present of  $\text{Li}_3\text{PO}_4$  crystalline phase from XRD, possible because of the small percentage present. However, preliminary result using  $^{31}\text{P}$  MAS NMR of 1 mol%  $\text{P}_2\text{O}_5$  glass did indicate possible formation of the  $\text{Li}_3\text{PO}_4$  phase in the heat treated glasses and even in the as-quenched glasses. For the composition containing 5 mol%  $\text{P}_2\text{O}_5$  XRD revealed crystalline  $\text{Li}_3\text{PO}_4$  in the as-quenched glass and after extend heat treatment. TEM revealed the presence of high density of fine volume nucleated crystals in the  $\text{P}_2\text{O}_5$  containing glasses, much higher than in the base lithium disilicate glass after similar heat treatment.

Mishima, Wakasuki and Ota (2004) studied the crystallization behavior of  $x\text{Li}_2\text{O}\cdot(1-x)\text{Na}_2\text{O}\cdot 2\text{SiO}_2$  glass doped with platinum (Pt). It was found that the addition of Pt induced the crystallization of  $\text{Li}_2\text{O}\cdot\text{SiO}_2$  in the interior of crystallized glasses with high  $\text{Na}_2\text{O}$  ( $x=0.4$  to  $0.6$ ) and  $\text{Li}_2\text{O}\cdot 2\text{SiO}_2$  were observed in crystallized glasses with high  $\text{Li}_2\text{O}$ .  $\text{SiO}_2$  were observed also in the range of  $x=0.6$  to  $0.8$ .



Morimoto (2006) investigated the effect of  $K_2O$  on the crystallization in  $Li_2O$ - $SiO_2$  glass. It was found that a small amount of  $K_2O$  affected the mechanism of phase separation and crystallization process, and  $K_2O$  suppressed the crystallization of  $Li_2O \cdot 2SiO_2$ , but promotes the precipitation of  $Li_2O \cdot SiO_2$  crystal.  $Li_2O \cdot SiO_2$  crystal can precipitate in  $Li_2O$  rich continuous phase containing  $K_2O$ .

Lithium disilicate glass-ceramics nucleated with  $P_2O_5$  are characterized by high body strength, 140-210 MPa, good fracture toughness,  $\approx 3 \text{ MPa} \cdot \text{m}^{1/2}$ , and moderate to high thermal expansion coefficient,  $80\text{-}130 \times 10^{-7} \text{ }^\circ\text{C}^{-1}$  (Pinkney, 2001).

Morimoto and Emem (2004) studied the properties of 77.7  $SiO_2$ :2.2  $Al_2O_3$ :18.8  $Li_2O$ :1.2  $P_2O_5$  (mol%). They found that the transparent glass-ceramics can be obtained by heat treatment below  $800^\circ\text{C}$ . The main crystalline phase is  $Li_2O \cdot 2SiO_2$ . The percent crystallinity and crystal size ranged from 60 to 70% and from 20 to 60 nm, respectively. The density of glass-ceramics increases with increasing heating temperature and time of crystallization. Fracture strength of transparent glass-ceramics increases linearly with crystal size ranging from 20-60 nm.

## **2.2 The Strengthening of Glass and Glass-ceramics by Ion Exchange**

The ion-exchange method has been useful in strengthening glass and in making gradient index lenses (Araujo, 2004). Ion exchange has been used for the increasing mechanical strength of glass and glass-ceramics for the past four decades because of its many advantages such as easy processing, available for any shapes of articles, easy to maintain the surface flatness and smoothness, etc (Izumitani, 1984). There are two types of ion exchange strengthening which differ substantially in theory and operation. The first type of ion exchange treatment is carried out above the strain

point of the glass. As the composition at the surface of glass change by ion exchange treatment so as to lower the thermal coefficient of expansion in the surface layer. As the glass is cooled, a compressive stress develops at the surface due to the expansion differential. This approach was taught by Hood and Stookey (1957) in U.S. Pat. No.2,779,136. The second type of ion exchange strengthening is characterized by treatment below the strain point of the glass, wherein surface compression is generated by substituting large ions from an external source (e.g., a molten salt bath) for smaller ions in the glass. Typically, the substitution is of sodium or potassium for lithium in the glass, or of potassium for sodium in the glass. The below-the-strain-point technique was first taught by Weber (1965) in U.S. Pat. No.3,218,220.

Generally, when the smaller cation (e.g.  $\text{Li}^+$  ion) in glass or glass-ceramics would be replaced by larger cation (e.g.  $\text{K}^+$  ion), the volume of glass and glass-ceramics expands and the compressive stresses arise in surface layer. The stress arisen is given by next equation (Stookey, 1954).

$$\sigma_s = \left(\frac{1}{3}\right) \cdot \frac{E}{1-\mu} \cdot \frac{\Delta V}{V} \quad (2.1)$$

where E is the Young's modulus,  $\mu$  Poisson's ratio and  $\Delta V/V$  the volume change without stresses.

On the other hand, the thermal expansion coefficient of ion exchanged layer changes. In this case, the stress arises by the difference in thermal expansion coefficient. The stress arisen of specimen by glazing may be given by the next equation.

$$\sigma_s = (\alpha_1 - \alpha_2) \cdot \Delta T \cdot \left[ \frac{E}{1-\mu} \right] \times \left( \frac{A_1}{A} \right) \quad (2.2)$$

where  $\alpha_1$  is the thermal expansion coefficient of base material,  $\alpha_2$  that of glaze,

$\Delta T$ =temperature difference,  $A_1$  cross section of glazed layer and  $A$  the cross section of base material.

In recent years a large volume of research on ion exchange strengthening has been carried out, particularly for lithium, sodium and magnesium aluminosilicate glass compositions based on the exchange of larger alkali ions for lithium or sodium using nitrate salt baths (Mallick and Holland, 2004). Notable work includes replacement of  $\text{Li}^+$  in lithium aluminosilicate glasses by  $\text{Na}^+$  from sodium salt baths. Similarly  $\text{Na}^+$  ions have been replaced in sodium aluminosilicate glasses by larger  $\text{K}^+$  ions from potassium salt baths.

Kistler studied the principle of stuffing of ion exchange in 1962. He treated soda-lime-silica glass in  $\text{KNO}_3$  melts at temperature below  $350^\circ\text{C}$  and found after sometime considerable compressive stress (up to 880 MPa) at the surface.

Zijlstra and Burggraaf (1968) mentioned an ion exchange process at high temperature involving the exchange of copper ions from a copper halide vapor for sodium ions in a window glass composition. Strength as high as 480 MPa was achieved in less than 1 hour.

Rinehart (1980) reported the ion exchange strengthening of specific soda-lime-silica glass compositions, which showed a maximum flexural strength value of 350 MPa for compression layer between 70 and 99  $\mu\text{m}$  thick.

Mallick and Holland (2004) investigated the strengthening of industrial grade sodium aluminosilicate glasses by dip coating. Li ion-exchange showed a significant flexural strength enhancement of 16-163% up to a maximum value of 506 MPa for container glass composition with progressively increasing net work modifier additions of alumina from 3 to 10 wt%. The result showed a linear relationship between square

root of exchange duration,  $t^{1/2}$ , and the layer thickness.

Glass-ceramics can also be strengthened by ion exchange techniques. Garfinkel (1980) studied  $\text{Li}^+ \leftrightarrow \text{Na}^+$  exchange in soda-alumina-silica glass containing  $\text{TiO}_2$ . They found that the low-expansion surface phase of  $\beta$ -spodumene solid solution simultaneous crystallization in the ion exchanged glass.

Karstetter and Voss (1967) reported that a fine grained glass-ceramics containing a large proportion of  $\beta$ -spodumene solid-solution crystals was strengthened by immersion in both molten sodium- and potassium-containing salt baths. Replacement of small  $\text{Li}^+$  ion by larger ion ( $\text{Li}^+$  and  $\text{K}^+$  ion) is believed to elastically deform the cation-oxygen bonds in the crystal lattice. The distortion caused by this ionic crowding directly produces a surface compression that typically results in modulus of rupture values on abraded samples of around 345 MPa, which is 241 MPa more than the normal body strength. Exchange normally takes place at relatively low temperature (500-600°C) in salt bath composed largely of  $\text{NaNO}_3$ . A compression layer typically a few mils in thickness is developed within several hours. The thermal stability of the resulting strength is not great because of the low exchange temperature. Similarly, stuffed  $\beta$ -quartz solid solution glass-ceramics derived from the crystallization of  $\text{Li}_2\text{O}-\text{Al}_2\text{O}_3-\text{SiO}_2$  glasses were also strengthened by  $\text{K}^+ \leftrightarrow \text{Li}^+$  exchange. However, the strengthening by  $\text{Na}^+ \leftrightarrow \text{Li}^+$  exchange could not be achieved, resulting from the formation of cracks on the surface (Morimoto, 1991).

Beall et al. (1967) studied the  $2\text{Li}^+ \leftrightarrow \text{Mg}^{2+}$  exchange in  $\beta$ -quartz solid solution glass-ceramics. Here glass-ceramics containing Mg-stuffed derivative of  $\beta$ -quartz as the major phase are placed in a high-temperature  $\text{Li}_2\text{SO}_4$  bath (800-900°C). Surface

compression in this case results from both ionic crowding and differential thermal expansion. The  $2\text{Li}^+ \leftrightarrow \text{Mg}^{2+}$  exchange result in an increase in the unit cell volume and a decrease in the thermal expansion coefficient from  $15$  to  $45 \times 10^{-7} / ^\circ\text{C}$ .

Duke, Macdowell and Karstetter (1967) studied the strengthening of nepheline ( $\text{Na}_2\text{O} \cdot \text{Al}_2\text{O}_3 \cdot 2\text{SiO}_2$ ) glass-ceramics by ion exchange, the glass-ceramics are ion exchanged in a  $\text{K}_2\text{SO}_4$ - $\text{KCl}$  salt bath at  $750^\circ\text{C}$ . In this case, crowding of the larger  $\text{K}^+$  ions in the smaller  $\text{Na}^+$  sites in the structure results in a displacive transformation to kalsilite ( $\text{K}_2\text{O} \cdot \text{Al}_2\text{O}_3 \cdot 2\text{SiO}_2$ ). This transformation normally involves a significant increase in specific volume, and it produces great surface compression in the glass-ceramics. Modulus of rupture values on rods ion exchanged in this manner and then abraded may average in excess of  $1378$  MPa.

Table 2.1 and Table 2.2 show the compositions and the strength of glass-ceramics obtained by different exchange baths (Uhlmann and Kreidl, 1980). All samples were tumble abraded for 15 min with 30 grit SiC before ion exchange process. The last three compositions represent strengthening by stuffing as a result of a phase transformation induced by ion exchange. The kalsilite ( $\text{KAlSiO}_2$ ) formed at the surface has a higher expansion coefficient than the nepheline body that would normally result in surface tensile forces and reduced strength. However, the stuffing process produces a net surface compression to yield strength as high as  $1378$  MPa. The difference in modulus of rupture of glass composition 8, 9 and 10 as shown in Table 2.2 due to the difference in expansion coefficient of them.

**Table 2.1** Compositions of representative glass-ceramics (Uhlmann and Kreidl, 1980).

Composition	1	2	3	4	5	6	7	8	9	10
SiO <sub>2</sub>	56	51	60	69	50	71	40	44	43	41
Al <sub>2</sub> O <sub>3</sub>	20	26	-	21	29	18	31	32	32	32
Li <sub>2</sub> O	-	-	-	5	-	2	-	-	-	-
Na <sub>2</sub> O	-	-	5	-	-	-	4	17	17	11
K <sub>2</sub> O	-	-	-	-	-	-	18	-	-	9
MgO	15	5	-	-	12	5	-	-	-	-
ZnO	-	8	-	-	-	-	-	-	-	-
BaO	-	-	35	-	-	-	-	-	-	-
TiO <sub>2</sub>	9	3	-	5	9	-	7	7	7	7
ZrO <sub>2</sub>	-	7	-	-	-	4	-	-	-	-
Crystal phases	$\alpha$ -Quartz spinel enstatite	$\alpha$ - Cristobalite spinel ZrO <sub>2</sub>	Barium silicate	$\beta$ - Spodumene rutile	$\beta$ -Quartz MgTi <sub>2</sub> O <sub>5</sub>	$\beta$ - Quartz ZrO <sub>2</sub>	Synthetic Kaliophilite	Nepheline anatase	Nepheline anatase	Nepheline anatase
Expansion coefficient, $\times 10^{-7}$ (23-300°C)	100	166	195	15	40	16	140	115	120	125

**Table 2.2** Strength of ion-exchanged glass-ceramics (Abraded) (Uhlmann and Kreidl, 1980).

Composition	Bath	Temperature (°C)	Time (Hr.)	Exchange	Surface phase	Modulus of rupture (MPa)
(A) Glass ceramics strengthened by expansion difference						
1	Li <sub>2</sub> SO <sub>4</sub>	950	24	2Li <sup>+</sup> →Mg <sup>2+</sup>	β-Quartz ss	986
2	Li <sub>2</sub> SO <sub>4</sub>	950	24	2Li <sup>+</sup> →Mg <sup>2+</sup>	β-Quartz ss	spalling
3	52%KCl 48%K <sub>2</sub> SO <sub>4</sub>	850	2	2K <sup>+</sup> →Ba <sup>2+</sup>	Glass	275
5	Li <sub>2</sub> SO <sub>4</sub>	850	8	2Li <sup>+</sup> →Mg <sup>2+</sup>	β-Quartz ss	1103
(B) Glass ceramics strengthened by stuffing mechanism						
4	85%NaNO <sub>3</sub> 15%Na <sub>2</sub> SO <sub>4</sub>	580	16	Na <sup>+</sup> →Li <sup>+</sup>	β-Spodumene ss	620
5	Li <sub>2</sub> SO <sub>4</sub>	850	8	2Li <sup>+</sup> →Mg <sup>2+</sup>	β-Quartz ss	1103
6	52%KCl 48%K <sub>2</sub> SO <sub>4</sub>	750	8	K <sup>+</sup> →Li <sup>+</sup>	β-Quartz ss	1006
7	52%KCl 48%K <sub>2</sub> SO <sub>4</sub>	730	8	K <sup>+</sup> →Na <sup>+</sup>	Kaliophilite	690
8	52%KCl 48%K <sub>2</sub> SO <sub>4</sub>	730	8	K <sup>+</sup> →Na <sup>+</sup>	Kalsilite	620
9	52%KCl 48%K <sub>2</sub> SO <sub>4</sub>	730	8	K <sup>+</sup> →Na <sup>+</sup>	Kalsilite	1234
10	52%KCl 48%K <sub>2</sub> SO <sub>4</sub>	730	8	K <sup>+</sup> →Na <sup>+</sup>	Kalsilite	1378

### 2.3 Stress Relaxation

Although the concentration of exchanging ions continually increases towards a maximum value, the resulting compressive stress rises and then decays with time when held at ion exchange temperatures. This effect is due to thermal relaxation, and can be significant if the exchange temperature is sufficiently high relative to the glass transition temperature of the glass. Prolonging the ion exchange process at high temperatures will eventually reduce the compressive stress (Abrams, 2004). Figure 2.1 illustrates this behavior for a  $\text{Na}_2\text{O}-\text{Al}_2\text{O}_3-\text{SiO}_2$  glass. This can be understood better if it is considered that the rate of buildup of the integral stress is proportional to the rate of ion exchange minus loss in stress due to relaxation of glass (Garfinkel, 1969). Thus, it may be written

$$\frac{d\sigma}{dt} = \frac{k}{t^{1/2}} - \frac{\sigma}{\tau} \quad (2.3)$$

where  $\sigma$  is the compressive stress,  $\tau$  is the relaxation time,  $t$  is the ion exchange time and  $k$  is constant.

The Eq. 2.3 has been simplified by Miller and Gordon (1931). It is easily verified that

$$\lim_{\tau \rightarrow \infty} \sigma = 2kt^{1/2} \quad (2.4)$$

and

$$\lim_{t \rightarrow \infty} \sigma = 0 \quad (2.5)$$

Thus, for very large relaxation times, the integral stress should increase linearly with the square root of the time of treatment as long as the sample remains infinite in extent. However, as the time of treatment becomes large with respect to the relaxation time  $\tau$ , the stress will begin to drop off from this linear relationship. The integral stress should exhibit a maximum value at  $t_{\text{max}} = 0.853\tau$ .



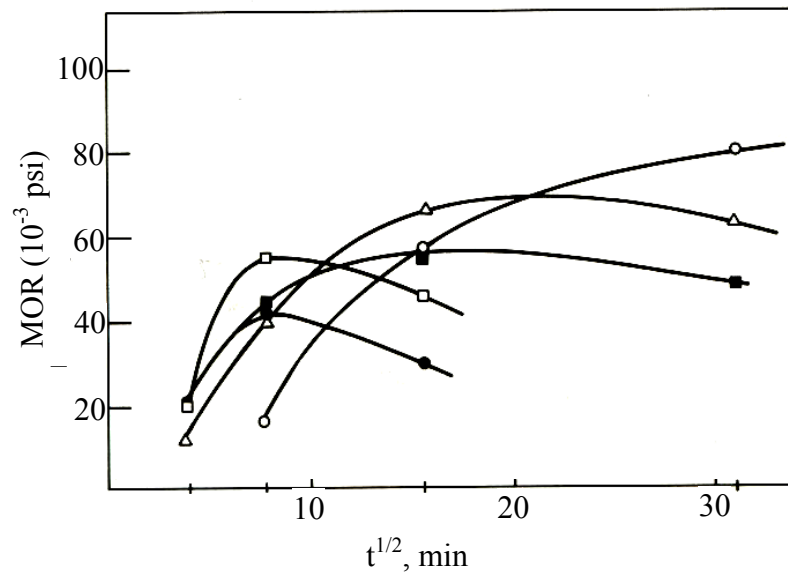


**Figure 2.1** Effect of temperature on the strength of potassium-exchanged  $1.1\text{Na}_2\text{O}-1\text{Al}_2\text{O}_3-4\text{SiO}_2$  glass. ○, 450°C; △, 500°C; ■, 525°C; □, 550°C; ●, 575°C (Uhlmann and Kreidl, 1980).

## 2.4 The Decrystallization of Glass-ceramics by Ion Exchange

Although the published literature on glass-ceramics and ions exchange is not extensive as that for glasses, additional information is directed to the books by Strnad (1986), McMilan (1979), Bach (1995), and Izumitani (1984).

The difficulty and problem of  $\text{Li}^+ \leftrightarrow \text{Na}^+$  ion exchange for  $\text{Li}^+$  containing glass-ceramics is caused by the destruction and disappearance of crystalline phase, such as lithium metasilicate [ $\text{Li}_2\text{O} \cdot \text{SiO}_2$ ], lithium disilicate [ $\text{Li}_2\text{O} \cdot 2\text{SiO}_2$ ] and lithium aluminium silicate [ $\beta$ -Quartz solid solution,  $\text{Li}_2\text{O} \cdot \text{Al}_2\text{O}_3 \cdot n\text{SiO}_2$ ].

Beall and Duke (1969) have reported first that crystalline phase of  $\beta$ -Quartz solid solution in low thermal expansion transparent glass-ceramics was destroyed and

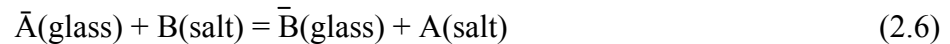
disappeared by  $\text{Li}^+ \leftrightarrow \text{Na}^+$  ion exchange. The structure of  $\beta$ -Quartz solid solution collapsed and disappeared due to the mismatch of crystal structure. In addition, they suggested that the pseudo amorphous phase has been formed.

Morimoto (1991) reported that an amorphous phase has been detected by FTIR spectra, however, the strengthening could be achieved by  $\text{Li}^+ \leftrightarrow \text{K}^+$  ion exchange in the same glass system as Beall and Duke (1969). Morimoto also reported that the unit volume of  $\beta$ -Quartz solid solution crystal decreased after  $\text{Li}^+ \leftrightarrow \text{Na}^+$  ion exchange, whilst it increased after  $\text{Li}^+ \leftrightarrow \text{K}^+$  ion exchange.

Tagantsev and Karapetyan (1999) investigated the decrystallization of crystallized glasses by ion exchange. They found that crystalline phase of lithium metasilicate ( $\text{Li}_2\text{O} \cdot \text{SiO}_2$ ) in photosensitive glass-ceramics disappeared by  $\text{Li}^+ \leftrightarrow \text{Na}^+$  exchange, and called this phenomenon as “Decrystallization”. They reported that this phenomenon took place based on the thermodynamics, and they considered the glass-ceramics as a liquid solution, with the microcrystals of  $\text{Li}_2\text{O} \cdot \text{SiO}_2$  crystals being a precipitate and the solvent is the glassy phase of glass-ceramics. The concentration of  $\text{Li}_2\text{O}$  in the vitreous constituent at the ion exchange temperature is presumed to be sufficient for the solution to be nearly saturated. Due to the Li-for-Na ion exchange process the concentration of  $\text{Li}_2\text{O}$  in a solvent (glassy phase) becomes lower and that fact gets the microcrystals of  $\text{Li}_2\text{O} \cdot \text{SiO}_2$  dissolved in glassy phase to keep the  $\text{Li}^+$  concentration be constant in glassy phase, and this process endured until all crystals have dissolved. Although they proposed the idea for the mechanism of this phenomenon, it has not been clearly explained yet. The chemical strengthening can be achieved by  $\text{Li}^+ \leftrightarrow \text{K}^+$  ion exchange (Morimoto, 1991).

## 2.5 The Theory of Ion Exchange

When a glass containing monovalent cation is placed into a molten salt containing another monovalent cation, ion exchange takes place. A generalized ion-exchange reaction can be written



where  $\bar{A}$  and  $\bar{B}$  are the counterions in the exchanger phase and A and B are the counterions in the liquid phase. Molten salts are required because of the temperature range needed before the cations in the glass become mobile with reference to the negatively charged oxygens of the rigid, immobile silicate network.

In binary ion exchange, the diffusing species A and B are charged, to diffuse at different rates. Thus there is a tendency for one ion to move faster than the other, leading to a buildup of electrical charge. There is, however, a gradient in electrical potential along with this charge, which acts to slow down the faster ion and speed up the slower one. Despite the difference in the mobilities of the two ions, the gradient in electrical potential forces the fluxes of two ions to be equal and opposite, thus preserving electrical neutrality.

The driving force for transport of species A or B is the negative of their gradients in total chemical potential. The total chemical or electrochemical potential is the sum of the gradient in activity and the gradient in electrical potential. This assertion is based upon the assumption that no gradient in pressure or gradients in temperature, are present in the system. With the additional assumption that the mobilities of the ions are the same in self-diffusion and inter-diffusion, the flux of diffusing species per unit time in the x direction is

$$J_A = -D_A \left[ \frac{\partial \bar{c}_A}{\partial x} \frac{\partial \ln \bar{a}_A}{\partial \ln \bar{c}_A} + \bar{c}_A \frac{FE}{RT} \right] \quad (2.7)$$

where  $D_A$  is the self-diffusion coefficients,  $c_A$  the ionic concentration,  $\bar{a}_A$  the activity of species A, and E is the potential gradient or electric field, F is Faraday constant, R is gas constant; a similar expression can be written for the flux  $J_B$ . Only univalent-for-univalent exchange is under consideration here. This set of flux equations is the Nernst-Planck equations.

The conditions of electrical neutrality require that  $J_A = -J_B$ . Since the number of negative exchange sites is constant and fixed,  $\partial c_A / \partial x = -\partial c_B / \partial x$

$$E = \frac{RT}{F} \left[ \frac{D_B - D_A}{\bar{c}_A D_A + \bar{c}_B D_B} \right] \frac{\partial \bar{c}_A}{\partial x} \frac{\partial \ln \bar{a}_A}{\partial \ln \bar{c}_A} \quad (2.8)$$

Substitution of Eq. (2.8) into Eq. (2.7) gives

$$J_A = \frac{D_A D_B}{N_A D_A + N_B D_B} \frac{\partial \ln \bar{a}_A}{\partial \ln \bar{c}_A} \quad (2.9)$$

where N is the cation fraction in the exchange; a similar equation can be written for  $J_B$ . The activity can be related to the concentration by

$$a_A = c_A^n \quad (2.10)$$

$n$  being a constant. By comparison with Fick's first law for diffusion, since  $\partial \ln a_A / \partial \ln c_A = n$  from Eq (2.10), the interdiffusion coefficient becomes

$$\bar{D} = \frac{D_A D_B}{N_A D_A + N_B D_B} n \quad (2.11)$$

For ideals solutions  $n=1$ , so one gets the commonly used relationship between the interdiffusion coefficient and self-diffusion coefficient of the individual cations.

These equation were first applied to the interdiffusion of hydrogen and sodium ions in polysulfonate exchangers in aqueous solution.

The temperature dependence of the interdiffusion and self-diffusion coefficients follows the Arrhenius equation

$$D = D_0 \exp\left(\frac{-E^\ddagger}{RT}\right) \quad (2.12)$$

In which  $E^\ddagger$  is the activation energy.

If the electrical current in an exchanger is carried by a single ionic species, then the electrical conductivity of the exchanger can be related to the diffusion coefficient of this species by Nernst-Einstein equation

$$D = \left[ \frac{\sigma RT}{c} \right] (zF)^2 \quad (2.13)$$

where  $\sigma$  is the specific conductivity in  $\Omega^{-1}\text{cm}^{-1}$ ,  $R$  is 8.314 J/deg mole,  $c$  the concentration of the diffusing species in moles/cm<sup>3</sup>,  $z$  the ionic value, and  $F$  is Faraday's constant which is equal to 96,500 C/equiv.

It has been found that the measured electrical conductivity of glass is less than that calculated from diffusion data (Uhlmann and Kreidl, 1980). These result have been interpreted in terms of a model that accounts for the difference in terms of the two kinds of processes. In this model a correlation factor  $f$ , which depends on the structure of the exchanger and on the transport mechanism, is used to modify the Nernst-Einstein equation so that

$$f = \frac{D_A}{D_\sigma} \quad (2.14)$$

where  $D_A$  is the measured self-diffusion coefficient, and  $D_\sigma$  the diffusion coefficient calculated from the conductivity with Equation (2.13). Thus  $f$  is a measured of the efficiency of the Nernst-Einstein equation. If diffusional motion is completely

random,  $f = 1$ . However,  $f$  is less than unity if the next jump depends upon the direction of the previous jump, i.e., the jump direction is not entirely random.

Experimental data for both self-diffusion and interdiffusion kinetics can be obtained by several techniques. To obtain self-diffusion coefficients, radioactive tracers are necessary. Weight change data has been used most extensively for interdiffusion measurements. The method is described individually below.

By measuring the weight of the exchanger before and after the exchange, the total amount in moles of A taken upper unit surface area of glass exposed to the molten salt is

$$Q_A = \frac{\Delta w}{S(M_A - M_B)} \quad (2.15)$$

where  $M$  is the gram-atomic weight,  $\Delta w$  is the change in weight of the sample following ion exchange, and  $S$  is the superficial area.

Integration of Fick's first law with constant mean integral interdiffusion coefficient  $D_{AB}$  gives

$$Q_A = 2C_{0,A} \left( \frac{D_{AB}t}{\pi} \right)^{1/2} \quad (2.16)$$

where  $C_{0,A}$  is the surface concentration per unit volume. Thus, the amount of material taken up by the exchanger is proportional to the square root of time. In order to double the amount of reaction at a given temperature, the time of treatment must be increased fourfold. If the inter-diffusion coefficient is a function of concentration, then  $D_{AB}$ , determined from Equation (2.16), will be some mean value over the initial and final concentration in the sample. In this case, the uptake is written

$$Q_A = \int_0^t J_A^0 dt = -2(D_{AB}^0 t)^{1/2} \left( \frac{\partial c_A}{\partial w} \right)_{w=0} \quad (2.17)$$

where  $w = x/(D_{AB}^0 t)^{1/2}$ ;  $J_A^0$  is the flux of A, and  $D_{AB}^0$  is the interdiffusion coefficient, respectively, at  $x=0$ . Thus,  $Q_A$  is still proportional to the square root time of exchange, because  $(\partial c_A / \partial w)_{w=0}$  is constant for a constant profile shape irrespective of the depth of exchange. The square-root-of-time law for uptake is well established for ion exchange of glass on molten salts. Figure 2.2 illustrates typical weight change data.

From the ion exchange reaction written in Equation (2.6), an equilibrium constant  $K_{AB}$  can be defined so that

$$K_{AB} = \frac{\hat{a}_B a_A}{\hat{a}_A a_B} \quad (2.18)$$

The  $\hat{a}_i$ s in Equation (2.18) are the respective activities in the exchanger phase and the  $a_i$ s are the respective activities in the liquid phase. The  $K_{AB}$  value of depend upon the reference state chosen to define activities. For the salt, it is convenient to use the pure material as reference state, so that

$$\lim_{N_A \rightarrow 1} = 1 \quad (2.19)$$

for component A, and similarly for component B. Here  $\gamma_A$  is the activity coefficient of component A. The reference state for the solid exchanger is that in which all of the exchangeable cations are of the ion in question.

Ion-exchange equilibrium is characterized by the ion-exchange isotherm, which is a graphical representation covering all experimental conditions at constant temperature. Of prime significance is the selectivity of the exchanger, i.e., the selection of one counterion in preference to the other by the ion exchanger. The equilibrium constant  $K_{AB}$  is an intergral measure of selectivity.

Certain assumptions must be used to get at the experimental quantities in Equation (2.6). The ratio of the activities of the ion in the exchanger is given by

$$\frac{\hat{a}_B}{\hat{a}_A} = \frac{\bar{N}_B}{\bar{N}_A^n} \quad (2.20)$$

where  $\bar{N}$  is the cation fraction. This has been referred to as n-type behavior in aqueous system.

Most of the molten nitrate mixtures used can be characterized as regular solutions (Uhlmann and Kreidl, 1980). Although the heat-of-mixing of these salts is a slight function of composition, the approximation is quite satisfactory. Therefore we may write

$$RT \ln \frac{\gamma_A}{\gamma_B} = A(1 - 2N_A) \quad (2.21)$$

where A is a constant independent of temperature. Substitution of Equations. (2.20) and (2.21) into Equation (2.18) yields

$$\log \frac{N_B}{N_A} - \frac{A}{2.303RT} (1 - 2N_A) = n \log \frac{\bar{N}_B}{\bar{N}_A} - \log K_{AB} \quad (2.22)$$

which is similar to the semiempirical relation proposed for aqueous exchange (Uhlmann and Kreidl, 1980). Thus a plot of  $\log \left( \frac{a_B}{a_A} \right)$  for the salt against  $\log \left( \frac{N_B}{N_A} \right)$

for the exchanger is characterized by a slope of n if  $K_{AB}$  is constant with concentration. Typical data are shown in Figures 2.3 and 2.4.



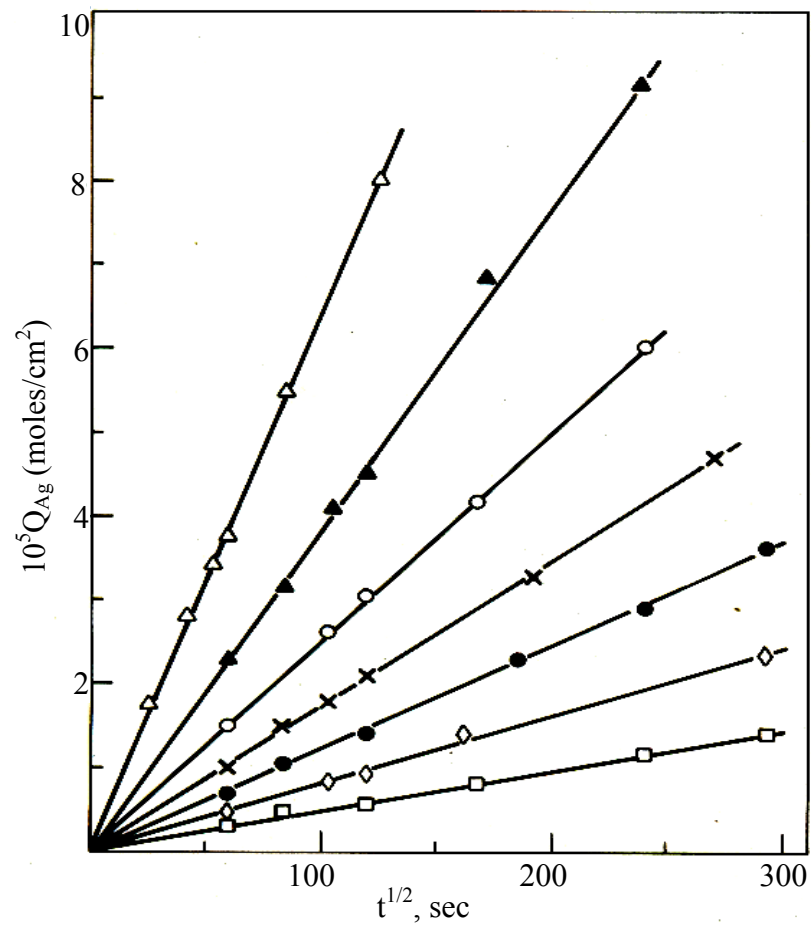


**Figure 2.2** Weight change as a function of  $t^{1/2}$ .  $\text{Ag}^+ \leftrightarrow \text{Li}^+$  ion exchange in 11.4 mole%  $\text{Li}_2\text{O}$ , 16.5 mole%  $\text{Al}_2\text{O}_3$ , 71.5 mole%  $\text{SiO}_2$  glass.  $\Delta$ , 395°C ;  $\blacktriangle$ , 352°C;  $\circ$ , 320°C ;  $\times$ , 306°C;  $\bullet$ , 277°C;  $\diamond$ , 254°C;  $\square$ , 228°C.

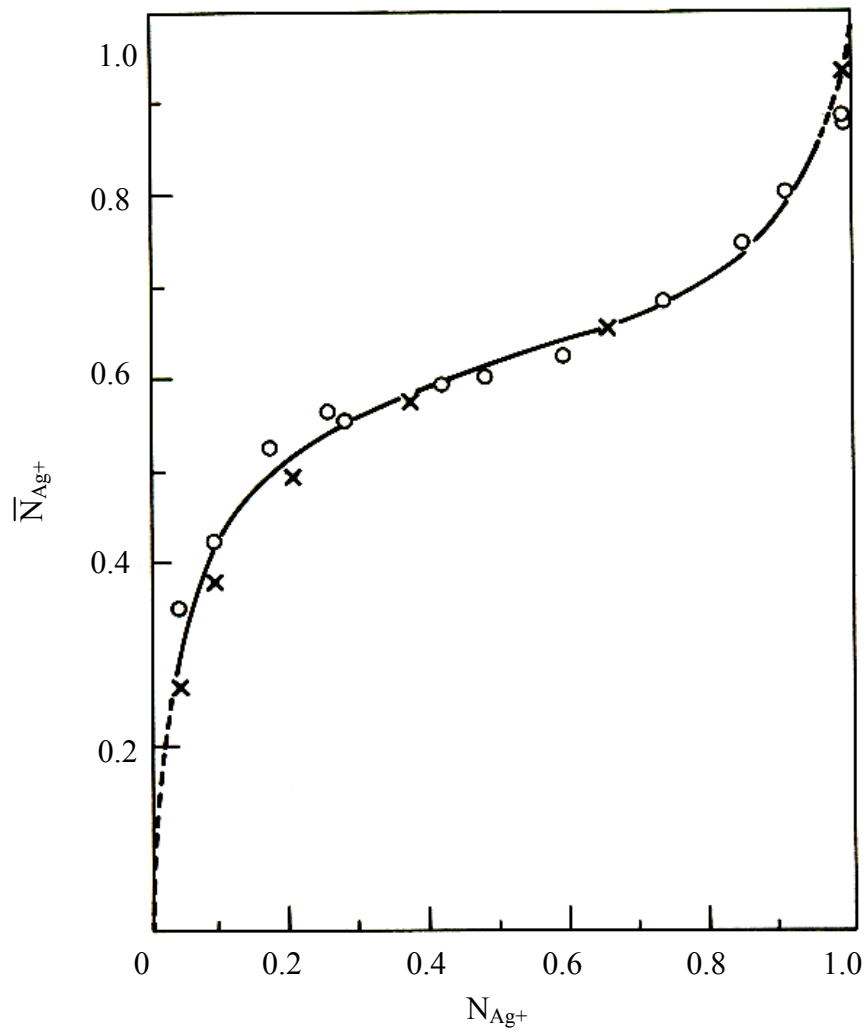


**Figure 2.3** Ion-exchange isotherm:  $\circ$ , 300°C;  $\times$ , 451°C;  $Ag^+ \leftrightarrow Li^+$  ion exchange in 11.4mole%  $Li_2O$ , 16.5mole%  $Al_2O_3$ , 71.5mole%  $SiO_2$  (Uhlmann and Kreidl, 1980).

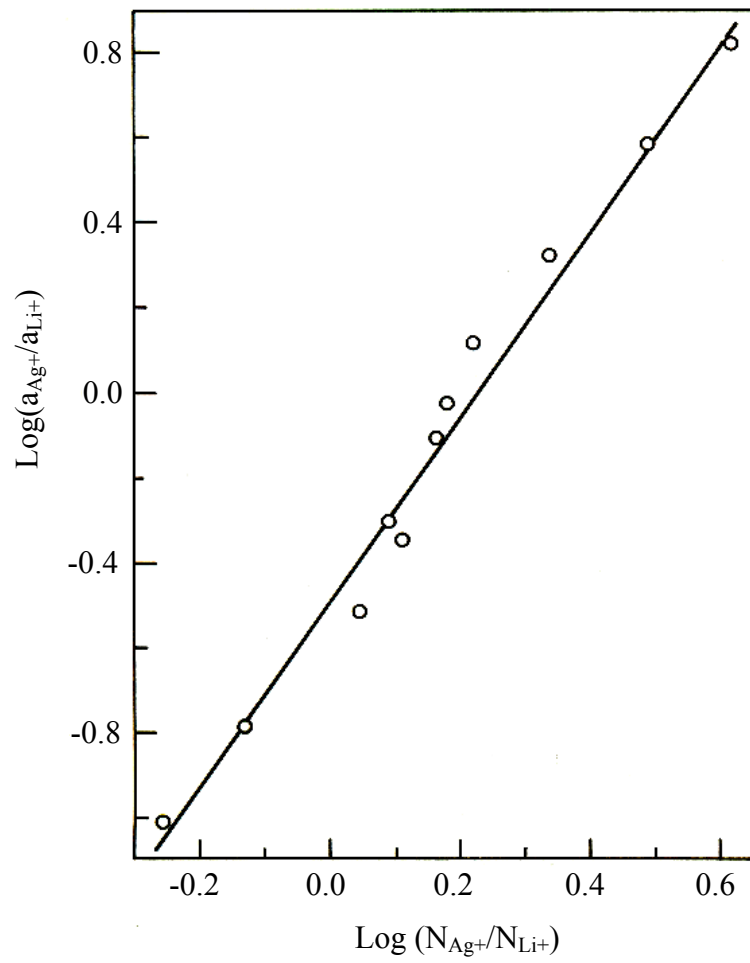


**Figure 2.4** Test of n-type behavior for exchange system  $\text{Ag}^+ \leftrightarrow \text{Li}^+$  at  $300^\circ\text{C}$ ;  $n=2.2$ ;  
 $w = -2.7 \text{ kcal mol}^{-1}$ ; 11.4 mole%  $\text{Li}_2\text{O}$ , 16.5 mole%  $\text{Al}_2\text{O}_3$ , 71.5 mole%  
 $\text{SiO}_2$  (Uhlmann and Kreidl, 1980).

# CHAPTER III

## EXPERIMENTAL

### 3.1 Materials

- High purity silica sand
- Aluminum oxide ( $\text{Al}_2\text{O}_3$ ) A-21, Sumitomo Chemical Ltd, Japan
- Lithium carbonate ( $\text{Li}_2\text{CO}_3$ ), Analytical reagent, Merck, Germany
- Di-Ammonium Hydrogen Orthophosphate [ $(\text{NH}_4)_2\text{HPO}_4$ ], Analytical reagent, Univar, Australia
- Potassium nitrate ( $\text{KNO}_3$ ), Reagent grade, Carlo erba
- Sodium nitrate ( $\text{NaNO}_3$ ), Reagent grade, Carlo erba
- Sodium sulphate ( $\text{Na}_2\text{SO}_4$ ), Reagent grade, Carlo erba

### 3.2 Sample Preparation

#### 3.2.1 Glass Melting

The composition of glass used was shown in Table 3.1

**Table 3.1** Chemical Composition of  $\text{Li}_2\text{O}$ - $\text{SiO}_2$  Glass.

	$\text{SiO}_2$	$\text{Al}_2\text{O}_3$	$\text{Li}_2\text{O}$	$\text{P}_2\text{O}_5$
Mol%	72.9	2.15	23.8	1.15
Weight%	80	4	13	3

$\text{Al}_2\text{O}_3$  was added to stabilize glass against phase separation and  $\text{P}_2\text{O}_5$  is common nucleating agent for lithium silicate glass-ceramics.

A batch corresponding to 200g of glass was mixed thoroughly and pre-calcined at 350 °C for overnight to remove  $\text{NH}_3$ . Then it was melted in a 100 ml Pt/Rh10 crucible at 1450 °C for 2hours with heating rate of 10 °C/min in an electric furnace. The molten glass was poured onto iron plate and crushed, and then it was melted one more time at the same condition to improve homogeneity.

### **3.2.2 Specimen Preparation**

Rods about 5 mm. diameter were freshly drawn and cut into 6 cm in length for the strength measurement. The molten glass was poured onto iron plate and pressed by another iron plate. The glass plate was cut into size of 2×20×20 mm for X-ray diffraction analysis (XRD). The samples were then annealed at 450 °C for 30 min and cooled to room temperature in the furnace.

The samples were heat treated at 500 °C for 15 hours for nucleation and 700 °C for 10 hours for crystallization with heating rate of 10 °C/min and cooled to room temperature in the furnace (Morimoto and Emem, 2004).

### **3.3 Ion Exchange**

The samples of glass and glass-ceramics were ion exchanged in  $\text{NaNO}_3$  and  $\text{KNO}_3$  molten bath under various condition (Salt/glass ratio is 10 by wt).

### 3.4 Material Characterization and Property Measurement

#### 3.4.1 Strength Measurement

The fracture strength was measured using Instron universal testing machine (Model 5565) with load cell of 5 kN according to ASTM C-158. The three point bending method was employed, and the strength of non-abraded specimens was measured. The span length and loading rate were 50 mm and 1 mm/min, respectively.

The fracture strength was calculated by next equation.

$$M = \frac{8PL}{\pi d^2} \quad (3.1)$$

Where:

M = fracture strength, MPa.

P = load at rupture, Newton.

L = Span length, mm.(millimeter).

d = diameter of specimen, mm.(millimeter).

Twelve specimens were used for strength measurement at each ion exchange condition. Maximum and minimum values were excluded to determine average fracture strength and standard deviation.

#### 3.4.2 X-ray Diffraction Analysis

Crystalline phase and lattice constant were determined by X-ray diffraction analysis (XRD). XRD data were collected on diffractometer (Bruker, AXS Model D5005) using Cu K<sub>α</sub> radiation at 40 kV and 40 mA.

Si powder was used as an internal standard for the measurement of lattice constant. The lattice constant of lithium disilicate ( $\text{Li}_2\text{O}\cdot 2\text{SiO}_2$ ) as monoclinic system was calculated as follow

$$\frac{1}{d^2} = \frac{h^2}{a^2 \sin^2 \beta} + \frac{k^2}{b^2} + \frac{l^2}{c^2 \sin^2 \beta} - \frac{2hl \cos \beta}{ac \sin^2 \beta} \quad (3.2)$$

The calculation of lattice constant was shown in Appendix A.

Crystalline size was calculated using Scherrer's equation.

$$D = \frac{0.9 \cdot \lambda}{\beta \cos \theta} \quad (3.3)$$

Where D is the crystalline size (Å),  $\lambda$  is the wavelength of X-ray (1.54 Å),  $\beta$  is the true half width (radian) and  $\theta$  is the diffraction angle (degree). True half width was determined by the Jones method (Nitta, 1975) (Appendix B), and  $\alpha$ -quartz was used as standard.

For example,  $\beta = 0.22^\circ (0.00384)$  radian at  $2\theta$  (degree) =  $24.92^\circ$ ,

$$\begin{aligned} D &= \frac{0.9 \cdot \lambda}{\beta \cos \theta} \\ &= \frac{0.9 \times 0.154 \text{ nm}}{0.0038 \times 0.9764} \\ &= 38 \text{ nm.} \end{aligned}$$

Percent crystallinity was determined using Ohlberg and Strickler's method (Ohlberg and Strickler, 1962) and was calculated using by

$$\text{Percent crystallinity (\%C)} = \frac{(I_g - I_x)}{(I_g - I_c)} \times 100 \quad (3.4)$$

Where  $I_g$  is the X-ray intensity of glass,  $I_x$  is the X-ray background intensity of the specimen and  $I_c$  that of the crystal at  $2\theta=23^\circ$ . The calibration curve

was obtained using mixture  $\alpha$ -quartz and a parent glass at various ratios, and showed a good linearity as shown in Figure 3.1. Detail of calculation was shown in Appendix C.

### **3.4.3 Scanning Electron Microscopy Analysis**

The strength measured samples were cut into 3 mm in length and were then coated with conductive material (gold) using Ion Sputtering Device (JEOL, JFC-110E). The surface structures of glasses and glass-ceramics after ion exchange were observed by scanning electron microscope (SEM, JEOL JSM 640).

### **3.4.4 Dilatometry Analysis**

A dilatometry analysis was carried out to determine the glass transition temperature ( $T_g$ ), dilatometric softening point ( $Y_p$ ) and thermal expansion coefficient ( $\alpha$ ) using fused silica push rod type (Netsch 402EP). Glass and glass-ceramics rod samples of 5mm $\times$ 25mm were heated from 30 °C to 600 °C at a heating rate of 5 °C/min.

### **3.4.5 Density Measurement of Glass and Glass-ceramic**

The density of glass and glass-ceramics was measured by He-gas substitution method using Accupyc 1330 (Micrometrics).

### **3.4.6 Differential Thermal Analysis**

A differential thermal analysis was carried out routinely to determine the nucleation and crystallization temperature using a Perkin-Elmer DTA-7. Glass sample was pulverized and sieved pass through 200 mesh screen. Powder sample was heated to 900 °C at a heating rate of 10 °C/min from room temperature.



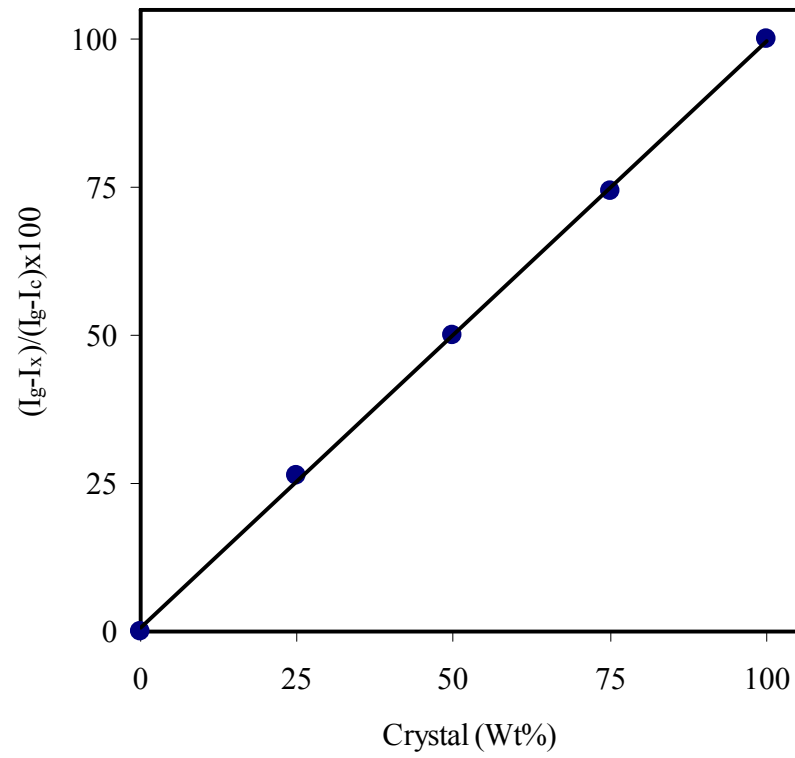


**Figure 3.1** Experimental determined crystallinity VS calculated crystallinity for mechanical mixtures of  $\alpha$ -quartz and parent glass.

## CHAPTER IV

### RESULTS AND DISCUSSION

#### 4.1 The Properties of $\text{Li}_2\text{O}\cdot 2\text{SiO}_2$ Glass and Glass-ceramics

The glass transition temperature ( $T_g$ ), dilatometric softening point ( $Y_p$ ), thermal expansion coefficient ( $\alpha$ ) and density of glass were  $476\text{ }^\circ\text{C}$ ,  $528\text{ }^\circ\text{C}$ ,  $83\times 10^{-7}\text{ }^\circ\text{C}^{-1}$  (30-300  $^\circ\text{C}$ ) and  $2.318\text{ g/cm}^3$ , respectively. The transparent glass-ceramics can be obtained by the heat treatment at  $500^\circ\text{C}$  for 15 h for nucleation and  $700^\circ\text{C}$  for 10 h for crystallization. XRD pattern of glass-ceramics is shown in Figure 4.1.

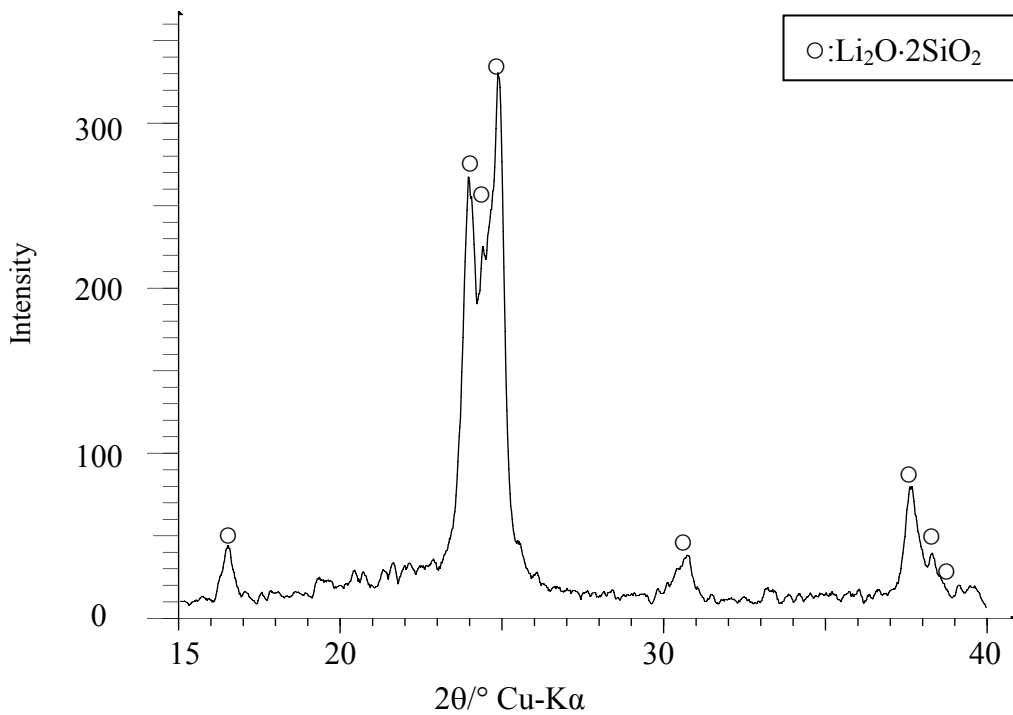


**Figure 4.1** XRD patterns of  $\text{Li}_2\text{O}\cdot 2\text{SiO}_2$  transparent glass-ceramics.

The crystal phase, percent crystallinity and crystallite size of glass-ceramics were  $\text{Li}_2\text{O}\cdot 2\text{SiO}_2$  crystal (JCPDS 40-0376), about 70% by weight and 40 nm respectively. The thermal expansion coefficient and density of transparent glass-ceramics were  $78\times 10^{-7} /^\circ\text{C}$  (30-300  $^\circ\text{C}$ ) and  $2.379 \text{ g/cm}^3$ . The density of glass-ceramics increased by about 2.63%, while the thermal expansion coefficient decreased by 6.02%. Properties of glass and glass-ceramics were summarized in Table 4.1.

**Table 4.1** Summary properties of  $\text{Li}_2\text{O}\cdot 2\text{SiO}_2$  glass and glass-ceramics.

	Glass	Glass-ceramic
Density ( $\text{g/cm}^3$ )	2.318	2.379
$T_g$ ( $^\circ\text{C}$ )	476	-
$Y_p$ ( $^\circ\text{C}$ )	528	-
$\alpha$ ( $^\circ\text{C}^{-1}$ )	$83\times 10^{-7}$	$78\times 10^{-7}$
Crystalline phase	-	$\text{Li}_2\text{O}\cdot 2\text{SiO}_2$
Crystallinity (%)	-	$\approx 70$
Crystallite size (nm)	-	$\approx 40$

## 4.2 The Strengthening of $\text{Li}_2\text{O}\text{-SiO}_2$ Glass by Ion Exchange

The appearance and fracture strength of glass before and after ion exchange for  $\text{Li}^+ \leftrightarrow \text{Na}^+$  and  $\text{Li}^+ \leftrightarrow \text{K}^+$  are shown in Table 4.2. Figure 4.2 shows the relation between fracture strength and ion exchange time.

The fracture strength increases at first and decreases drastically later, and the crack was observed in unchanged layer by naked eye with progress of ion exchange for  $\text{Li}^+ \leftrightarrow \text{Na}^+$  at  $450^\circ\text{C}$  for 4 hours. The maximum value of fracture strength of  $251 \pm 13$  MPa was obtained by  $\text{Li}^+ \leftrightarrow \text{K}^+$  exchange at  $450^\circ\text{C}$  for 4 hours.

**Table 4.2** Fracture strength of glass before and after  $\text{Li}^+ \leftrightarrow \text{Na}^+$  and  $\text{Li}^+ \leftrightarrow \text{K}^+$  exchange.

Ion exchange condition ( $^\circ\text{C}$ -Time)	Fracture strength(MPa)	
	$\text{Li}^+ \leftrightarrow \text{Na}^+$	$\text{Li}^+ \leftrightarrow \text{K}^+$
Glass (Blank sample)	$146 \pm 27$	$146 \pm 27$
450 $^\circ\text{C}$ - 15 min.	$175 \pm 8$	-
- 30 min.	$160 \pm 7$	-
- 1 h	$156 \pm 12$	$180 \pm 28$
- 4 h	35(crack)	$251 \pm 13$
- 9 h	Crack	$155 \pm 15$
-16 h	Crack	$86 \pm 19$

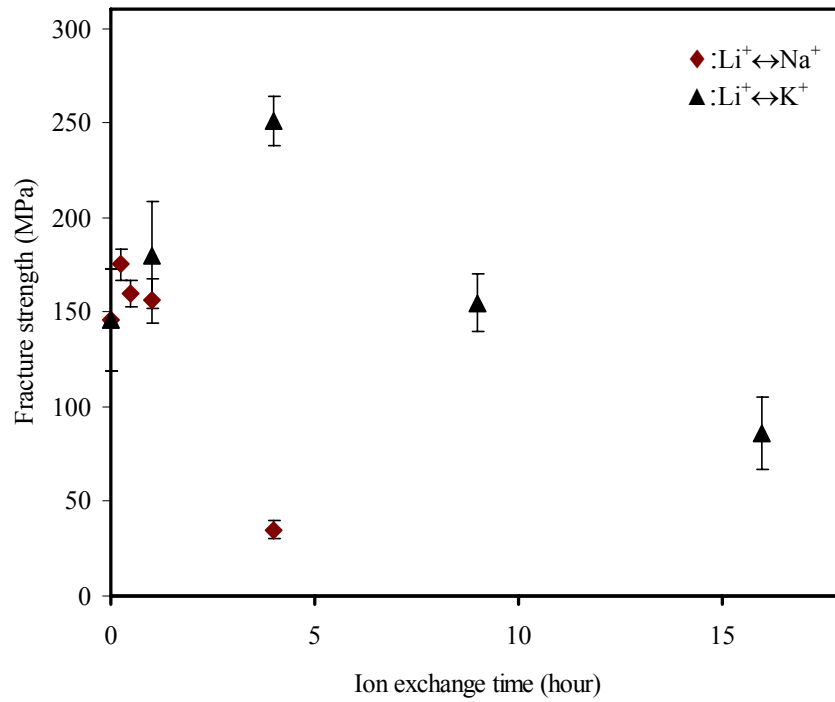


**Figure 4.2** The relation between fracture strength of  $\text{Li}_2\text{O}\cdot 2\text{SiO}_2$  glass and  $\text{Li}^+ \leftrightarrow \text{Na}^+$  and  $\text{Li}^+ \leftrightarrow \text{K}^+$  exchange time.

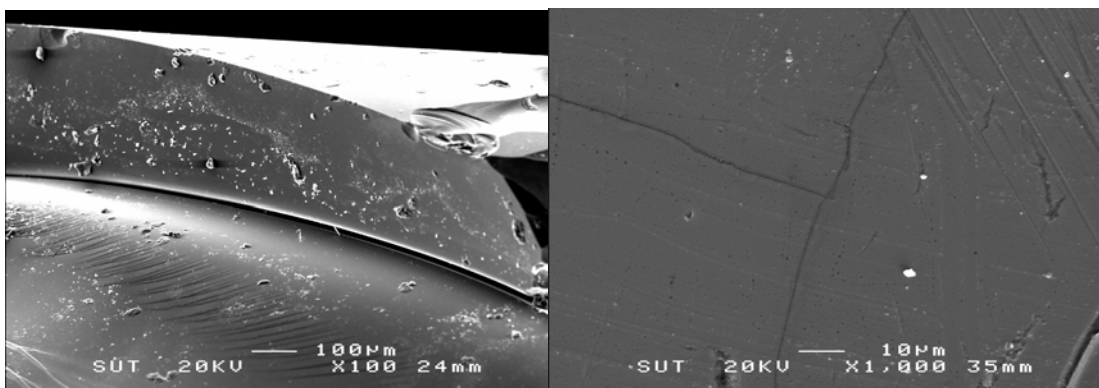


**Figure 4.3** SEM photos of the surface of  $\text{Li}_2\text{O}\cdot 2\text{SiO}_2$  glass after ion exchange.

(a)  $\text{Li}^+ \leftrightarrow \text{Na}^+$  exchange at  $450^\circ\text{C}$  for 4 hours.

(b)  $\text{Li}^+ \leftrightarrow \text{K}^+$  exchange at  $450^\circ\text{C}$  for 16 hours.

Fig. 4.3 shows SEM photos of the surface of glass after ion exchange. It is interesting to note that the ion exchange layer peels off from the surface and a hair-like crack is observed on the surface just below the peeled off layer for  $\text{Li}^+ \leftrightarrow \text{Na}^+$  exchange. On the contrary, for  $\text{Li}^+ \leftrightarrow \text{K}^+$  exchange, crack is observed on the surface. Thus the surface of glass shows the unusual behavior after ion exchange. The relation between this unusual behavior of surface and the fracture strength will be discussed below.

Generally, it is well known that the brittle materials like glasses are weak in tensile stress, and the ion exchange strengthening can be achieved due to the compressive stress arisen in the surface layer by the replacement of smaller ions in glass by larger foreign ions. This method is called “Crowding” (Stookey, 1954). The maximum compressive stress arisen by this mechanism may be given:

$$\sigma_c = \left(\frac{1}{3}\right) \cdot \left[\frac{E}{1-\mu}\right] \cdot \left(\frac{\Delta V}{V}\right) \quad (4.1)$$

Where  $V$  the volume of glass,  $\Delta V$  the volume change by ion exchange without stress at room temperature,  $E$  the Young’s modulus and  $\mu$  the Poisson’s ratio. This equation indicates that the larger  $\Delta V$  gives the larger compressive stress.

Density, molar volume and thermal expansion coefficient of Li-, Na- and K-glasses which according to Volf (1988) were calculated as shown in Appendix D and summarized in Table 4.3. By substituting  $\left(\frac{\Delta V}{V}\right)$  from Table 4.3 into equation (4.1) the compressive stress arisen by  $\text{Li}^+ \leftrightarrow \text{Na}^+$  and  $\text{Li}^+ \leftrightarrow \text{K}^+$  can be calculated. Calculated compressive stress for  $\text{Li}^+ \leftrightarrow \text{Na}^+$  and  $\text{Li}^+ \leftrightarrow \text{K}^+$  is expected to be significantly large because  $\left(\frac{\Delta V}{V}\right)$  of  $\text{Li}^+ \leftrightarrow \text{Na}^+$  and  $\text{Li}^+ \leftrightarrow \text{K}^+$  are comparatively high.

**Table 4.3** The calculated density, molar volume and thermal expansion coefficient of Li-, Na- and K-glasses (Uhlmann and Kreidl, 1980).

Materials	Calculated			
	Density (g/cm <sup>3</sup> )	Molar volume (cm <sup>3</sup> /mole)	$\Delta V/V$ (Li <sup>+</sup> ↔R <sup>+</sup> )*(%)	$\alpha$ ( $\times 10^{-7} \text{ }^\circ\text{C}^{-1}$ )
Li-glass	2.34	23.37	-	88.8
Na-glass	2.44	25.52	9.20	118.0
K-glass	2.48	28.26	20.92	135.1

\*R<sup>+</sup> is alkali ion.

Figure.4.4 shows the schematic representation of dimension change during ion exchange. The volume change ( $\Delta V$ ) in equation (4.1) was based on the assumption as shown in case A, ideal case. However, the volume change of glass by ion exchange shown in case B, actual case; that is, much smaller than in case A. As a result the observed compressive stresses arisen are lower than the calculated values.

It is very interesting to note that the peeling and crack occur despite a large compressive stress arisen in ion exchange layer. This behavior can not be observed in usual ion exchange process. In the early stage of ion exchange discussed here, peeling and crack were not observed, therefore, the compressive stress arisen affects effectively on the increase in fracture strength. The increasing in the thickness of ion exchanged layer caused the increasing of the volume change of ion exchanged layer. Therefore, the crack and the peeling can be generated in that layer. The compressive stress arises in ion exchanged layer and simultaneously tensile stress also generates in original glass to compensate the stress. Thus, with progress of ion exchange, the peeling and crack formation take place and the submicroscopic crack (hair-like crack in figure 4.3) which acts as stress concentrator, would be formed perpendicular to the

surface and finally the fracture strength decreases drastically in the later stage of ion exchange.

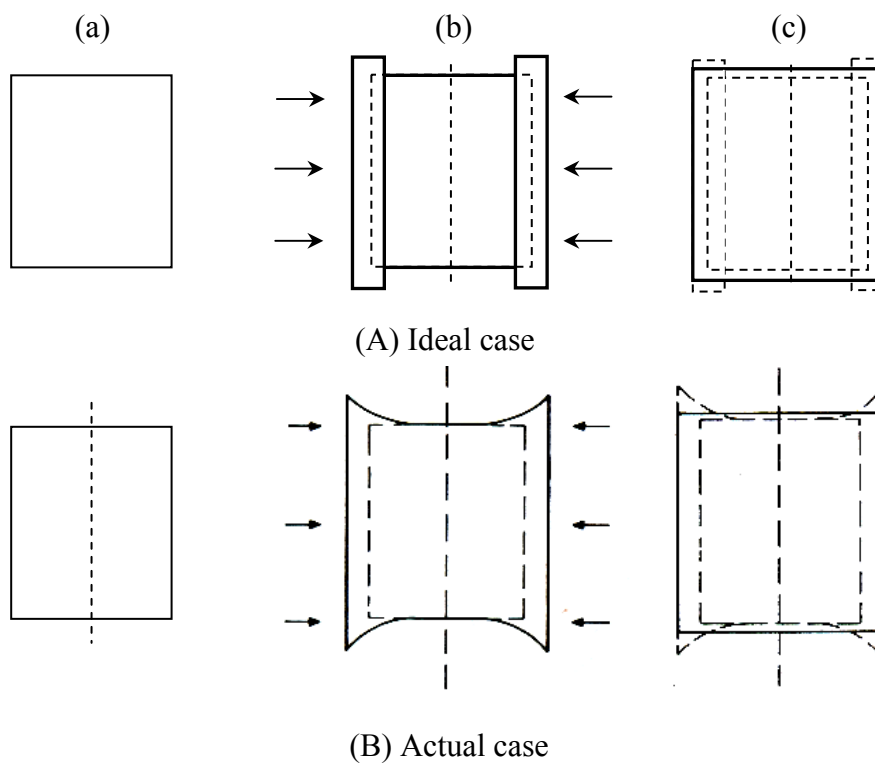


**Figure. 4.4** Schematic representation of ideal and actual dimension change after ion exchange (Varshneya, 1994).

(a). No ion exchange.

(b). Ion exchanged and unrestrained.

(c). Ion exchanged and restrained



### 4.3 The Strengthening of $\text{Li}_2\text{O}\cdot 2\text{SiO}_2$ Transparent Glass-ceramics by Ion Exchange

The fracture strength of glass-ceramics before and after ion exchange is shown in Table 4.4 and Table 4.5. The relationships between fracture strength of glass-ceramics and ion exchange time for  $\text{Li}^+ \leftrightarrow \text{Na}^+$  and  $\text{Li}^+ \leftrightarrow \text{K}^+$  are shown in Figure 4.5 and Figure 4.6, respectively. The change in fracture strength of glass-ceramics with time shows the similar tendency to that of glass. However, the ion exchange time of glass-ceramics is longer than that of glass. This suggests that the rate of ion exchange of glass-ceramics is smaller than that of glass (Figure 4.2).

The fracture strength of glass-ceramics increases gradually and reaches the maximum, and then decreases. However, the fracture strength does not drop below original strength. The maximum fracture strength of  $487 \pm 15$  MPa was obtained without surface crack by  $\text{Li}^+ \leftrightarrow \text{K}^+$  exchange at  $500^\circ\text{C}$  for 9 hours. This is about 3 times greater than that of original glass-ceramics.

Figure 4.7 shows SEM photos of surface of glass-ceramics after ion exchange. The similar behavior to glass was observed. The ion exchanged layer peels off from the surface layer for  $\text{Li}^+ \leftrightarrow \text{Na}^+$  exchange (at  $550^\circ\text{C}$  for 16 hours). On the other hand, crack was observed on the surface of glass-ceramics for  $\text{Li}^+ \leftrightarrow \text{K}^+$  exchange (at  $550^\circ\text{C}$  for 16 hours).

**Table 4.4** Fracture strength of  $\text{Li}_2\text{O}\cdot 2\text{SiO}_2$  transparent glass-ceramics before and after  $\text{Li}^+ \leftrightarrow \text{Na}^+$  exchange.

Ion exchange condition (°C-Time)	Fracture strength(MPa)
Glass-Ceramics	167±27
400 °C -1.5 h	263±15
-2.5 h	301±20
- 4 h	296±18
450 °C - 1 h	345±24
- 4 h	379±34
- 9 h	180±13
550 °C - 1 h	189±33
- 4 h	200±19
- 9 h	236±10
- 16 h	178±20

**Table 4.5** Fracture strength of  $\text{Li}_2\text{O}\cdot 2\text{SiO}_2$  transparent glass-ceramics before and after  $\text{Li}^+ \leftrightarrow \text{K}^+$  exchange.

Ion exchange condition (°C-Time)	Fracture strength(MPa)
Glass-Ceramics	167±27
450 °C - 4 h.	255±17
- 9 h.	331±40
- 16 h.	381±25
- 25 h.	355±35
500°C - 4 h	300±10
- 9 h	487±15
- 16 h.	451±5
- 25 h.	360±17
550C - 4 h.	220±11
- 9 h.	246±15
- 16 h.	333±29
- 25 h.	256±25

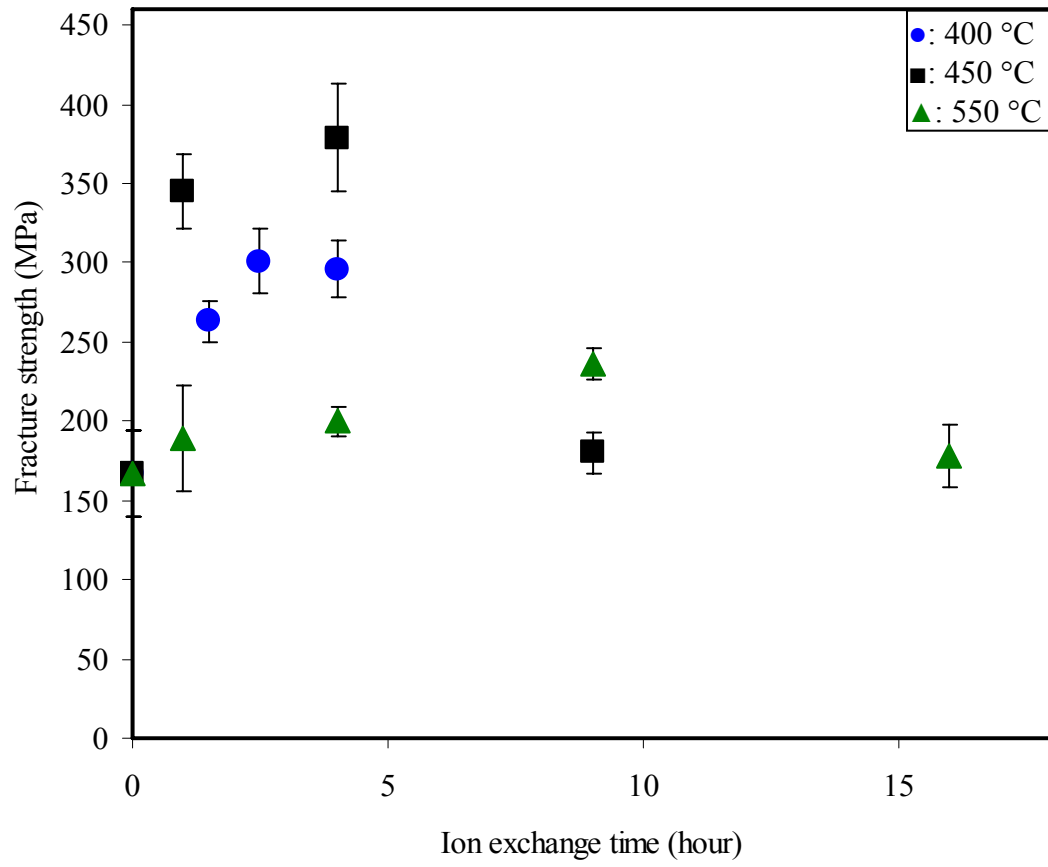


**Figure 4.5** The relation between fracture strength of  $\text{Li}_2\text{O}\cdot 2\text{SiO}_2$  transparent glass-ceramics and  $\text{Li}^+ \leftrightarrow \text{Na}^+$  exchange time.

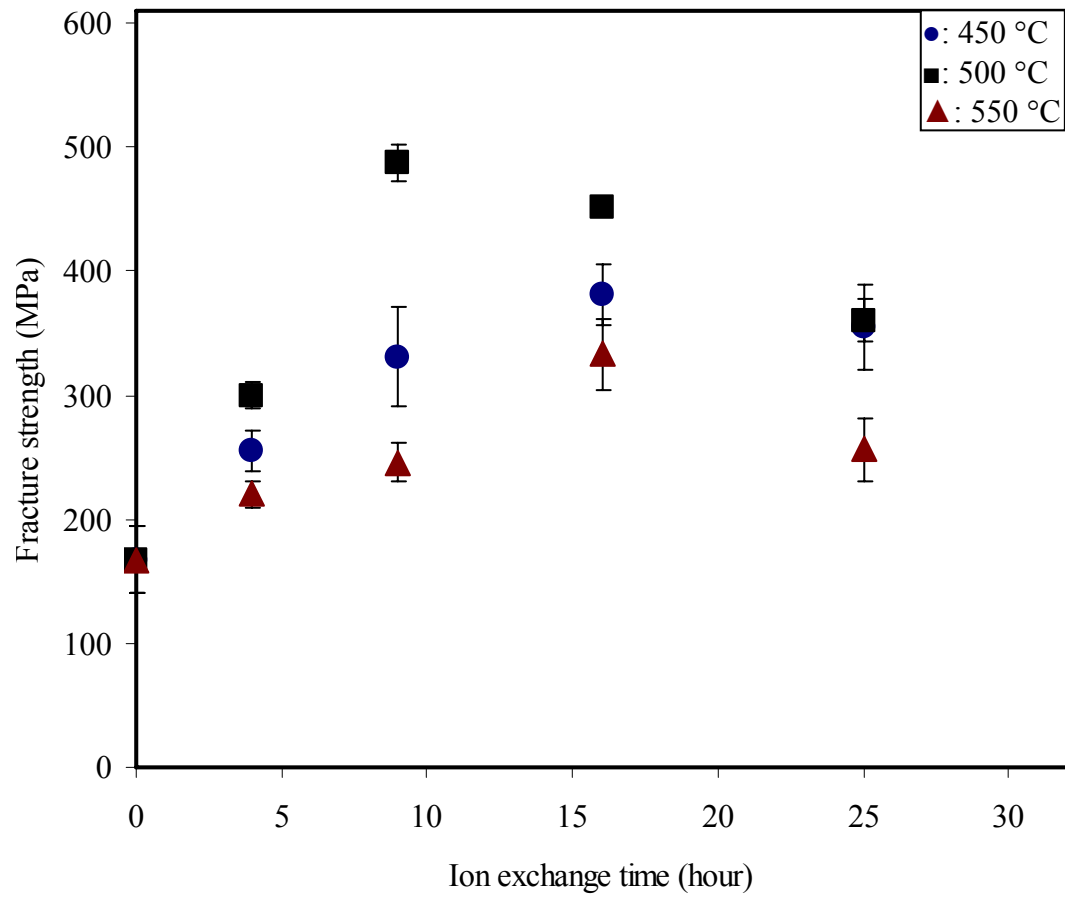


**Figure 4.6** The relation between fracture strength of  $\text{Li}_2\text{O}\cdot 2\text{SiO}_2$  transparent glass-ceramics and  $\text{Li}^+ \leftrightarrow \text{K}^+$  exchange time.

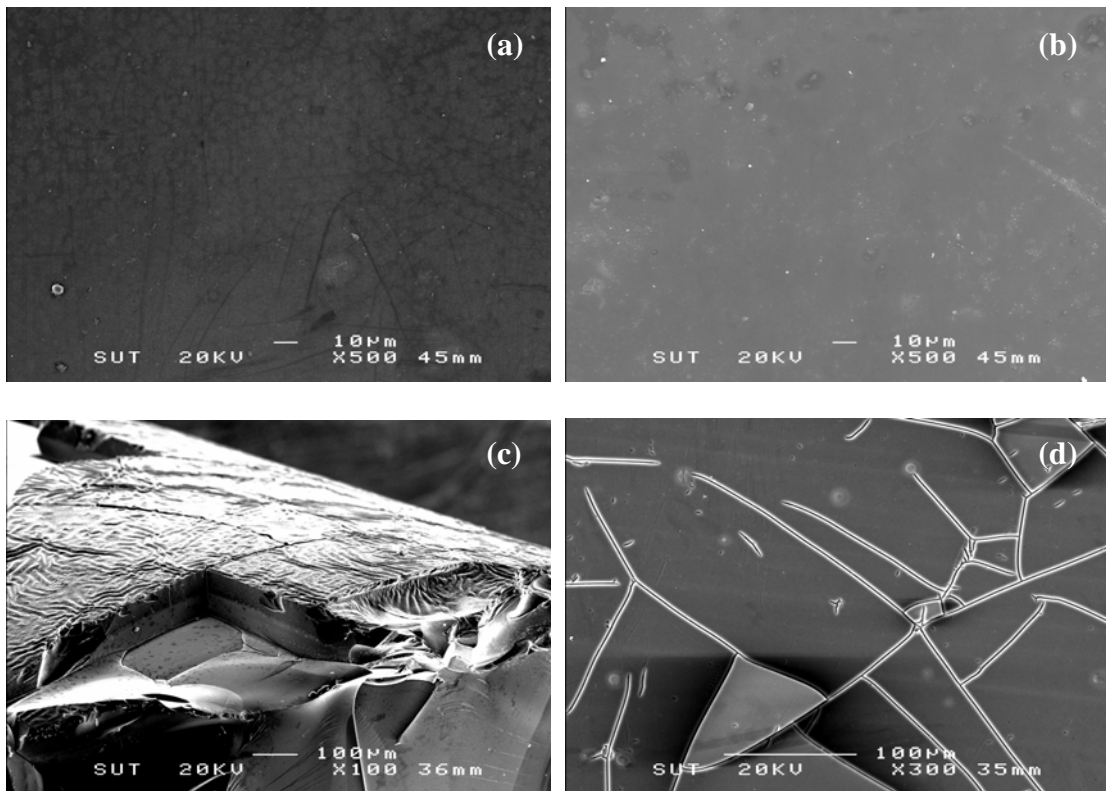


**Figure 4.7** The SEM photos of the surface of  $\text{Li}_2\text{O}\cdot 2\text{SiO}_2$  transparent glass-ceramics after ion exchange.

- (a)  $\text{Li}^+ \leftrightarrow \text{Na}^+$  exchange at  $400^\circ\text{C}$  for 4 hours.
- (b)  $\text{Li}^+ \leftrightarrow \text{K}^+$  exchange at  $500^\circ\text{C}$  for 9 hours.
- (c)  $\text{Li}^+ \leftrightarrow \text{Na}^+$  exchange at  $550^\circ\text{C}$  for 16 hours.
- (d)  $\text{Li}^+ \leftrightarrow \text{K}^+$  exchange at  $550^\circ\text{C}$  for 16 hours.

The increase in the fracture strength of glass-ceramics may be interpreted by “Crowding” as discussed before. However, it should be note that the crystal phase of higher density of  $\text{Li}_2\text{O}\cdot 2\text{SiO}_2$  disappeared and convert to lower density of glassy phase by  $\text{Li}^+ \leftrightarrow \text{Na}^+$  and  $\text{Li}^+ \leftrightarrow \text{K}^+$  exchange of glass-ceramics. This phenomenon was

called as “Amorphization” and will be discussed later. Therefore, the volume change is controlled by two factors, amorphization and the volume change by ion exchange discussed previously, and may be larger than that of glass. Thus, the larger compressive stress generation may be expected for glass-ceramics by ion exchange.

The fracture strength does not decrease below initial fracture strength, despite the crack and peeling were observed on the surface of glass-ceramics. This suggests that submicroscopic flaws were not formed on the surface of glass-ceramics and hence, higher fracture strength than glass. Also, the result show that the fracture strength depends on temperature and time of ion exchange, the lesser the fracture strength as self-annealing of samples are accelerated. The decrease in the fracture strength of glass-ceramics seems to be due to the stress relaxation.

The volume change of ion exchanged layer strongly depends on the alkali content in the base glass. The glass discussed here contains about 24 mol% of  $\text{Li}_2\text{O}$ . These peeling and crack formation seems to be the characteristics of high alkali containing glasses by ion exchange.

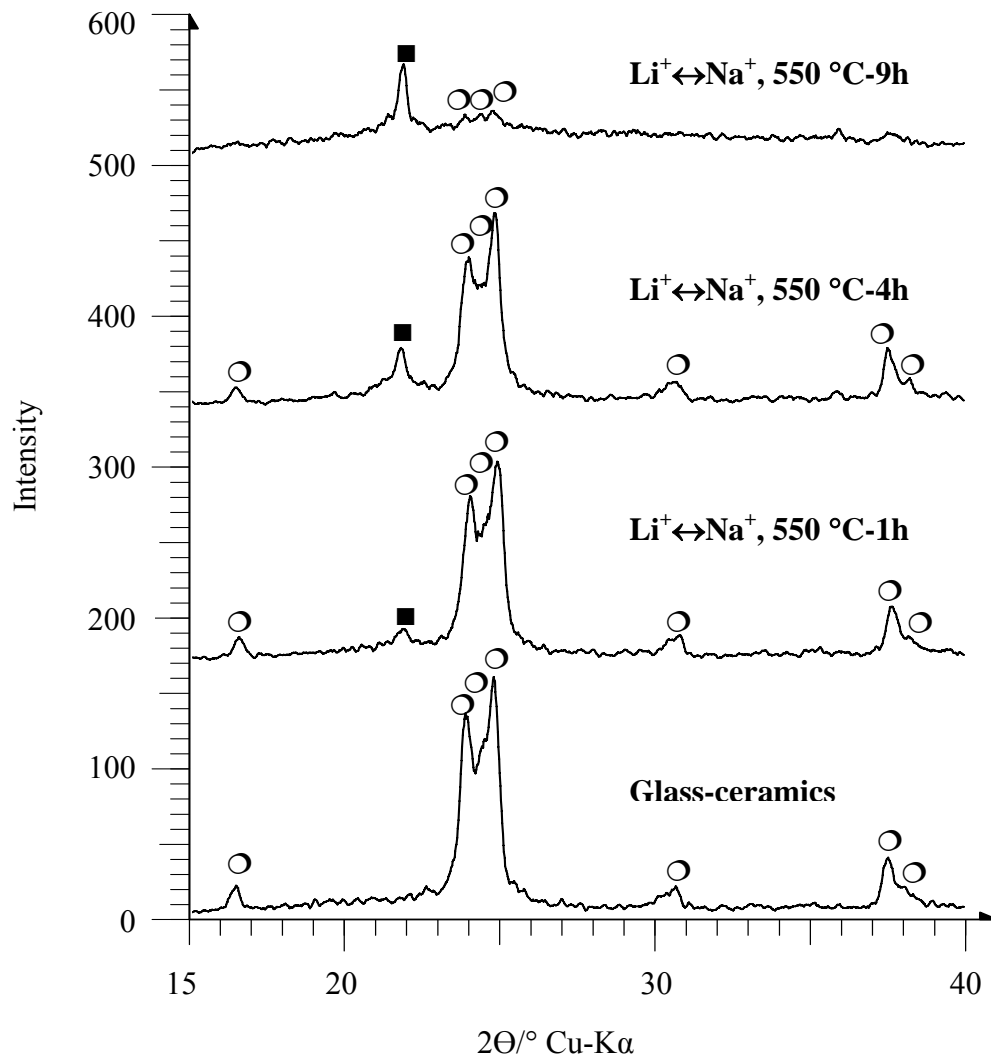


**Figure 4.8** XRD patterns of  $\text{Li}_2\text{O}\cdot 2\text{SiO}_2$  transparent glass-ceramics (plate specimens)

before and after  $\text{Li}^+ \leftrightarrow \text{Na}^+$  exchange.  $\circ$ :  $\text{Li}_2\text{O}\cdot 2\text{SiO}_2$ ,  $\blacksquare$ : Cristobalite.



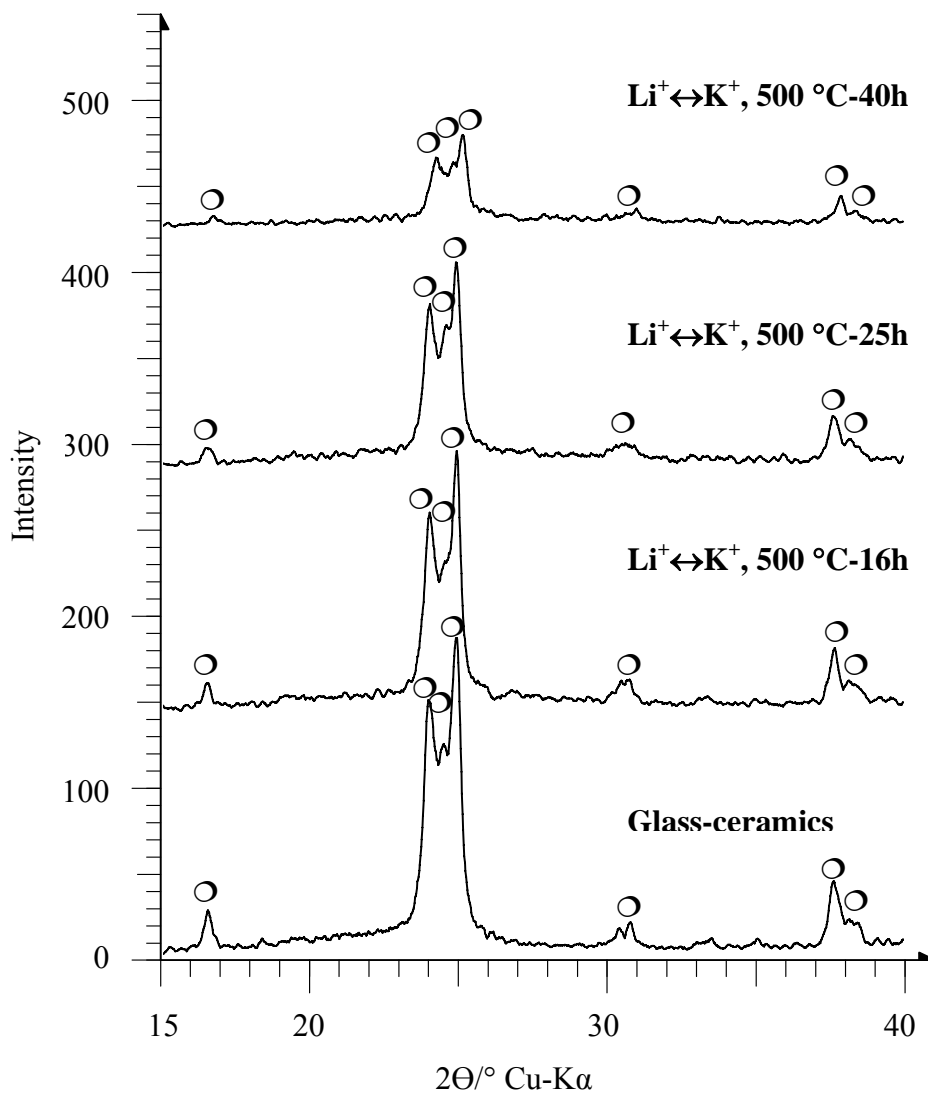


**Figure 4.9** XRD patterns of Li<sub>2</sub>O·2SiO<sub>2</sub> transparent glass-ceramics (plate specimens)

before and after Li<sup>+</sup> ↔ K<sup>+</sup> exchange. ○ : Li<sub>2</sub>O·2SiO<sub>2</sub>.

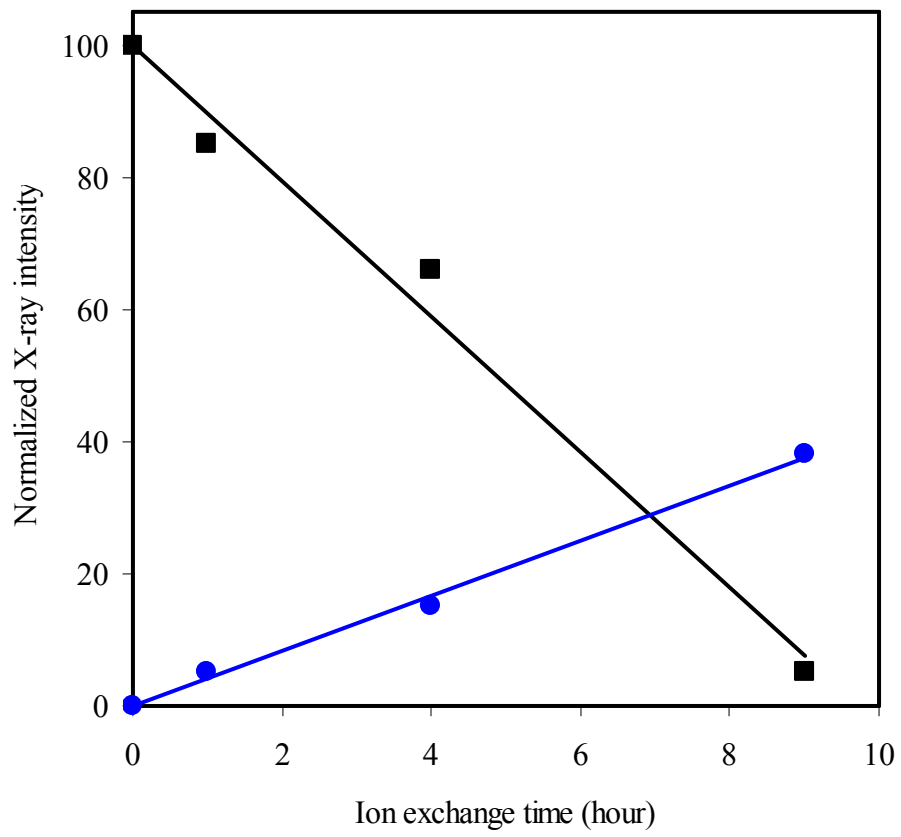


**Figure 4.10** Relation between normalized X-ray intensity of the strongest peak of  $\text{Li}_2\text{O}\cdot 2\text{SiO}_2$  crystal (■) ( $2\theta=24.8^\circ$ ) and  $\text{SiO}_2$  crystal (●) ( $2\theta=21.8^\circ$ ) in  $\text{Li}_2\text{O}\cdot 2\text{SiO}_2$  transparent glass-ceramics and  $\text{Li}^+ \leftrightarrow \text{Na}^+$  ion exchange time at  $550^\circ\text{C}$ .

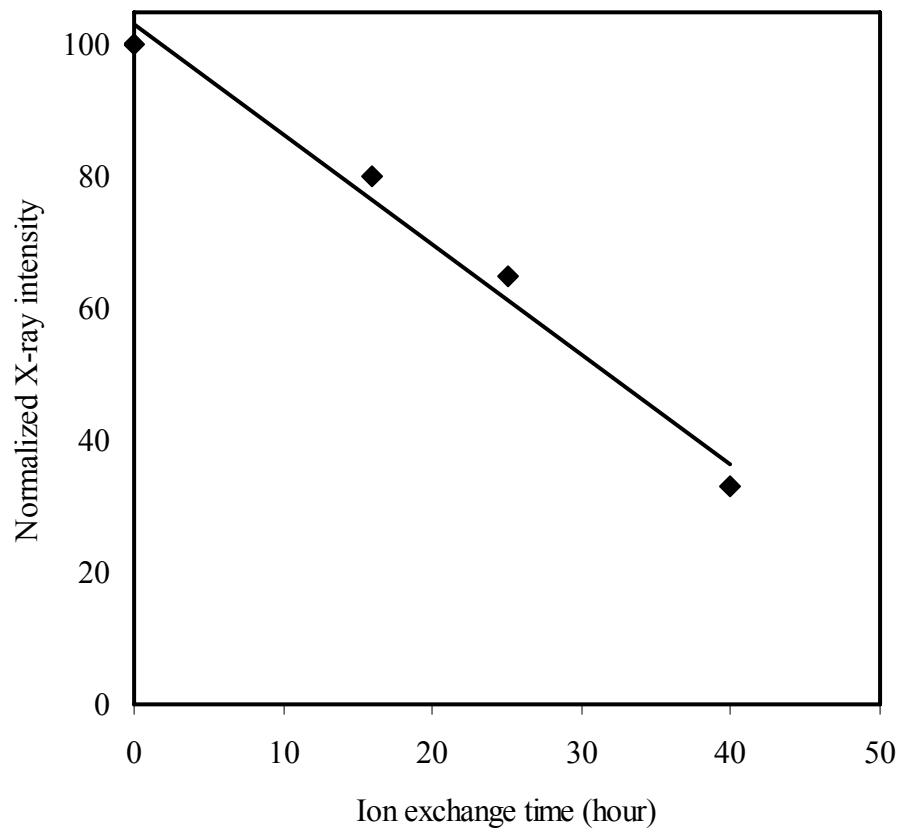


**Figure 4.11** Relation between normalized X-ray intensity of the strongest peak of  $\text{Li}_2\text{O}\cdot 2\text{SiO}_2$  crystal ( $2\theta=24.8^\circ$ ) in  $\text{Li}_2\text{O}\cdot 2\text{SiO}_2$  transparent glass-ceramics and  $\text{Li}^+ \leftrightarrow \text{K}^+$  ion exchange time at  $500^\circ\text{C}$ .

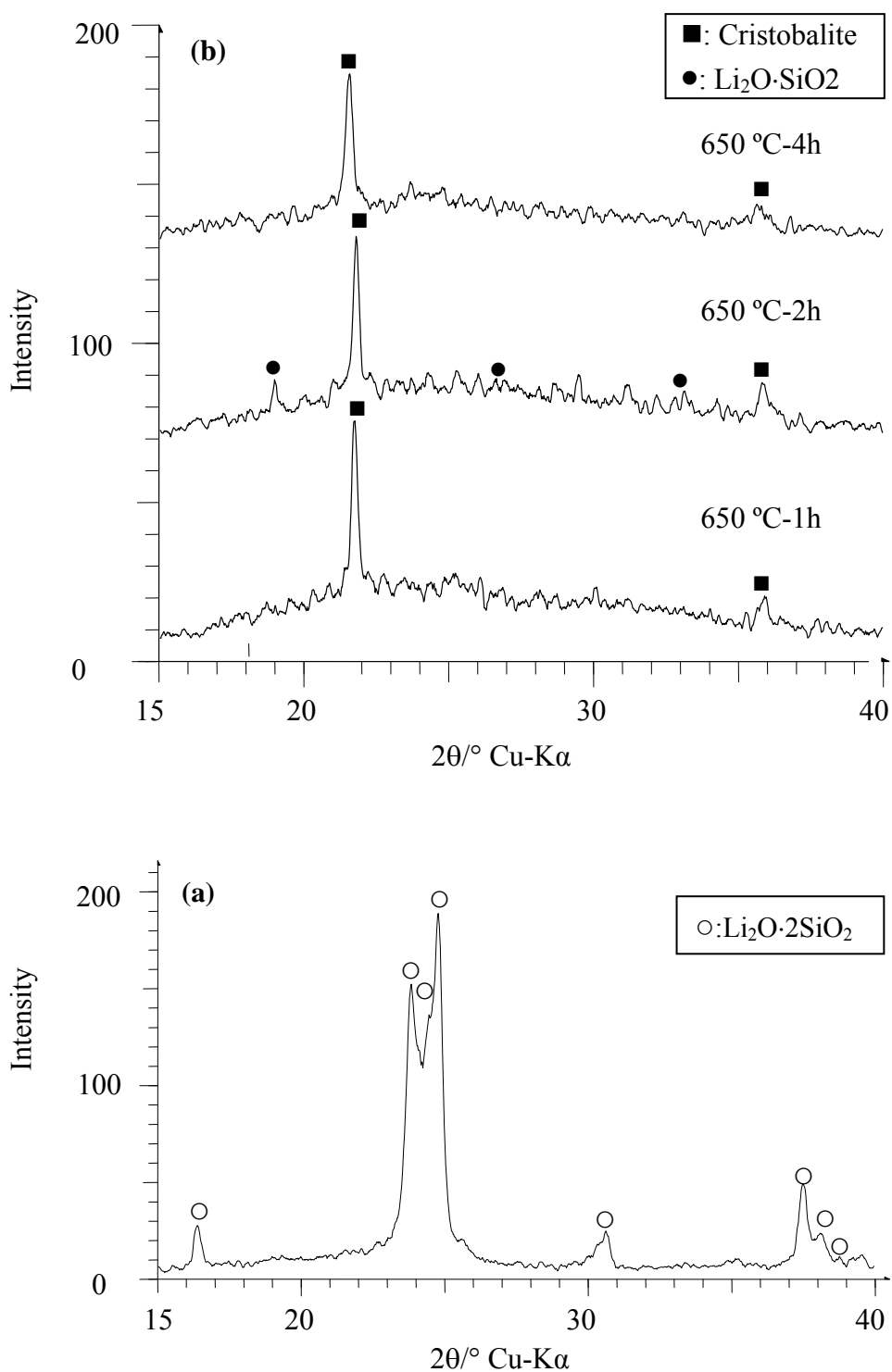


**Figure 4.12** XRD patterns of  $\text{Li}_2\text{O}\cdot 2\text{SiO}_2$  transparent glass-ceramics, (a) before and (b) after  $\text{Li}^+ \leftrightarrow \text{Na}^+$  exchange at  $650^\circ\text{C}$ .

#### 4.4 The Amorphization of $\text{Li}_2\text{O}\cdot 2\text{SiO}_2$ Transparent Glass-ceramics by Ion Exchange.

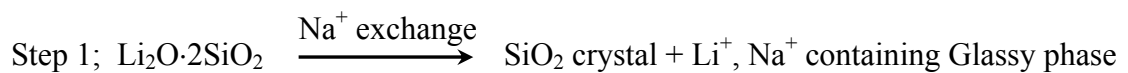
The plate samples of glass-ceramics were ion exchanged in molten salt baths under various conditions to investigate the effect of the ion exchange process on structure of  $\text{Li}_2\text{O}\cdot 2\text{SiO}_2$  crystal in lithium silicate transparent glass-ceramics.

Figures 4.8 and 4.9 show the XRD patterns of glass-ceramics before and after ion exchange for  $\text{Li}^+ \leftrightarrow \text{Na}^+$  and  $\text{Li}^+ \leftrightarrow \text{K}^+$ , respectively. The XRD results showed XRD peaks of  $\text{Li}_2\text{O}\cdot 2\text{SiO}_2$  crystal and its X-ray intensity decreased and finally disappeared after ion exchange while a diffraction peak of cristobalite appeared at around  $2\theta=22^\circ$  after  $\text{Li}^+ \leftrightarrow \text{Na}^+$  exchange. This indicates that the  $\text{Li}_2\text{O}\cdot 2\text{SiO}_2$  crystal was disappeared by ion exchange process.

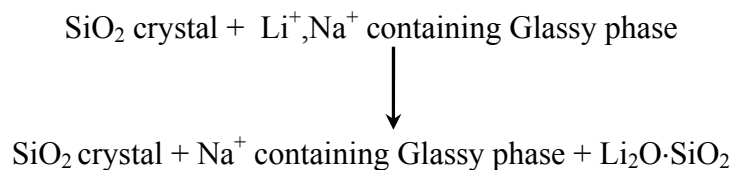
Figure 4.10 and 4.11 show the relationship between normalized X-ray intensity of the strongest peak of  $\text{Li}_2\text{O}\cdot 2\text{SiO}_2$  crystal ( $2\theta=24.8^\circ$ , [111]) and time of ion exchange (t) of glass-ceramics for  $\text{Li}^+ \leftrightarrow \text{Na}^+$  and  $\text{Li}^+ \leftrightarrow \text{K}^+$ , respectively. The good linearity was obtained, and this indicates that the rate of disappearance of  $\text{Li}_2\text{O}\cdot 2\text{SiO}_2$  crystal is proportional to the time of ion exchange and this process is dominant process. According to Garfinkel (1970), the ion exchange process of glass in molten salts was evaluated by  $(Dt)^{1/2}$ , where D is the interdiffusion coefficient at the ion exchange temperature and t is the ion exchange time. If ion exchange would be dominant process, the rate process should be expressed by  $\sqrt{t}$ .

Figure 4.12 shows the XRD patterns of glass-ceramics before and after ion exchange at high temperature ( $650^\circ\text{C}$ ). It was observed that the XRD peaks of  $\text{Li}_2\text{O}\cdot 2\text{SiO}_2$  crystal disappeared completely in ion exchanged layer and a diffraction

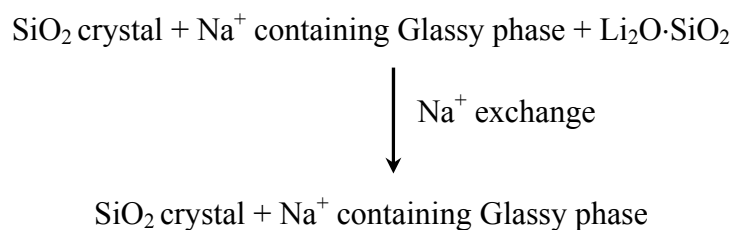
peaks of Cristobalite starts to appear by  $\text{Li}^+ \leftrightarrow \text{Na}^+$  exchange for 1 hour. It is interesting to notice that a diffraction peaks of  $\text{Li}_2\text{O}\cdot\text{SiO}_2$  appears at first and disappears again with progress of ion exchange. This indicate that the  $\text{Li}_2\text{O}\cdot\text{SiO}_2$  crystal precipitate in  $\text{Li}_2\text{O}\text{-SiO}_2$  glass-ceramics by  $\text{Li}^+ \leftrightarrow \text{Na}^+$  at high temperature ( $650^\circ\text{C}$ ). There are two cases for the crystallization of  $\text{Li}_2\text{O}\cdot\text{SiO}_2$  crystal in  $\text{Li}_2\text{O}\text{-SiO}_2$  glass, one is the high  $\text{Li}_2\text{O}$  containing glass (West and Glasser,1971; Jacquin et al.,1995) and another is mixed alkali  $\text{Li}_2\text{O}\text{-SiO}_2$  glass (Mishima, 2004;Morimoto, 2006). In the latter case, the studies reported by Mishima (2004), used similar glass system. The crystallization of  $x\text{Li}_2\text{O}\cdot(1-x)\text{Na}_2\text{O}\cdot 2\text{SiO}_2$  glass doped with 0.005wt% platinum (Pt) was investigated. It was found that the crystallization of  $\text{Li}_2\text{O}\cdot\text{SiO}_2$  crystal was observed in the range of  $x \geq 0.8$  at heat treatment of  $450^\circ\text{C}$  for 5 hours and  $600^\circ\text{C}$  for 1 hour. This suggest that  $\text{Na}_2\text{O}$  induced the precipitation of  $\text{Li}_2\text{O}\cdot\text{SiO}_2$  crystal in  $\text{Li}_2\text{O}\text{-SiO}_2$  glass system. Above phenomena can be interpreted as follows;



Step 2;



Step 3;



Step 1, the  $\text{Li}_2\text{O}\cdot 2\text{SiO}_2$  crystal disappeared by  $\text{Li}^+ \leftrightarrow \text{Na}^+$  exchange and converted to  $\text{Li}^+$ ,  $\text{Na}^+$  containing glassy phase in ion exchanged layer, and the  $\text{Na}^+$  concentration also increases in glassy phase. Step 2,  $\text{Li}_2\text{O}\cdot \text{SiO}_2$  crystal starts to precipitate in  $\text{Li}^+ \leftrightarrow \text{Na}^+$ -containing glassy phase and Step 3, the  $\text{Li}_2\text{O}\cdot \text{SiO}_2$  crystal disappears finally by subsequent ion exchange.

The cristobalite starts to precipitate and grows in contrast to the disappearance of  $\text{Li}_2\text{O}\cdot 2\text{SiO}_2$  crystal with progress of  $\text{Li}^+ \leftrightarrow \text{Na}^+$  exchange, but not in  $\text{Li}^+ \leftrightarrow \text{K}^+$  exchange. This indicates that  $\text{Na}_2\text{O}$  reduces crystallization temperature of cristobalite and promotes the precipitation of cristobalite in  $\text{Li}_2\text{O}\text{-Na}_2\text{O}\text{-SiO}_2$  glassy phase (Mishima, 2004).

Thus it is clear that the  $\text{Li}_2\text{O}\cdot 2\text{SiO}_2$  crystals disappear during ion exchange. This phenomenon was found about 40 years ago by Beall and Duke (1969). They found the disappearance of  $\beta$ -quartz solid solution in low thermal expansion transparent glass-ceramics by  $\text{Li}^+ \leftrightarrow \text{Na}^+$  exchange, and concluded that this is due to the formation of pseudo amorphous phase. Recently, Tagantsev and Karapetyan (1999) found the same phenomenon in photosensitive chemically machinable glass-ceramics based on  $\text{Li}_2\text{O}\cdot \text{SiO}_2$  crystal and called this phenomenon as “Decrystallization” which was called as “Amorphization” in present work. Tagantsev and Karapetyan explained that “Amorphization” took place based on thermodynamics, consider  $\text{Li}_2\text{O}\cdot \text{SiO}_2$  glass-ceramics as liquid solution, with the microcrystals of  $\text{Li}_2\text{O}\cdot \text{SiO}_2$  being as precipitates and the solvent is glassy phase of glass-ceramics. Due to the ion exchange process the concentration of  $\text{Li}_2\text{O}$  in the glassy phase becomes lower. The  $\text{Li}_2\text{O}\cdot \text{SiO}_2$  crystals can dissolve in glassy phase to

keep the  $\text{Li}^+$  concentration in glassy phase being constant, and this process endures until all crystals have dissolved in glassy phase. This suggests that the ion exchange reaction takes place only in glassy phase and the glassy phase plays an important role in “Amorphization” process. Figure 4.13 illustrates Amorphization mechanism according to Tagantsev and Karapetyan.

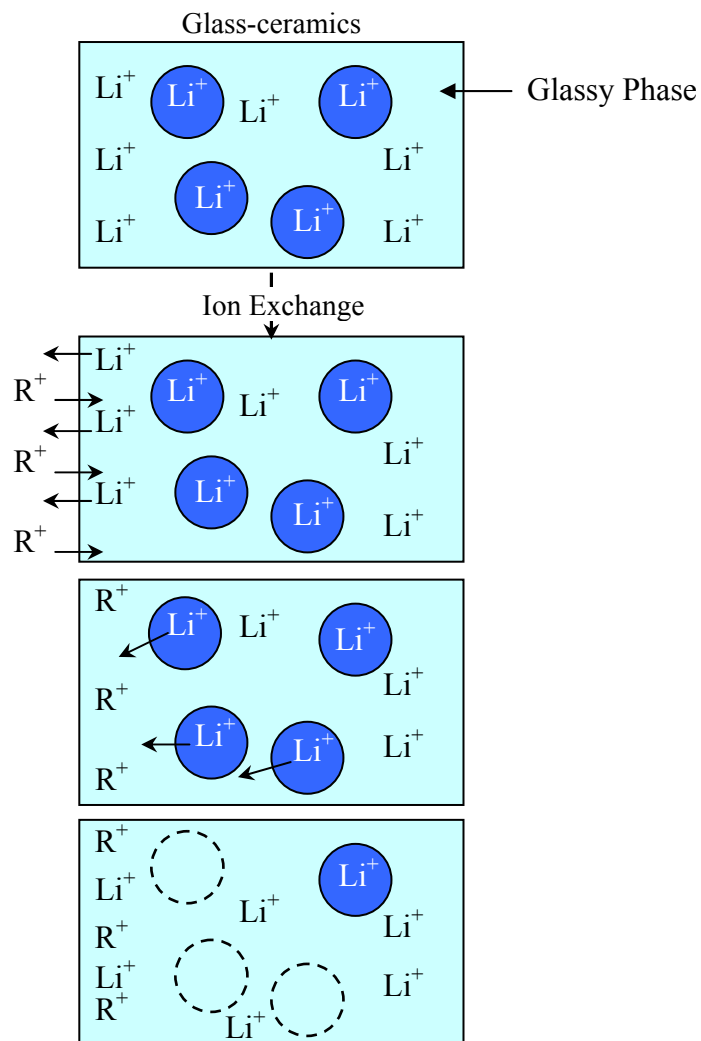


**Figure 4.13** Schematic representation of amorphization by ion exchange according to

Tagantsev and Karapetyan (1999),  $\bullet$ :  $\text{Li}_2\text{O}\cdot\text{SiO}_2$ ,  $\text{R}^+$ : alkali.



According to their idea, the “Amorphization” should not occur by the ion exchange reaction between foreign ions ( $\text{Na}^+$ ) and  $\text{Li}^+$  ion in  $\text{Li}_2\text{O}\cdot\text{SiO}_2$  and  $\text{Li}_2\text{O}\cdot 2\text{SiO}_2$  crystals directly without glassy phase.

In order to confirm the “Amorphization” of polycrystalline  $\text{Li}_2\text{O}\cdot 2\text{SiO}_2$  by ion exchange reaction,  $\text{Li}_2\text{O}\cdot 2\text{SiO}_2$  polycrystalline powder was synthesized by the conventional solid state reaction of silica and  $\text{Li}_2\text{CO}_3$  powder, and then ion exchange reaction was carried out in  $\text{NaNO}_3$  molten salts at  $550^\circ\text{C}$ . Figure 4.12 shows the XRD patterns of synthesized polycrystalline  $\text{Li}_2\text{O}\cdot 2\text{SiO}_2$  before and after  $\text{Li}^+\leftrightarrow\text{Na}^+$  ion exchange. The synthesized powder consists of  $\text{Li}_2\text{O}\cdot 2\text{SiO}_2$  crystal with a small amount of  $\text{Li}_2\text{O}\cdot\text{SiO}_2$  crystals. It is clearly observed that the X-ray intensity of  $\text{Li}_2\text{O}\cdot\text{SiO}_2$  and  $\text{Li}_2\text{O}\cdot 2\text{SiO}_2$  crystals decreases with the progress of ion exchange reaction. The  $\text{Li}_2\text{O}\cdot\text{SiO}_2$  crystal disappears in early stage of ion exchange. This indicates that the “Amorphization” occurs by ion exchange reaction.

The lattice constant of  $\text{Li}_2\text{O}\cdot 2\text{SiO}_2$  crystal in glass-ceramics before and after ion exchange was measured and the results are shown in Table 4.6. The unit cell volume of polycrystalline  $\text{Li}_2\text{O}\cdot 2\text{SiO}_2$  is slightly larger than that of JCPDS 40-0376. It seems that the polycrystalline  $\text{Li}_2\text{O}\cdot 2\text{SiO}_2$  forms solid solution with  $\text{SiO}_2$ . The average unit cell volume of  $\text{Li}_2\text{O}\cdot 2\text{SiO}_2$  crystal increases slightly for  $\text{Li}^+\leftrightarrow\text{K}^+$  exchange, whilst it decreases very slightly at first and increases later for  $\text{Li}^+\leftrightarrow\text{Na}^+$  exchange. The change in unit cell volume is quite small but is observed always in ion exchange, and this phenomenon consistent with Morimoto (1991) on the ion exchange of low thermal expansion transparent glass-ceramics based on  $\beta$ -quartz solid solution. This suggest that the ion exchange reaction takes place between foreign ions and  $\text{Li}^+$  ion in

$\text{Li}_2\text{O}\cdot 2\text{SiO}_2$  crystal. In fact, the chemical strengthening can be achieved in  $\text{Li}^+$  containing glass-ceramics by ion exchange at much higher temperature ( $800^\circ\text{C}$ ) (Uhlmann and Kreidl, 1980). However, the formation of  $\text{Li}_2\text{O}\cdot 2\text{SiO}_2$  solid solution crystal with  $\text{Na}^+$  might not be allowed by the ion exchange at lower temperature discussed here. Thus, the amorphization takes place eventually followed by the change in unit cell volume. It seems, therefore, that the replacement of  $\text{Li}^+$  ion in  $\text{Li}_2\text{O}\cdot 2\text{SiO}_2$  crystal by larger foreign ions results in the deformation of disilicate crystal structure and it causes the destruction of crystal structure in  $\text{Li}_2\text{O}\cdot 2\text{SiO}_2$  glass-ceramics.

Table 4.7 shows the crystal structure of three disilicate crystals. They have the same monoclinic structure but the lattice constant of these crystals is different significantly. The  $\text{Li}_2\text{O}\cdot 2\text{SiO}_2$  crystal has a layer structure ( $\text{Si}_2\text{O}_5$ ), which is very puckered (Wells, 1975), and  $\text{Li}^+$  ion places between layers. The ionic radius of these ions are  $0.68 \text{ \AA}$  ( $\text{Li}^+$ ),  $0.97 \text{ \AA}$  ( $\text{Na}^+$ ) and  $1.33 \text{ \AA}$  ( $\text{K}^+$ ), respectively. According to the ion exchange between crystals in glass-ceramics and molten salts (Beall and Duke, 1983), the unit cell volume of  $\text{Li}_2\text{O}\cdot 2\text{SiO}_2$  crystal should increase by  $\text{Li}^+ \leftrightarrow \text{Na}^+$  and  $\text{Li}^+ \leftrightarrow \text{K}^+$  exchange. However, the unit cell volume decreases by  $\text{Li}^+ \leftrightarrow \text{Na}^+$  exchange. This suggests that the cation site might be different.

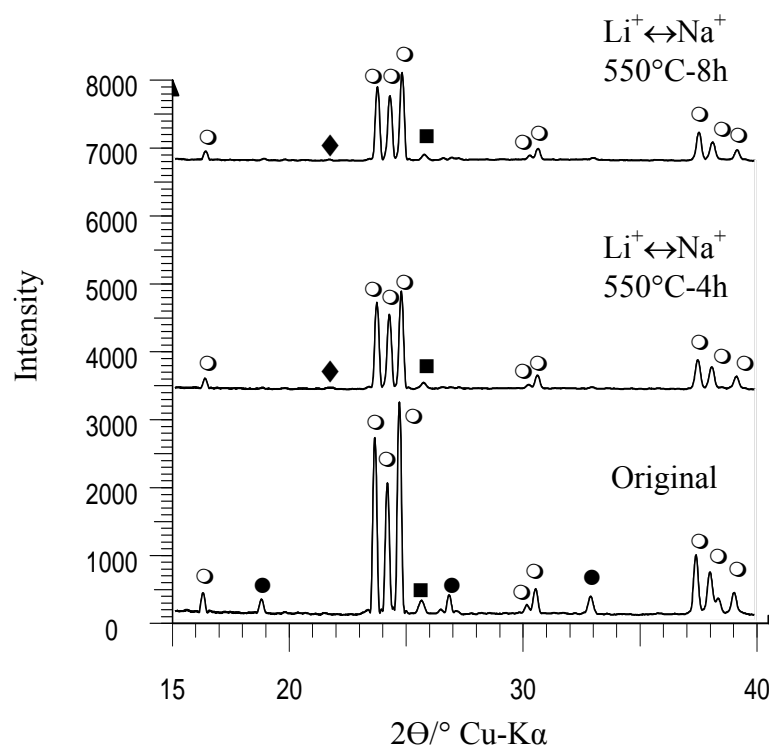


**Figure 4.14** XRD patterns of synthesized  $\text{Li}_2\text{O}\cdot 2\text{SiO}_2$  crystal before and after

$\text{Li}^+\leftrightarrow\text{Na}^+$  exchange at 550 °C. ○:  $\text{Li}_2\text{O}\cdot 2\text{SiO}_2$ , ●:  $\text{Li}_2\text{O}\cdot\text{SiO}_2$ , ◆:

Cristobalite, ■: Quartz.

**Table 4.6** Lattice constant of  $\text{Li}_2\text{O}\cdot 2\text{SiO}_2$  crystal before and after ion exchange.

Sample No.	a(Å)	b(Å)	c(Å)	$V_o(\text{Å})^3$
Original glass-ceramics	$5.87\pm 0.009$	$14.51\pm 0.026$	$4.80\pm 0.002$	$408.45\pm 0.72$
$\text{Li}^+\leftrightarrow\text{Na}^+$ 550 C-1 h.	$5.82\pm 0.017$	$14.53\pm 0.0034$	$4.81\pm 0.005$	$407.31\pm 1.23$
550 C-4 h.	$5.81\pm 0.020$	$14.61\pm 0.035$	$4.82\pm 0.004$	$408.87\pm 0.76$
$\text{Li}^+\leftrightarrow\text{K}^+$ 550 C-9 h.	$5.88\pm 0.020$	$14.53\pm 0.021$	$4.80\pm 0.003$	$409.97\pm 0.68$
550 C-16 h.	$5.88\pm 0.017$	$14.49\pm 0.039$	$4.80\pm 0.003$	$409.16\pm 0.31$
550 C-25 h.	$5.87\pm 0.025$	$14.53\pm 0.045$	$4.81\pm 0.006$	$409.68\pm 0.68$
JCPDS 40-0376	5.822	14.6	4.775	405.9

**Table 4.7** Crystal structure and lattice constant of alkali disilicate crystals.

Crystal	System	JCPDS	a(Å)	b(Å)	c(Å)	$\beta$ (Å)	V <sub>0</sub> (Å)
		No.					
Li <sub>2</sub> O·2SiO <sub>2</sub>	Momoclinic	40-0376	5.822	14.6	4.775	90.0	405.9
Na <sub>2</sub> O·2SiO <sub>2</sub>	Momoclinic	23-0529	12.329	4.848	8.133	104.2	471.2
K <sub>2</sub> O·2SiO <sub>2</sub>	Momoclinic	26-1331	9.72	25.26	14.24	90.0	3496.3

## CHAPTER V

### CONCLUSION

The chemical strengthening of  $\text{Li}_2\text{O}\cdot 2\text{SiO}_2$  transparent glass-ceramics was investigated and the following results were obtained.

1) The fracture strength of glass and glass-ceramics increased first and then decreased, and the crack formation and peeling of ion exchanged layer were observed for both  $\text{Li}^+ \leftrightarrow \text{Na}^+$  and  $\text{Li}^+ \leftrightarrow \text{K}^+$  ion exchange.

2) The volume change by  $\text{Li}^+ \leftrightarrow \text{Na}^+$  and  $\text{Li}^+ \leftrightarrow \text{K}^+$  ion exchange is very large. This large volume change causes the peeling and crack formation of ion exchanged layer in glass and glass-ceramics.

3) The maximum value of fracture strength of glass of  $251 \pm 13$  MPa was obtained by  $\text{Li}^+ \leftrightarrow \text{K}^+$  ion exchange at  $450^\circ\text{C}$  for 4 hours.

4) The maximum fracture strength of glass-ceramics of  $487 \pm 15$  MPa was obtained without surface crack by  $\text{Li}^+ \leftrightarrow \text{K}^+$  ion exchange at  $500^\circ\text{C}$  for 9 hours.

5) The fracture strength of glass decreases due to the cracks generated in unexchanged layer of glass with progress of ion exchange.

6) Submicroscopic flaws are not formed on the surface of unexchanged layer of glass-ceramics after ion exchange process. Nevertheless, the fracture strength of glass-ceramics was decreased due to the occurring of the stress relaxation.

Also, the amorphization phenomenon was investigated in  $\text{Li}_2\text{O}\cdot 2\text{SiO}_2$  crystal system transparent glass-ceramics by ion exchange and the following results were obtained.

1)  $\text{Li}_2\text{O}\cdot 2\text{SiO}_2$  crystals were disappeared with progress of  $\text{Li}^+ \leftrightarrow \text{Na}^+$  and  $\text{Li}^+ \leftrightarrow \text{K}^+$  ion exchange and this phenomenon was called as “Amorphization”.

2) The cristobalite precipitated and grew in  $\text{Li}_2\text{O}\text{-SiO}_2$  glass-ceramics with progress of  $\text{Li}^+ \leftrightarrow \text{Na}^+$  exchange.

3) The  $\text{Li}_2\text{O}\text{-SiO}_2$  crystal precipitated at first and disappeared again with progress of  $\text{Li}^+ \leftrightarrow \text{Na}^+$  exchange at 650 °C.

4) The unit cell volume of  $\text{Li}_2\text{O}\cdot 2\text{SiO}_2$  crystal increases slightly for  $\text{Li}^+ \leftrightarrow \text{K}^+$  exchange, whilst it decreases at first and increases later for  $\text{Li}^+ \leftrightarrow \text{Na}^+$  exchange. This suggests that the ion exchange between foreign ions and  $\text{Li}^+$  ions in  $\text{Li}_2\text{O}\cdot 2\text{SiO}_2$  crystal occurs directly.

5) The occurrence of Amorphization in  $\text{Li}_2\text{O}\text{-SiO}_2$  transparent glass-ceramics was due to the ion exchange between  $\text{K}^+$  or  $\text{Na}^+$  and  $\text{Li}^+$  in  $\text{Li}_2\text{O}\cdot 2\text{SiO}_2$  crystals directly.

## REFERENCES

- Abrams, M.B., Shen, J., and Green, D.J. (2004). Residual stress measurement in ion-exchanged glass by iterated birefringance and etching. **J. Testing Eval.** 32(2):1-7
- Andreev, N. S.(1978). Scattering of visible light by glasses undergoing phase separation and homogenization. **J. Non-Cryst. Solids.** 30:99-126.
- Arun, K. V. (1994). **Fundamental of inorganic glasses.** New York:Academic Press.
- Araujo, R. (2004). Thermodynamics of ion exchange. **J. Non-Cryst. Solids.** 349:230-233
- Beall, G.H., and Duke, D.A. (1969). Transparent glass-ceramics. **J. Mater. Sci.** 4: 340-52.
- Beall, G.H., Karstetter, B.R., and Rittler, H.L. (1967). Crystallization and chemical strengthening of stuffed  $\beta$ -quartz glass-ceramics. **J. Amer. Ceram. Soc.** 50 :99–108.
- Beall, G.H., and Pinckney, L.R. (1999). Nanophase glass-ceramics. **J. Amer. Ceram. Soc.** 82:5-16.
- Bach, H. (1995). **Low thermal expansion glass-ceramics.** Berlin:Springer.
- Clausbruch, S.C., Schweiger, M., Holand, W., and Rheinberger, V. (2000). The Effect of  $P_2O_5$  on the crystallization and microstructure of glass-ceramics in the  $SiO_2-Li_2O-K_2O-ZnO-P_2O_5$  system. **J. Non-Cryst. Solids.** 263&264:388-394.

- Duke, D. A., Macdowell, J. F., and Karstetter, B. R. (1967). Crystallization and chemical strengthening of nepheline glass-ceramics. **J. Amer. Ceram. Soc.**, 50:77-81.
- Garfinkel, H. M. (1980). Chemical strengthening of glass. In D. R. Uhlmann and N. J. Kreidl (eds). **Glass Science and Technology**. 5:253.
- Headley, T.J., and Loehman, R.E. (1984). The crystallization of a glass-ceramics by epitaxial-growth. **J. Amer. Ceram. Soc.** 67:620.
- Hench, L.L., Freiman, S.W., and Kinser, D.L. (1971). The Early stages of crystallization in a  $\text{Li}_2\text{O}-2\text{SiO}_2$  Glass,” *Phys. Chem. Glasses*. **Phys. Chem. Glasses**. 12:58-63.
- Hood, K.P., and Stookey, S.D. (1957). Method of making a glass article of high mechanical strength and article made thereby. **US Patent No 2779136** (Unpublished manuscript)
- Hopper, R.W.(1985). “Stochastic Theory of Scattering from Idealized Spinodal Structure”. **J. Non-Cryst. Solids**. 70:111-142.
- Igbal, Y., James, P.F., Jais, U.S., Jordery, S., and Lee W.E. (1998). Crystallisation of silicate and phosphate glasses. **J. Non-Cryst. Solids**. 219:17-29.
- Izumitani, T. (Ed.). (1984). “**New Glasses And Their Properties**”. Tokyo:Kei-ei System Kenkyu-sho.[in Japanese].
- Jacquin, J.R., and Tomozawa, M. (1995). Crystallization of lithium metasilicate from lithium disilicate. **J. Non-Cryst. Solids**.190:233-237.
- James, P.F. (1982). Nucleation and crystallization in glasses. In J.H. Simmons, D.R. Uhlmann and G.H. Beall (eds). **Advances in ceramics**. Columbus:American Ceramic Society.



- Kalinina, A., and Filipovich, V. N. (1964). The structure of glass-catalyzed crystallization of glass. In E.A. Porai-Koshits (Ed.). **The structure of glass**. New York:Consultan Bureau.3:53.
- Karstetter, B.R., and Voss, R.O. (1967). Chemical strengthening of glass-ceramics in the system  $\text{Li}_2\text{O}-\text{Al}_2\text{O}_3-\text{SiO}_2$ . **J. Amer. Ceram. Soc.**50:133-137.
- Kerker, M. (1969). **The scattering of light**. New York:Academic Press.
- Kingery, W.D., Bowen, H.C., and Uhlmann, D.R. (1976). **Introduction to Ceramics** (2<sup>nd</sup> ed):New York John:Wiley and Sons.
- Kistler, S. S. (1962). Stresses in glass produced by non-uniform exchange of monovalent ions. **J. Am. Ceram. Soc.** 45:59-68.
- Mallick ,K.K., and Holland, D. (2004). Strengthening of container glasses by ion-exchange dip coating. **J. Non-Cryst. Solids**. 351:2524-2536.
- McMillan, P.W. (1979). **Glass-Ceramics**. London:Academic Press.
- Mishima et al. (2004). Nucleation Behavior of  $\text{Li}_2\text{O}-\text{Na}_2\text{O}-\text{SiO}_2$  glass doped with platinum. **J. Ceram. Soc. Japan**.112:350-353.
- Morimoto, S. (1991). Research on Functionnal Glasses through Phase Separation and Crystalization.**Ph. D. Thesis**, Tokyo University, Japan.
- Morimoto, S. (2004). Formation, absorption and emission spectra of  $\text{Cr}^{4+}$  ions in  $\text{Li}_2\text{O}-\text{SiO}_2$  system transparent glass-ceramics. **J. Ceram. Soc. Japan**. 112: pp.486-490.
- Morimoto, S., and Emem, W. (2004). Strength of  $\text{Li}_2\text{O}-\text{SiO}_2$  system transparent glass-Ceramics. **J. Ceram. Soc. Japan**, 112, pp.259-62.
- Morimoto, S. (2006). Effect of  $\text{K}_2\text{O}$  on the crystallization in  $\text{Li}_2\text{O}-\text{SiO}_2$  system of glass. **J. Ceram. Soc. Japan**.114(2):195-198.

- Nitta, I. (1975). **X-ray Crystallography**. Tokyo:Maruzen. 1: 489.
- Ohlberg, S. M., and Strickler, D. W. (1962). Determination of percent crystallinity of partly devitrified glass by X-ray diffraction. **J. Am. Ceram. Soc.** 45 (4):170–171.
- Pinkney, L.R. (2001). Glass ceramics. **Encyclopedia of Materials Science and Technology**. 4:3535-3540
- Reinhart, D.W. (1980). Ion exchange strengthening of soda-lime-silica glass. **US Patent No 4192689** (Unpublished manuscript)
- Soares, Jr., Zanotto, E. D., Fokin, V. M., and Jain, H. (2003). TEM and XRD study of early crystallization of lithium disilicate glasses. **J. Non-Cryst. Solids**. 331:217-227.
- Stookey, S.D. (1954). Recent Developments in Radiation Sensitive Glasses. **Ind. Eng. Chem.** 46:174-176.
- Strnad, Z. (1986). **Glass-Ceramic Materials**. Amsterdam:Elsevier.
- Tagantsev, D.K., and Karapetyan, G.O. (1999). Decrystallization of crystallized glass by ion exchange. **J. Non-Cryst. Solids**. 255:185-92.
- Uhlmann, D.R. and Kreidl, N.J. (1980). **Glass Science and Technology**. London:Academic Press.5:254-255.
- Weber, N.(1965). Strengthened glass article and method of producing same. **US Patent No 3218220** (Unpublished manuscript).
- Wells, A.F. (1975). **Structural Inorganic Chemistry** (4th ed.). Oxford:Clarendon Press.
- West, A.R. and Glasser, F.P. (1971). **Advances in nucleation and crystallization in glasses**. Columbus:American Ceramic Society.

- Wu, X., Yuan, H., Yen, W.M., and Aitken, B.G. (1996). Compositional dependence of the luminescence from Cr<sup>4+</sup>-doped calcium aluminate glass. **J. Luminescence**, 66&67:285-89.
- Zijlstra, A. L., and Burggraaf, A. J. (1968). Fracture phenomena and strength properties of chemically and physically strengthened glass. **J. Non-Crystalline Solids** 1:49-68.

## **APPENDIX A**

### **THE CALCULATION OF LATTICE CONSTANT**

Si powder (JCPDS 027-1402) was used as an internal standard for the measurement of lattice constant.

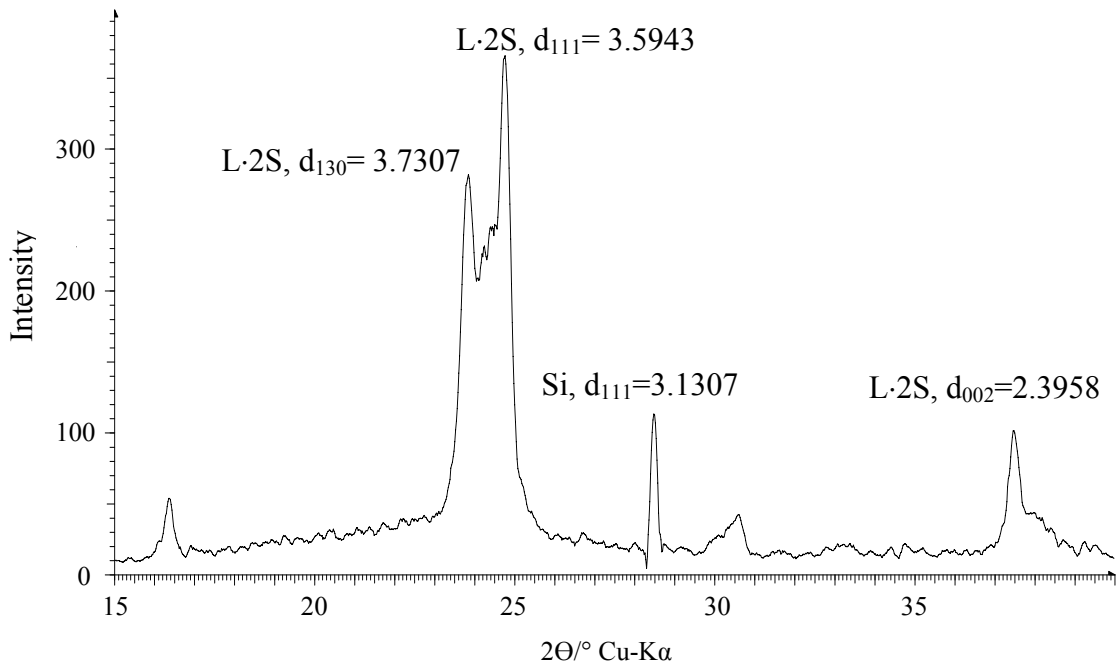


**Figure A1** XRD pattern of  $\text{Li}_2\text{O}\cdot 2\text{SiO}_2$  glass-ceramics (500°C-15h, 700°C-15h)

$$\Delta d = d_{111} (\text{Si, JCPDS 27-1402}) - d_{111} (\text{Si, Observed})$$

$$\Delta d = 3.1355 - 3.1307$$

$$\Delta d = 0.0048 \text{ \AA}$$

The lattice constant of lithium disilicate ( $\text{Li}_2\text{O}\cdot 2\text{SiO}_2$ ) as monoclinic system was calculated as follow

$$\frac{1}{d^2} = \frac{h^2}{a^2 \sin^2 \beta} + \frac{k^2}{b^2} + \frac{l^2}{c^2 \sin^2 \beta} - \frac{2hl \cos \beta}{ac \sin^2 \beta} \quad (\text{A1})$$

Where

$$\beta = 90^\circ \text{ (JCPDS 40-0376).}$$

$$(hkl) = (130);$$

$$d_{130} = d_{130}(\text{Observed}) + \Delta d$$

$$d_{130} = 3.731 + 0.0048$$

$$d_{130} = 3.7358 \text{ \AA}$$

$$\frac{1}{3.7358^2} = \frac{1^2}{a^2} + \frac{3^2}{b^2} + \frac{0^2}{c^2} \quad (\text{A2})$$

$$(hkl) = (111);$$

$$d_{111} = d_{111}(\text{Observed}) + \Delta d$$

$$d_{111} = 3.5943 + 0.0048$$

$$d_{111} = 3.5991 \text{ \AA}$$

$$\frac{1}{3.5991^2} = \frac{1^2}{a^2} + \frac{1^2}{b^2} + \frac{1^2}{c^2} \quad (\text{A3})$$

$$(hkl) = (002);$$

$$d_{002} = d_{002}(\text{Observed}) + \Delta d$$

$$d_{002} = 2.3958 + 0.0048$$

$$d_{002} = 2.4006 \text{ \AA}$$

$$\frac{1}{2.4006^2} = \frac{0^2}{a^2} + \frac{0^2}{b^2} + \frac{2^2}{c^2} \quad (\text{A4})$$

From equation (1), (2), (3)

$$a = 5.8629 \text{ \AA}$$

$$b = 14.5397 \text{ \AA}$$

$$c = 4.8014 \text{ \AA}$$

The volume  $V$  of the unit cell of lithium disilicate ( $\text{Li}_2\text{O}\cdot 2\text{SiO}_2$ ) as monoclinic system was calculated as follow

$$V = abcsin\beta \quad (\text{A5})$$

$$V = (5.8629)(14.5397)(4.8014)\sin 90^\circ$$

$$V = 409.2991 \text{ (\AA)}^3$$

## **APPENDIX B**

### **THE CALCULATION OF CRYSTALLITE SIZE**

#### **BY X-RAY DIFFRACTION TECHNIQUE**



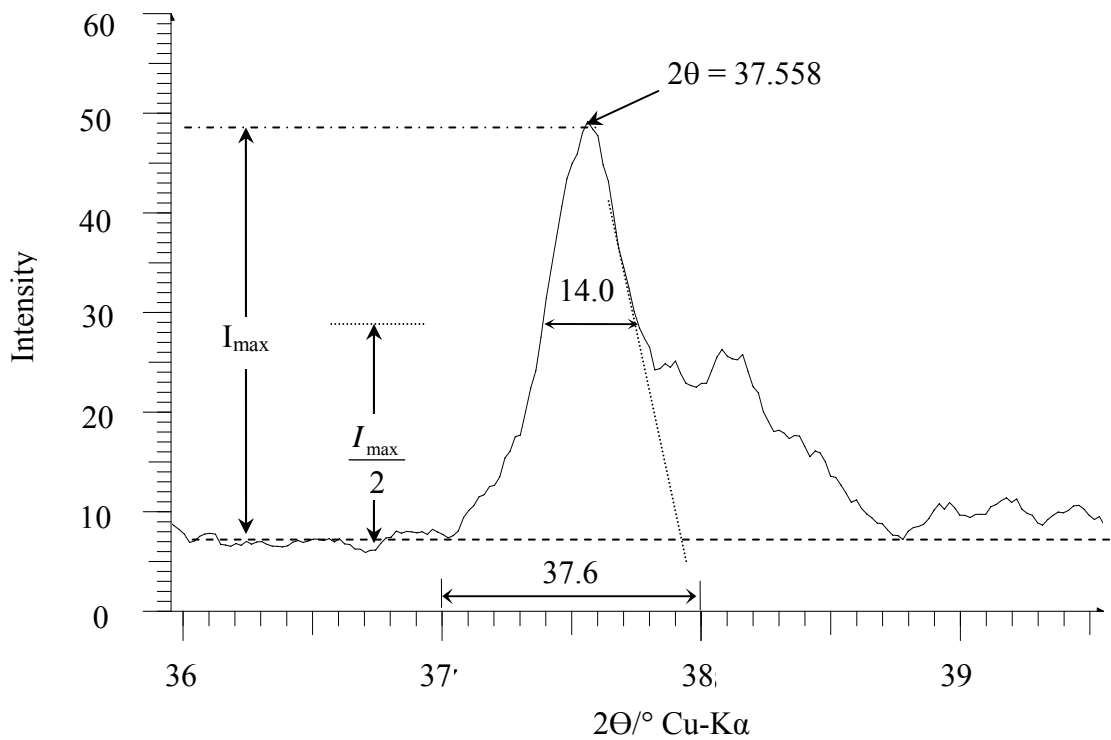


**Figure B1** XRD pattern of transparent  $\text{Li}_2\text{O-SiO}_2$  glass-ceramics (500°C-15h, 700°C-10h).

From above Figure,

$$\text{Observed line broadening} = \frac{14.0}{37.6} = 0.372^\circ$$

By Jone's Method,

Observed line broadening  $\rightarrow$  True line broadening (Figure B2)

$$0.372^\circ \rightarrow 0.220^\circ$$

$$\frac{0.22^\circ}{360^\circ} = \frac{\beta}{2\pi}$$

$$\beta = 0.00384 \text{ radian}$$

$$2\theta = 37.558^\circ$$

$$\theta = 18.779^\circ$$

Crystalline size was calculated using Scherrer's equation.

$$D = \frac{0.9 \cdot \lambda}{\beta \cos \theta} \quad (\text{B1})$$

Where

D = crystalline size (nm).

$\lambda$  = wavelength of X-ray (1.54Å).

$\beta$  = true half width (radian).

$\theta$  = diffraction angle (degree).

From equation (B1),

$$\begin{aligned} D &= \frac{0.9 \times 1.54}{0.00384 \cos 18.779^\circ} \\ &= 381 \text{ \AA} \\ &= 38.1 \text{ nm} \end{aligned}$$

X-ray Line Broadening For AgCl Precipitated In Glass

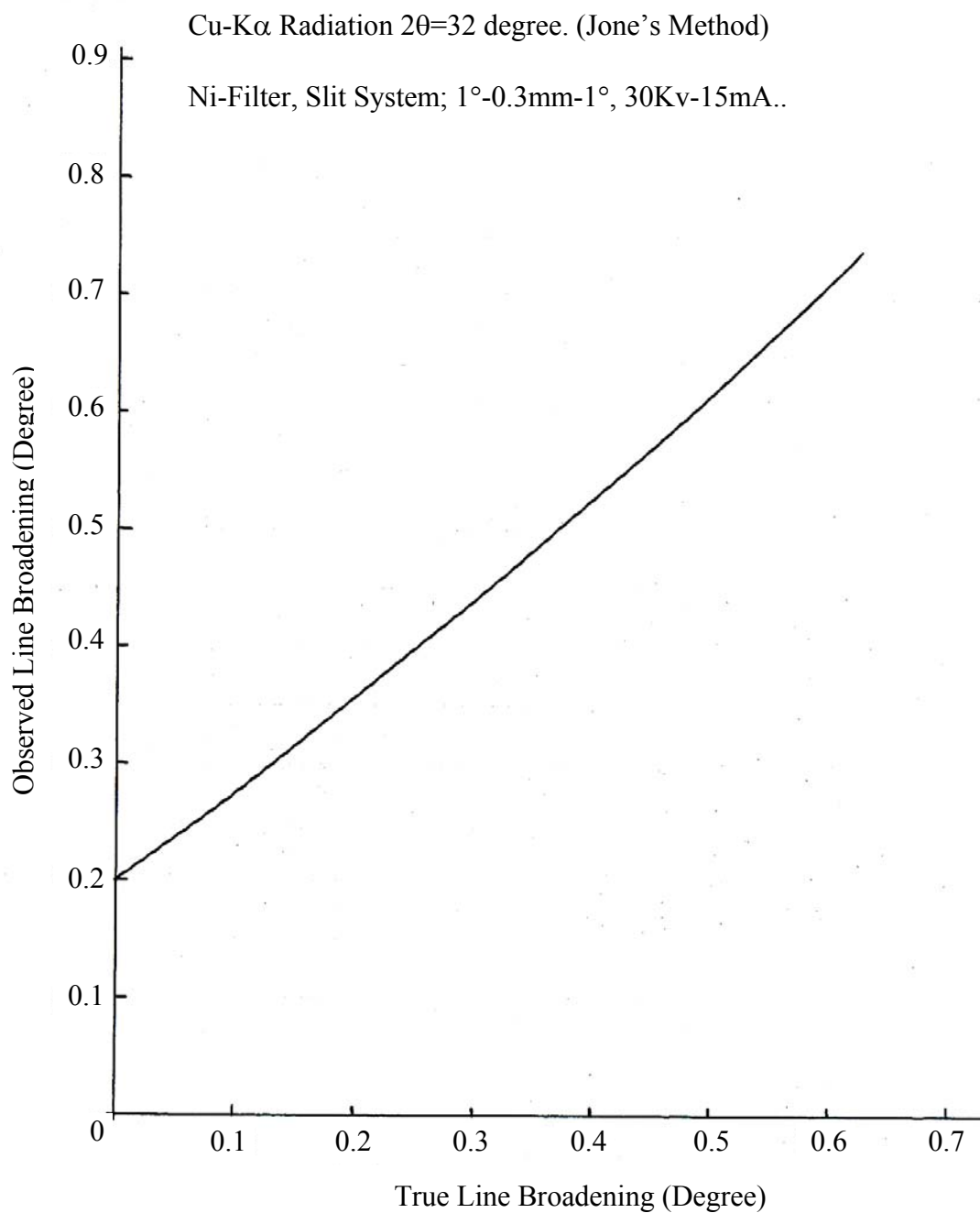


**Figure B2** Calibration curve of X-ray line broadening for AgCl precipitated in glass by Jone's method (Nitta, 1975).

## **APPENDIX C**

### **THE CALIBRATION CURVE OF $\text{Li}_2\text{O}\cdot 2\text{SiO}_2$ GLASS**

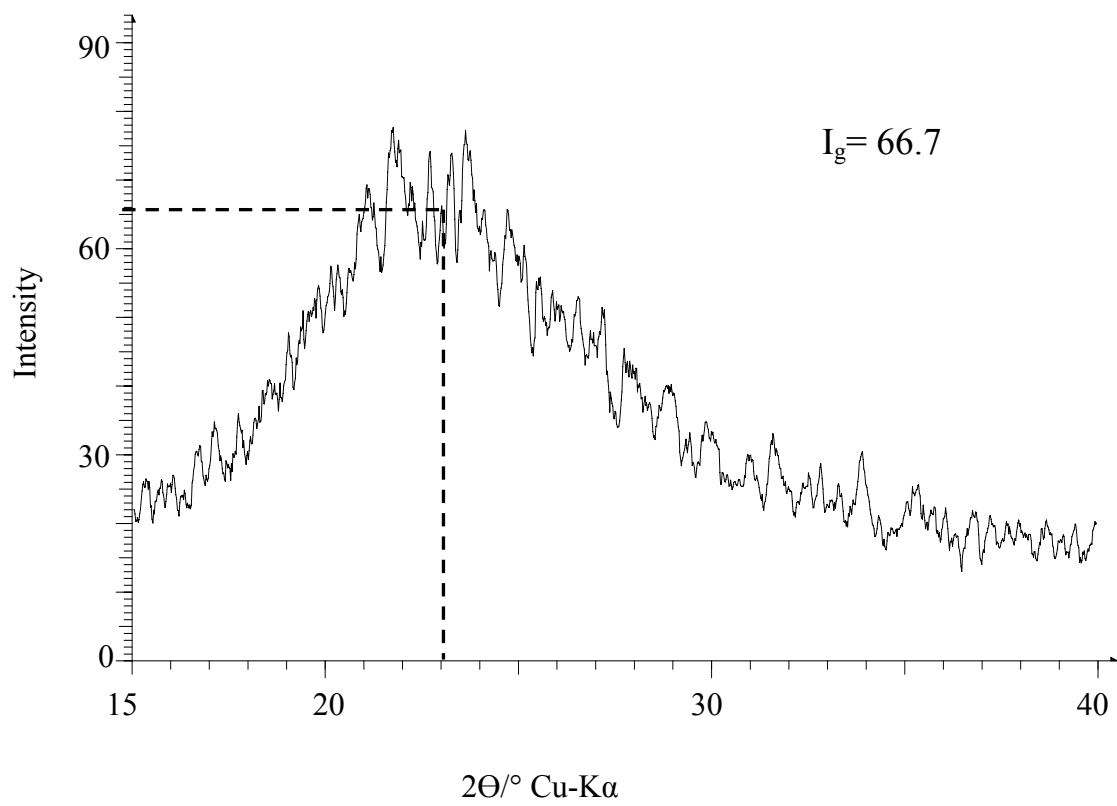


**Figure C1** XRD pattern of  $\text{Li}_2\text{O-SiO}_2$  glass (100% Glass)

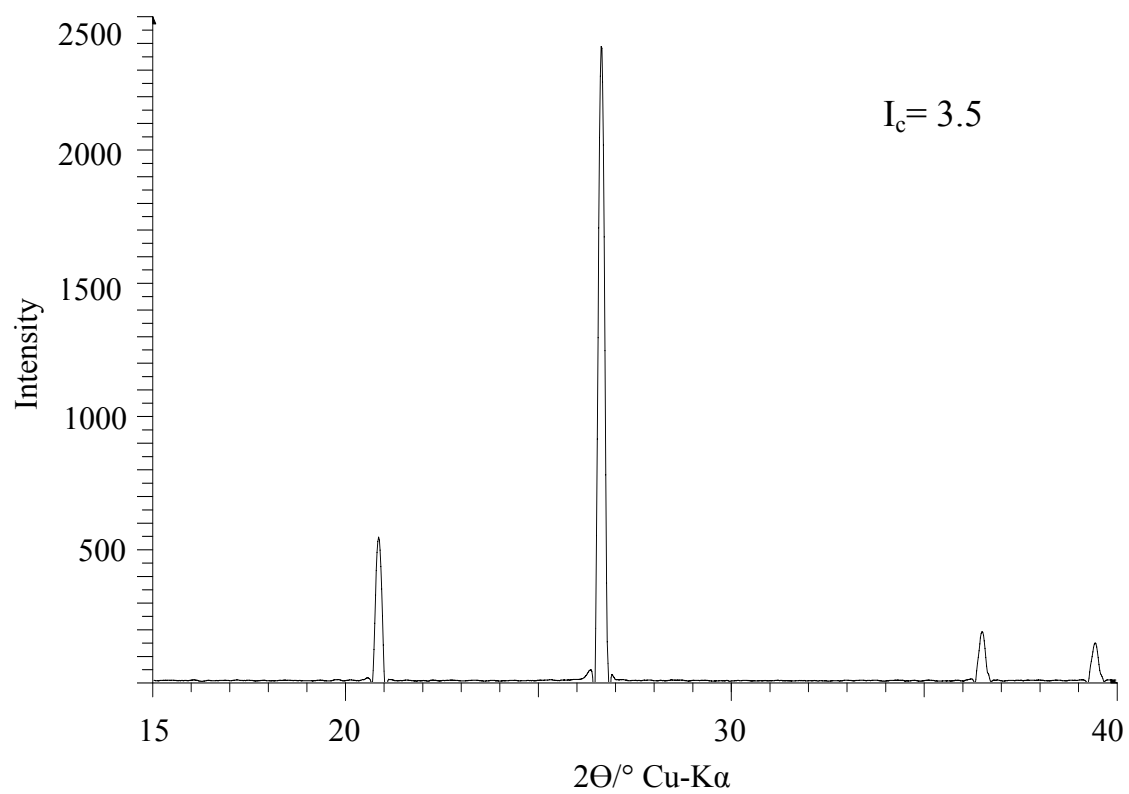


**Figure C2** XRD pattern of Quartz (100% Crystal)

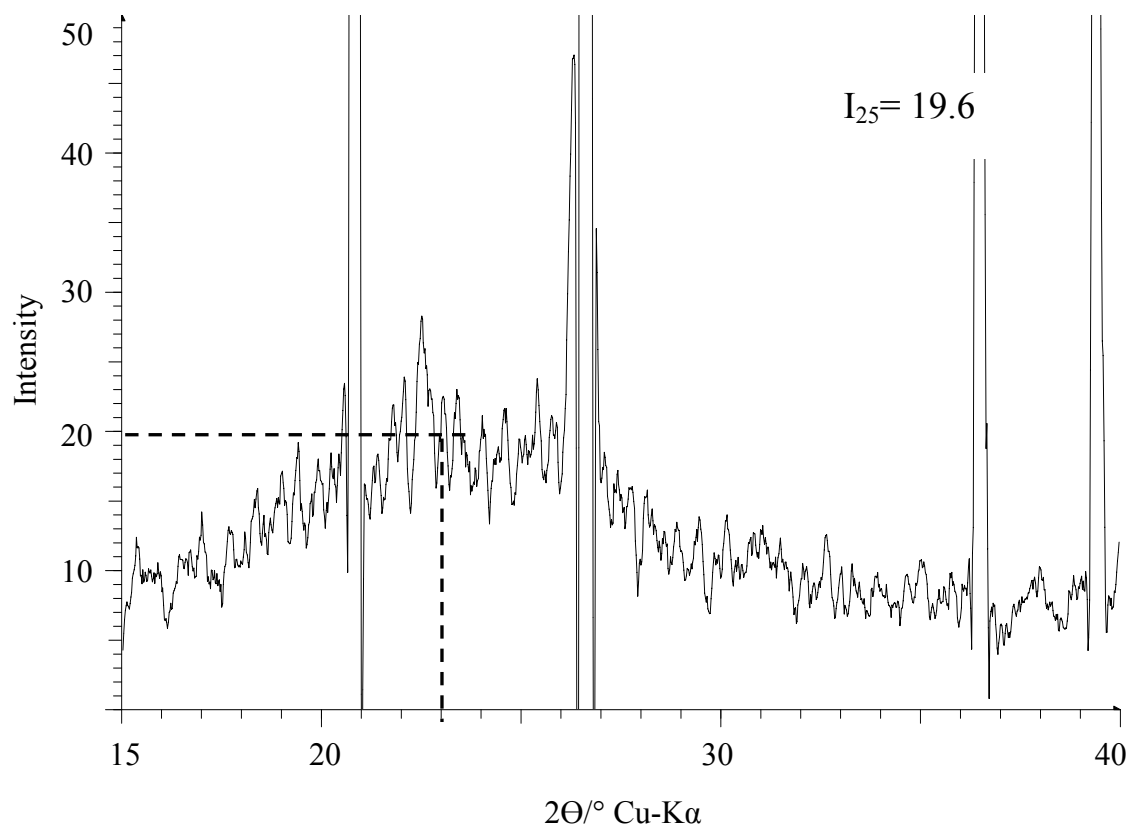


**Figure C3** XRD pattern of 25% Li<sub>2</sub>O-SiO<sub>2</sub> glass + 75% Quartz.

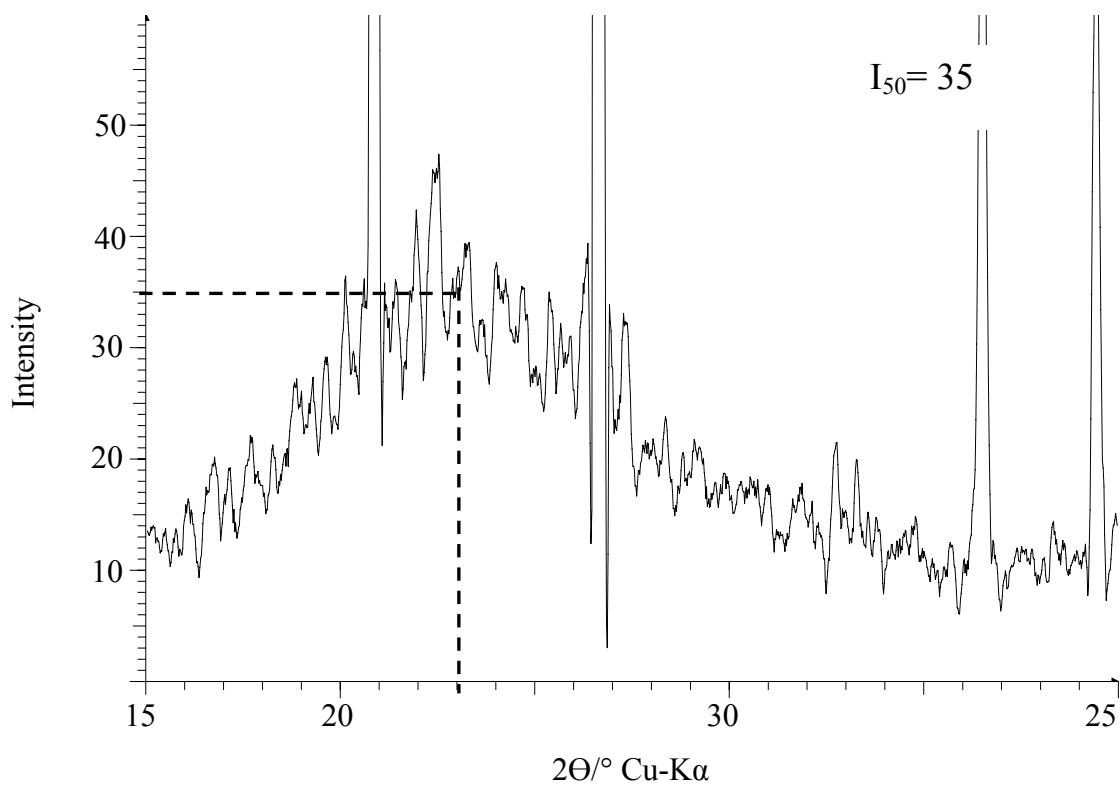


**Figure C4** XRD pattern of 50% Li<sub>2</sub>O-SiO<sub>2</sub> glass + 50% Quartz



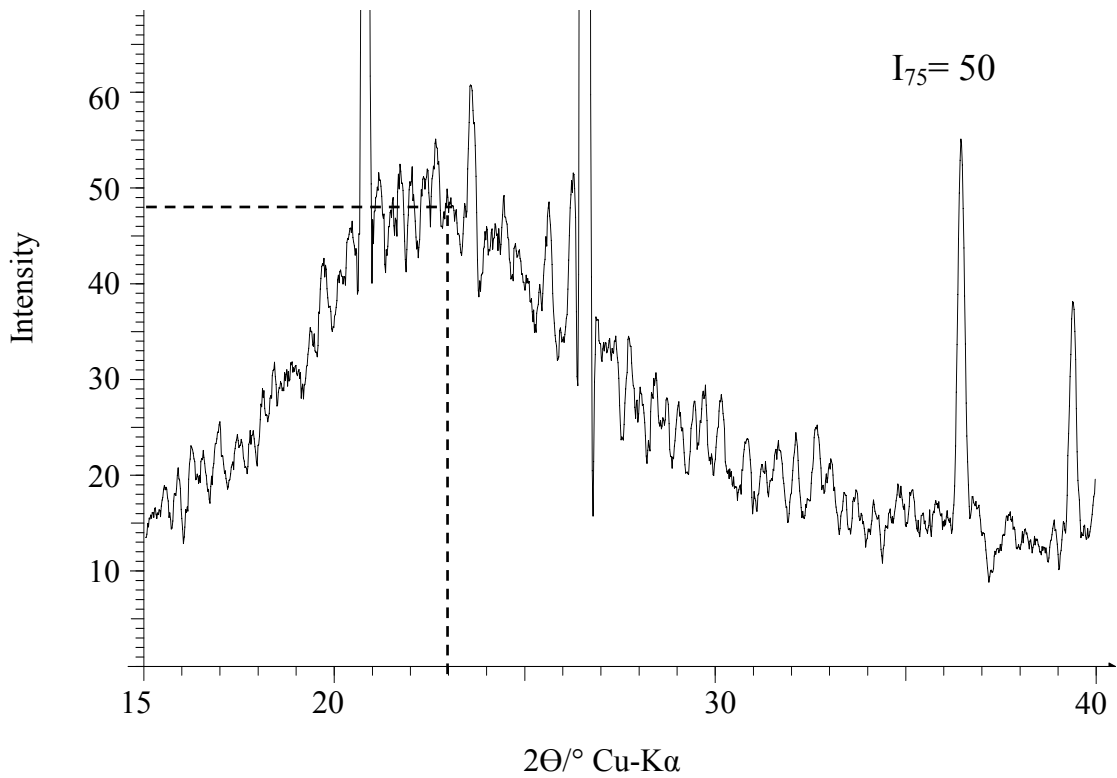


**Figure C5** XRD pattern of 75%  $\text{Li}_2\text{O-SiO}_2$  glass + 25% Quartz

Percent crystallinity was determined using Ohlberg and Strickler's method (Ohlberg and Strickler, 1962) and was calculated using by

$$\text{Percent crystallinity}(\%C) = \frac{(I_g - I_x)}{(I_g - I_c)} \times 100 \quad (\text{C1})$$

Where

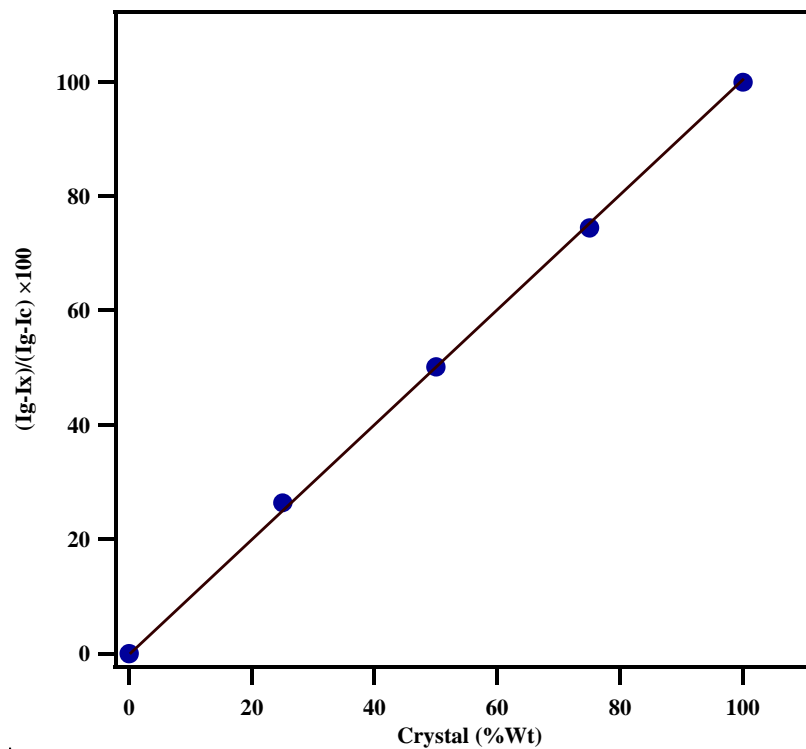
$I_g$  is the X-ray intensity of glass at  $2\theta=23^\circ$ .

$I_x$  is the X-ray background intensity of the mixtures at  $2\theta=23^\circ$ .

$I_c$  is the X-ray background intensity of the Quartz at  $2\theta=23^\circ$ .

**Table C1** The calculation of crystallinity using Ohlberg and Strickler's method.

Mixture		$I_g$	$I_c$	$I_x$	$\frac{I_g - I_x}{I_g - I_c} \times 100$
Glass	Quartz				
100	0	66.7	3.5	66.7	0
75	25	66.7	3.5	19.6	74.53
50	50	66.7	3.5	35	50.16
25	75	66.7	3.5	50	26.42
0	100	66.7	3.5	3.5	100

**Figure C6** Experimental determined crystallinity VS calculated crystallinity for mechanical mixtures of  $\alpha$ -quartz and parent glass.

## **APPENDIX D**

**THE CALCULATION OF DENSITY, MOLAR VOLUME**

**AND THERMAL EXPANSION COEFFICIENT OF**

**$\text{Li}_2\text{O}\cdot 2\text{SiO}_2$  GLASS**

**Table D1** The Calculation of density, molar volume and thermal expansion coefficient Li<sub>2</sub>O-SiO<sub>2</sub> glass.

Composition				Molar Volume (cm <sup>3</sup> /mol)		Thermal expansion coefficient (10 <sup>-7</sup> )	
Oxide	Wt %	Mole	Mole Fraction X <sub>i</sub>	Volume V <sub>i</sub>	V <sub>i</sub> ×X <sub>i</sub>	α <sub>i</sub>	α <sub>i</sub> ×X <sub>i</sub>
SiO <sub>2</sub>	80	1.332	0.728	26.30	19.15	32.2	23.44
Al <sub>2</sub> O <sub>3</sub>	4	0.039	0.022	40.40	0.89	-30	-0.66
Li <sub>2</sub> O	13	0.435	0.238	11.00	2.62	270	64.26
P <sub>2</sub> O <sub>5</sub>	3	0.021	0.012	59.5	0.71	140	1.68
<b>Total</b>	100	1.827	1	V <sub>glass</sub> =	23.37	α <sub>glass</sub> =	88.72
<b>Weight</b> of glass = $\frac{100}{1.827} = 54.74$ g/mol				<b>Density</b> of glass = $\frac{54.74}{23.37} = 2.34$ g/cm <sup>3</sup>			

**Table D2** The Calculation of density, molar volume and thermal expansion coefficient of Na<sub>2</sub>O-SiO<sub>2</sub> glass.

Composition				Molar Volume (cm <sup>3</sup> /mol)		Thermal expansion coefficient (10 <sup>-7</sup> )	
Oxide	Wt %	Mole	Mole Fraction, X <sub>i</sub>	Volume V <sub>i</sub>	V <sub>i</sub> ×X <sub>i</sub>	α <sub>i</sub>	α <sub>i</sub> ×X <sub>i</sub>
SiO <sub>2</sub>	70.2	1.169	0.728	26.30	19.15	32.2	23.44
Al <sub>2</sub> O <sub>3</sub>	3.5	0.035	0.022	40.40	0.89	-30	-0.66
Na <sub>2</sub> O	23.7	0.382	0.238	20.2	4.76	395	94.01
P <sub>2</sub> O <sub>5</sub>	2.6	0.019	0.012	59.5	0.72	140	1.68
<b>Total</b>	100	1.605	1	V <sub>glass</sub> =	25.52	α <sub>glass</sub> =	118.47
<b>Weight</b> of glass = $\frac{100}{1.605} = 62.31$ g/mol				<b>Density</b> of glass = $\frac{62.42}{26.58} = 2.44$ g/cm <sup>3</sup>			

**Table D3** The Calculation of density, molar volume and thermal expansioncoefficient of K<sub>2</sub>O-SiO<sub>2</sub> glass.

Composition				Molar Volume (cm <sup>3</sup> /mol)		Thermal expansion coefficient (10 <sup>-7</sup> )	
Oxide	Wt %	Mole	Mole Fraction X <sub>i</sub>	Volume V <sub>i</sub>	V <sub>i</sub> ×X <sub>i</sub>	α <sub>i</sub>	α <sub>i</sub> ×X <sub>i</sub>
SiO <sub>2</sub>	62. 5	1.041	0.728	26.80	23.35	32.2	23.44
Al <sub>2</sub> O <sub>3</sub>	3.1	0.031	0.022	40.40	1.01	-30	-0.66
K <sub>2</sub> O	32. 0	0.340	0.238	34.1	3.07	465	110.67
P <sub>2</sub> O <sub>5</sub>	2.4	0.017	0.012	59.5	0.833	140	1.68
<b>Total</b>	100	1.429	1	V <sub>glass</sub> =	28.26	α <sub>glass</sub> =	135.13
<b>Weight</b> of glass = $\frac{100}{1.429} = 69.98$ g/mol				<b>Density</b> of glass = $\frac{69.98}{28.26} = 2.48$ g/cm <sup>3</sup>			

**Figure D4** Property factor of oxide in glass composition by A.A. Appen (Volf, 1988).

Oxide	Formula weight (g/mol)	Volume $V_i$ (cm <sup>3</sup> /mol)	Refractive Index $\eta_i$	Mean Dispersion $\delta_i$	Thermal Expansion $\alpha_i$ ( $10^{-7}$ ) 20-400°C	Elastic Modulus $E_i^*$ (GPa)	Modulus of rigidity $G_i^*$ (GPa)	Dielectric Constant $\epsilon_i^{**}$	Surface Tension $\sigma_i^{***}$ (dyn/cm)	Range Mol%
SiO <sub>2</sub>	60.06	27.25-26.10	1.459-1.475	675	5-38	7.15-6.5	3.0-2.7	3.8	290	100-45
TiO <sub>2</sub>	79.9	20.5	2.08-2.23	5000-6200	-15~30	17.1	6.95	25.5	250	0-25
ZrO <sub>2</sub>	123.2	-	2.17	-	-60	-	-	-	350	0-15
SnO <sub>2</sub>	150.7	-	-	-	-45	-	-	-	350	0-10
B <sub>2</sub> O <sub>3</sub>	69.6	18.5-38.0	1.46-1.71	640-900	-50~0	1.0-18.0	0-7.5	3-8	-	0-30
Al <sub>2</sub> O <sub>3</sub>	101.9	40.4(30.0)	1.52(1.70)	850	-30	11.4	4.95	9.2	580	0-20
Cr <sub>2</sub> O <sub>3</sub>	152.0	-	-	-	-	-	-	-	-	0-5
Sb <sub>2</sub> O <sub>3</sub>	291.5	-	2.55	7700	75	-	-	-	-	0-5
BeO	25.0	7.8	1.595	890	45	10.9	4.6	13.8	390	0-30
MgO	40.3	12.5(13.5)	1.61(1.57)	1110	60	9.2	3.8	15.4	520	0-25
CaO	56.1	14.4	1.73	1480	130	11.15	4.95	17.4	510	0-25
SrO	103.6	18.0	1.77	1630	160	9.65	4.5	18.0	490	0-30
BaO	153.4	22.0	1.88	1890	200	6.25	1.75	20.5	470	0-40
ZnO	81.4	14.5	1.71	1650	50	6.0	2.90	14.4	450	0-20
CdO	128.4	17.0-18.2	1.805-1.925	2270-2930	115	5.7	2.75	17.2	430	0-20
PbO	223.2	21.0-23.5	2.15-2.35	5280-7400	130-190	4.3	1.45	22.0	-	0-50
MnO	70.9	-	-	-	105	6.1	2.6	13.8	390	0-25
FeO	71.8	-	-	-	55	5.2	1.9	16.0	490	0-20
CoO	74.9	-	-	-	50	8.5	3.65	15.2	430	0-20

Oxide	Formula weight	Volume $V_i$ (cm <sup>3</sup> /mol)	Refractive Index $\eta_i$	Mean Dispersion $\delta_i$	Thermal Expansion $\alpha_i$ (10 <sup>-7</sup> ) 20-400°C	Elastic Modulus $E_i^*$ (GPa)	Modulus of rigidity $G_i^*$ (GPa)	Dielectric Constant $\epsilon_i^{**}$	Surface Tension $\sigma_i^{***}$ (dyn/cm)	Range Mol%
NiO	74.7	-	-	-	50	12.9	5.0	13.4	400	0-15
CuO	79.6	-	-	-	30	-	-	-	-	0-10
Li <sub>2</sub> O	29.9	11.0(11.9)	1.695(1.655)	1380(1300)	270(270)	8.0(10.5)	3.0(4.0)	14.0(15.0)	295	0-30
Na <sub>2</sub> O	62.0	20.2(20.6)	1.59(1.575)	1420(1400)	395(410)	5.95(4.7)	1.75(1.5)	17.6(17.6)	295	0-25
K <sub>2</sub> O	94.2	34.1*(33.5)	1.575*(1.595)	1300*(1320)	465*(500)	4.1(-1.0)	1.1(-0.5)	16.0(20.3)	-	0-20
Cs <sub>2</sub> O	281.8	-	1.7(1.74-1.8)	-	-	-	-	-	-	0-10
P <sub>2</sub> O <sub>5</sub>	142.0	59.5	-	-	140	-	-	-	-	0-10
UO <sub>2.7</sub>	280.8	-	-	-	20	-	-	-	-	0-10
CaF <sub>2</sub>	78.1	-	-	-	180	-	-	-	420	0-15
Na <sub>2</sub> SiF <sub>6</sub>	188.1	-	-	-	340	-	-	-	-	0-8
Na <sub>3</sub> AlF <sub>6</sub>	210.0	-	-	-	480	-	-	-	-	0-8
CdS	144.5	-	-	-	200	-	-	-	-	0-5

Bracket () of Al<sub>2</sub>O<sub>3</sub> can be applied to the glasses containing no strong basic oxide (alkali, BaO and SrO).

Bracket () of MgO is abnormal value, and can be applied to only narrow region of Na<sub>2</sub>O(K<sub>2</sub>O)-MgO-SiO<sub>2</sub> system.

Bracket () of R<sub>2</sub>O can be applied to R<sub>2</sub>O-SiO<sub>2</sub> system (R<sub>2</sub>O<30mol%)

Symbol \* of K<sub>2</sub>O can be applied to Na<sub>2</sub>O containing glass. For a practical glass: V=34.5,  $\eta_i = 1.560$ ,  $\delta_i = 1250$ ,  $\alpha_i=425$ .

\*:  $\times 10^{-3}$  Kg/mm<sup>2</sup>, \*\*: at  $4.5 \times 10^8$ Hz, \*\*\*: at 1300°C.

## **APPENDIX E**

# **THE CALCULATION OF NORMALIZED X-RAY INTENSITY**



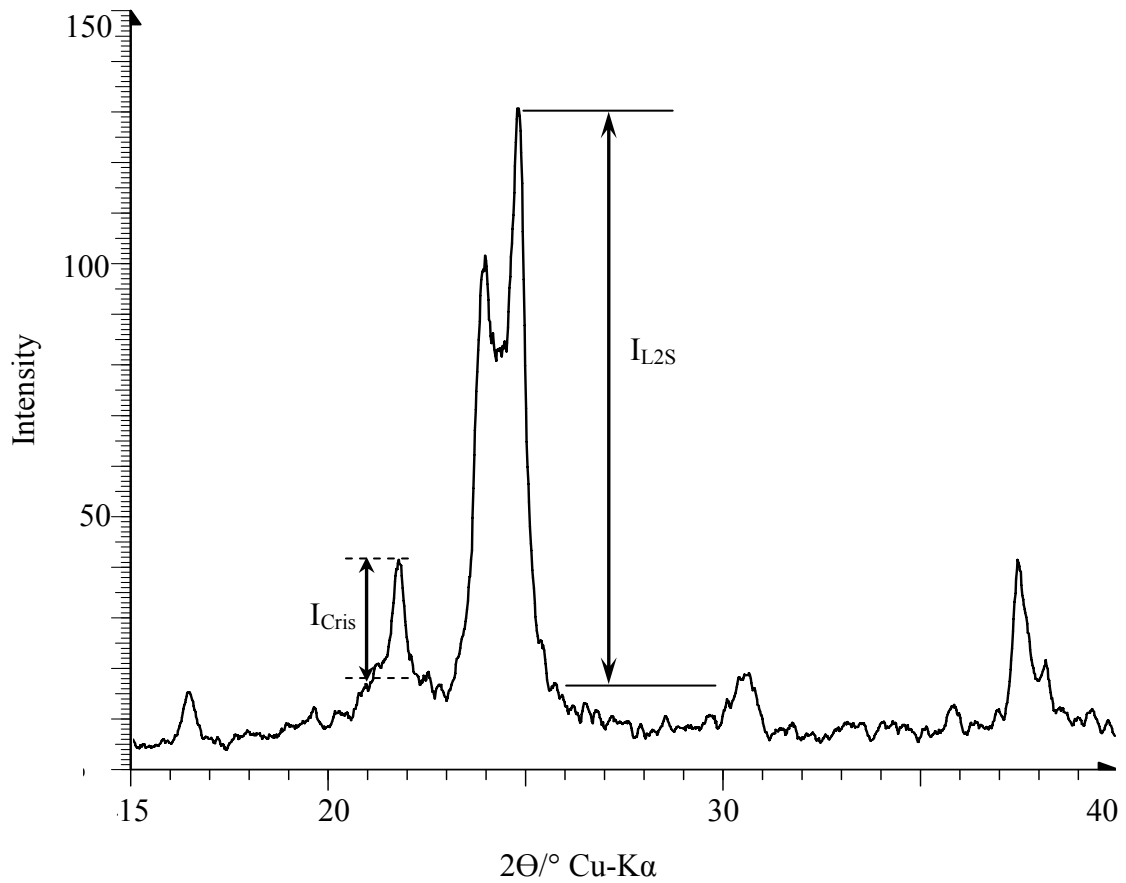


**Figure E1** XRD pattern of  $\text{Li}_2\text{O}\cdot 2\text{SiO}_2$  transparent glass-ceramics after  $\text{Li}^+ \leftrightarrow \text{Na}^+$  exchange at 550 °C for 4 hours.

$I_{\text{Cris}}$  = Observed X-ray intensity of Cristobalite in glass-ceramics.

$I_{\text{L2S}}$  = Observed X-ray intensity of strongest peak of  $\text{Li}_2\text{O}\cdot 2\text{SiO}_2$ .

**Table E1** Observed X-ray intensity and normalized X-ray intensity of  $\text{Li}_2\text{O}\cdot 2\text{SiO}_2$  and Cristobalite in glass-ceramics before and after ion exchange.

Ion Exchange Condition	Observed X-ray intensity		Normalized X-ray intensity	
	$I_{\text{L2S}}$	$I_{\text{Cris}}$	$I_{\text{L2S}}$	$I_{\text{Cris}}$
Original Glass-ceramics	170	0	100	0
$\text{Li}^+ \leftrightarrow \text{Na}^+$ , 550°C-1hour	140	9	82	5.3
$\text{Li}^+ \leftrightarrow \text{Na}^+$ , 550°C-4hour	119	29	70	17.1
$\text{Li}^+ \leftrightarrow \text{Na}^+$ , 550°C-9hour	12	44	7	25.9

## **APPENDIX F**

### **X-RAY DIFFRACTION FILES**

**Table F1** X-ray diffraction file of Silicon (JCPDS 027-1402).

Pattern : 00-027-1402		Radiation = 1.540598		Quality : High		
Si	d (Å)	I	h	k	l	
Silicon	3.13550	100	1	1	1	
Silicon, syn	1.92010	55	2	2	0	
Lattice : Face-centered cubic S.G. : Fd-3m (227)	1.63750	30	3	1	1	
a = 5.43088 b = c =	1.35770	6	4	0	0	
$\alpha = \beta = \gamma = Z =$	1.24590	11	3	3	1	
Temperature of data collection: Pattern taken at 25(1) °C	1.10860	12	4	2	2	
	1.04520	6	5	1	1	
Sample source or locality: This sample is NBS Standard Reference Material No.640	0.96000	3	4	4	0	
	0.91800	7	5	3	1	
General comments: a0 uncorrected refraction.	0.85070	8	6	2	0	
Additional pattern: T0 replace 00-005-0565 and 00-026-1481	0.82820	3	5	3	3	
Color: Gray						
Data collecting flag: Ambient.						
Natl. Bur. Stand. (U.S.) Monogr. 25, volume 13, page 35(1976) CAS Number: 7440-21-3						
Radiation : CuK $\alpha$ 1 Filter : Monochromator crystal						
Lambda : 1.54060 d-sp : Diffractometer						
SS/FOM : F11=443(0.0019,13)						
Internal Standard : W						

**Table F2** X-ray diffraction file of lithium silicate (JCPDS 029-0828)

Pattern : 00-029-0828	Radiation = 1.540598		Quality : High		
Li <sub>2</sub> SiO <sub>3</sub>	d (Å)	I	h	k	l
	4.69000	100	0	2	0
Lithium silicate	3.30100	65	1	1	1
Lattice : Base-centered orthorhombic	2.70800	65	1	3	0
S.G. : Ccm21 (36)	2.70000	45	2	0	0
	2.34200	19	1	3	1
a = 5.39750      b = 9.39740      c = 4.66150	2.33100	20	0	0	2
a/b = 0.57436      c/b = 0.49604      Z = 4	2.09100	7	2	2	1
Mol. Weight = 89.97      Volume[CD] = 236.44	2.08500	5	1	1	2
	1.77470	4	1	5	0
D <sub>x</sub> = 2.527	1.76670	9	1	3	2
	1.76380	8	2	0	2
Sample preparation: Made by heating a 1:1 molar mixture of Li <sub>2</sub> CO <sub>3</sub> and silica gel at 860 °C for 5 minutes, followed by grinding and reheating to 1200 °C for several minutes.	1.65630	7	2	4	1
	1.65220	7	3	1	1
	1.56650	12	0	6	0
	1.56050	15	3	3	0
	1.47470	3	1	1	3
Additional pattern: To replace 00-015-0519	1.41050	1	2	4	2
	1.40790	1	3	1	2
Additional diffraction line(s): Plus 8 reflections to 0.9337	1.35470	3	2	6	0
Structure: Isostructural with Na <sub>2</sub> SiO <sub>3</sub> and Li <sub>2</sub> GeO <sub>3</sub> .	1.34750	5	1	3	3
	1.30010	5	0	6	2
	1.29650	8	3	3	2
Additional pattern: See ICSD 4261 (PDF 01-070-1788)	1.25440	3	1	7	1
	1.24950	2	4	2	1
	1.17470	2	0	8	0
Color: Colorless	1.17100	2	2	6	2
	1.16810	2	2	4	3
Data collecting flag: Ambient.	1.13500	3	4	4	1
	1.07700	1	2	8	0
Natl. Bur. Stand. (U.S.) Monogr. 25, volume 13, page 35(1976) CAS Number: 7440-21-3	1.07590	1	3	7	0
	1.07000	1	2	0	4
	1.04880	1	0	8	2
Radiation : CuKα1      Filter : Monochromator crystal	1.04520	1	5	1	1
Lambda : 1.54060      d-sp : Not given	1.04410	1	0	4	4
SS/FOM : F30=45(0.0107,62)	1.02530	1	1	9	0
Internal Standard : Ag	1.02120	2	2	6	3
	1.01880	1	4	0	3
	1.00130	1	1	9	1

**Table F3** X-ray diffraction file of cristobalite (JCPDS 039-1425)

Pattern : 00-039-1425	Radiation = 1.540598		Quality : High		
SiO <sub>2</sub>	d (Å)	I	h	k	l
Silicon Oxide	4.03974	100	1	0	1
Cristobalite, syn	3.51470	1	1	1	0
Lattice : Tetragonal	3.13592	8	1	1	1
S.G. : P41212 (92)	2.84116	9	1	0	2
a = 4.9732      c = 6.92360      Z = 4	2.48740	4	2	0	0
Mol. Weight = 60.08      Volume[CD]= 171.24	2.46750	1	1	1	2
	2.34170	2	2	0	1
D <sub>x</sub> =2.331	2.11791	2	2	1	1
	2.01957	4	2	0	2
Sample preparation: Cristobalite was prepared by Trans Tech Company using Berkley 5 micron MIN-U-SIL(R). A two kilogram sample was heated at 1600 °C for 8 hours. The sample was then air quenched, treated with 6N HCl and then jet-milled. The +325 mesh fraction was then remove by sieving.	1.92935	4	1	1	3
	1.87147	1	2	1	2
Structure: The structure was determined by Peacor(1).	1.75907	1	2	2	0
Additional pattern: See ICSD 4261 (PDF 01-070-1788)	1.73033	2	0	0	4
Color: Colorless	1.69221	1	2	0	3
	1.63488	3	1	0	4
	1.61217	1	3	0	1
	1.60131	1	2	1	3
	1.57207	1	3	1	0
	1.56745	2	2	2	2
	1.53356	2	3	1	1
	1.49520	2	3	0	2
Temperature of data collection: The temperature was ≈25 °C.	1.43165	1	3	1	2
	1.42102	1	2	0	4
Polymorphism: There are a number of others forms of SiO <sub>2</sub>	1.39908	2	2	2	3
	1.36560	1	2	1	4
Additional pattern: To replace 00-011-0695 and validated by calculated pattern.	1.35277	1	3	2	1
	1.34650	1	3	0	3
Data collecting flag: Ambient.	1.33398	1	1	0	5
	1.29976	1	3	1	3
Wong-Ng, W., McMurdie, H., Paretzkin, B., Hubbard, C., Dragoo, A. NBS, Gaithersburg, MD, USA., ICDD Grant-in-Aid (1988).	1.28133	1	3	2	2
	1.23318	1	2	2	4
	1.22375	1	4	0	1
	1.20599	1	4	1	0
Radiation : CuKα1      Filter : Monochromator crystal	1.18427	1	3	2	3
Lambda : 1.54060      d-sp : Diffractometer	1.17576	1	2	1	5
SS/FOM : F30=83(0.0100,36)	1.16384	2	3	1	4
Internal Standard : W FP	1.15546	1	3	3	1
	1.11050	1	3	3	2

**Table F4** X-ray diffraction file of lithium silicate (JCPDS 027-1402)

Pattern : 00-027-1402	Radiation = 1.540598		Quality : High		
$\alpha$ -Li <sub>2</sub> Si <sub>2</sub> O <sub>5</sub>	d (Å)	I	h	k	l
Lithium Silicate	7.22800	9	0	2	0
	5.42000	19	1	1	0
	3.73700	66	1	3	0
Lattice : Base-centered monoclinic	3.65500	48	0	4	0
S.G. : Cc (9)	3.58100	100	1	1	1
a = 5.82200      b = 14.6000      c = 4.77500	2.93000	7	1	3	1
a/b = 0.39877    c/b = 0.32705 $\beta$ = 90.0	2.90800	13	2	0	0
Z = 4	2.70200	6	2	2	0
	2.42900	4	0	6	0
Color: White	2.38800	28	0	0	2
Additional pattern: To replace 00-017-0447.	2.35000	18	2	2	1
Sample preparation: Prepared at MRC-Mound Lab.,	2.29000	11	1	5	1
Miamisburg, Ohio, USA, by Kramer, D., via a	2.05400	10	2	4	1
modified method by Glasser, F., Phy. Chem.	2.00200	8	0	4	2
Glasses, 8 224 (1967)	1.96290	14	1	7	0
Additional pattern: See ICSD 15414 (PDF 01-072-	1.86260	4	2	6	0
0102)	1.84610	7	2	0	2
General comments: Room temperature form of	1.83280	5	0	8	0
Li <sub>2</sub> Si <sub>2</sub> O <sub>5</sub>	1.80370	10	3	3	0
Data collecting flag: Ambient.	1.79430	8	2	2	2
	1.78460	1	3	1	1
Cantrell, J., Miami University, Oxford, Ohio, USA.,	1.76960	4	1	5	2
ICDD Grant-in-Aid (1989)	1.73380	4	2	6	1
	1.70460	1	0	6	2
Radiation : CuK $\alpha$ 1    Filter : Monochromator crystal	1.65020	4	2	4	2
Lambda : 1.54060      d-sp : Diffractometer	1.52820	1	3	5	1
SS/FOM : F11=443(0.0019,13)	1.52570	8	1	1	3
Internal Standard : W	1.48390	5	1	9	1
	1.47100	7	2	6	2
	1.45990	1	0	10	0

**Table F5** X-ray diffraction file of quartz (JCPDS 046-1045).

Pattern : 00-046-1045	Radiation = 1.540598		Quality : High		
SiO <sub>2</sub>	d (Å)	I	h	k	l
Silicon Oxide	4.25499	16	1	0	0
Quartz, syn	3.34347	100	1	0	1
Lattice : Hexagonal	2.45687	9	1	1	0
S.G. : P3221 (154)	2.28149	8	1	0	2
a = 4.91344      c = 5.40524      Z = 3	2.23613	4	1	1	1
Mol. Weight = 60.08      Volume[CD]= 113.01	2.12771	6	2	0	0
	1.97986	4	2	0	1
D <sub>x</sub> =2.649      D <sub>m</sub> = 2.660      I/I <sub>cor</sub> = 3.41	1.81796	13	1	1	2
	1.80174	1	0	0	3
	1.67173	4	2	0	2
Additional pattern: See ICSD 174 (PDF 01-085-0335)	1.65919	2	1	0	3
Color: White	1.60827	1	2	1	0
	1.54153	9	2	1	1
	1.45289	2	1	1	3
Temperature of data collection: Pattern taken at 23(1) °C.	1.41841	1	3	0	0
General comments: Low temperature quartz	1.38210	6	2	1	2
General comments: 2θ determination based on profile fit method.	1.37496	7	2	0	3
Additional pattern: To replace 00-033-1161.	1.37188	5	3	0	1
Data collecting flag: Ambient.	1.28791	2	1	0	4
	1.25595	3	3	0	2
	1.22832	1	2	2	0
	1.19982	2	2	1	3
Kern, A., Eysel, W., Mineralogisch-Petrograph. Inst., Univ. Heidelberg, Germany., ICDD Grant-in-Aid (1993)	1.19779	1	2	2	1
	1.18399	2	1	1	4
	1.18017	2	3	1	0
	1.15298	1	3	1	1
Radiation : CuKα1      Filter : Monochromator crystal	1.14065	1	2	0	4
Lambda : 1.54060      d-sp : Diffractometer	1.11455	1	3	0	3
SS/FOM : F30=83(0.0100,36)	1.08155	2	3	1	2
Internal Standard : Si	1.06380	1	4	0	0
	1.04772	1	1	0	5
	1.04380	1	4	0	1
	1.03461	1	2	1	4
	1.01490	1	2	2	3
	0.98958	1	1	1	5
	0.98725	1	3	1	3
	0.97834	1	3	0	4
	0.97617	1	3	2	0



## **APPENDIX G**

### **CHARACTERIZATION DATA REPORT**

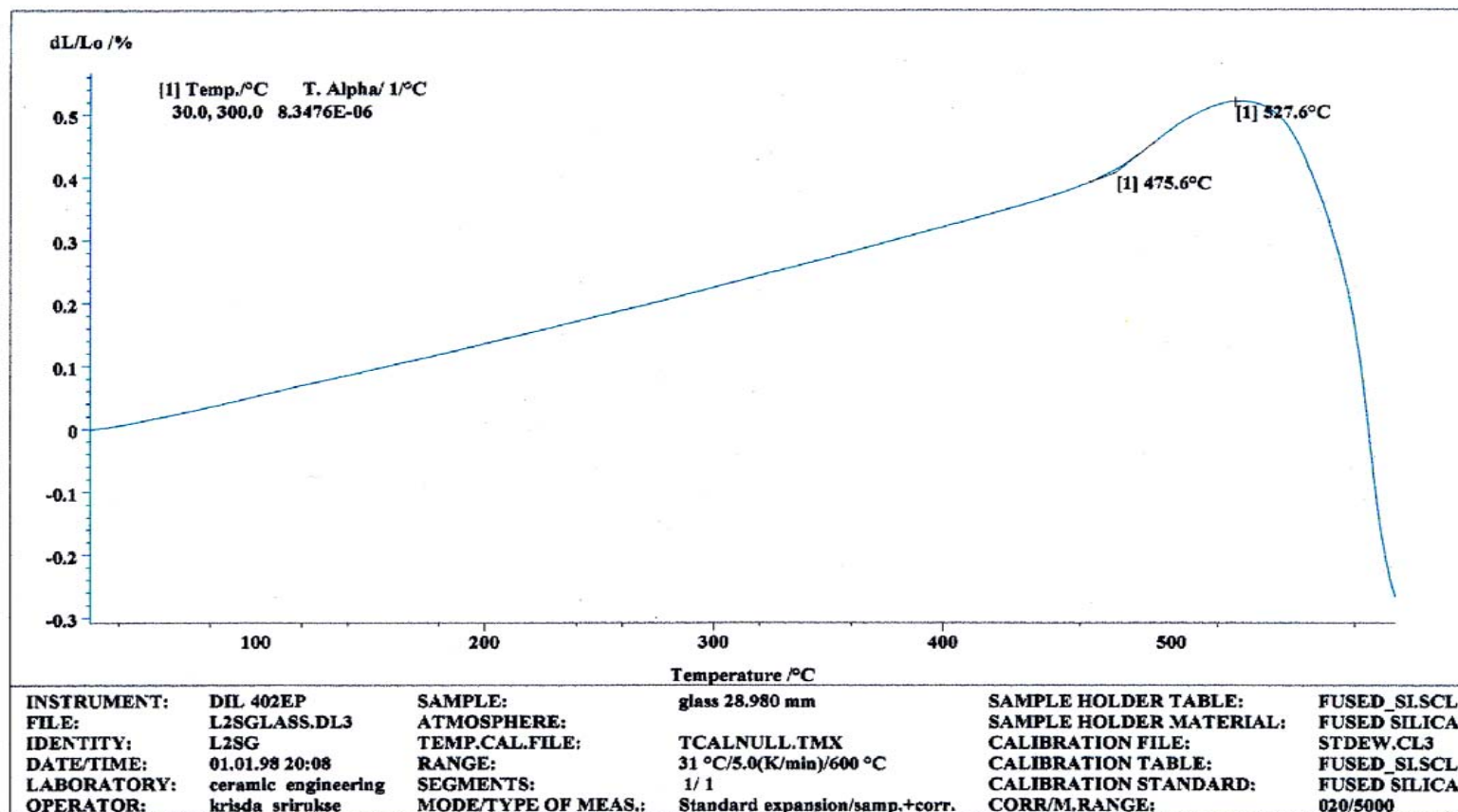
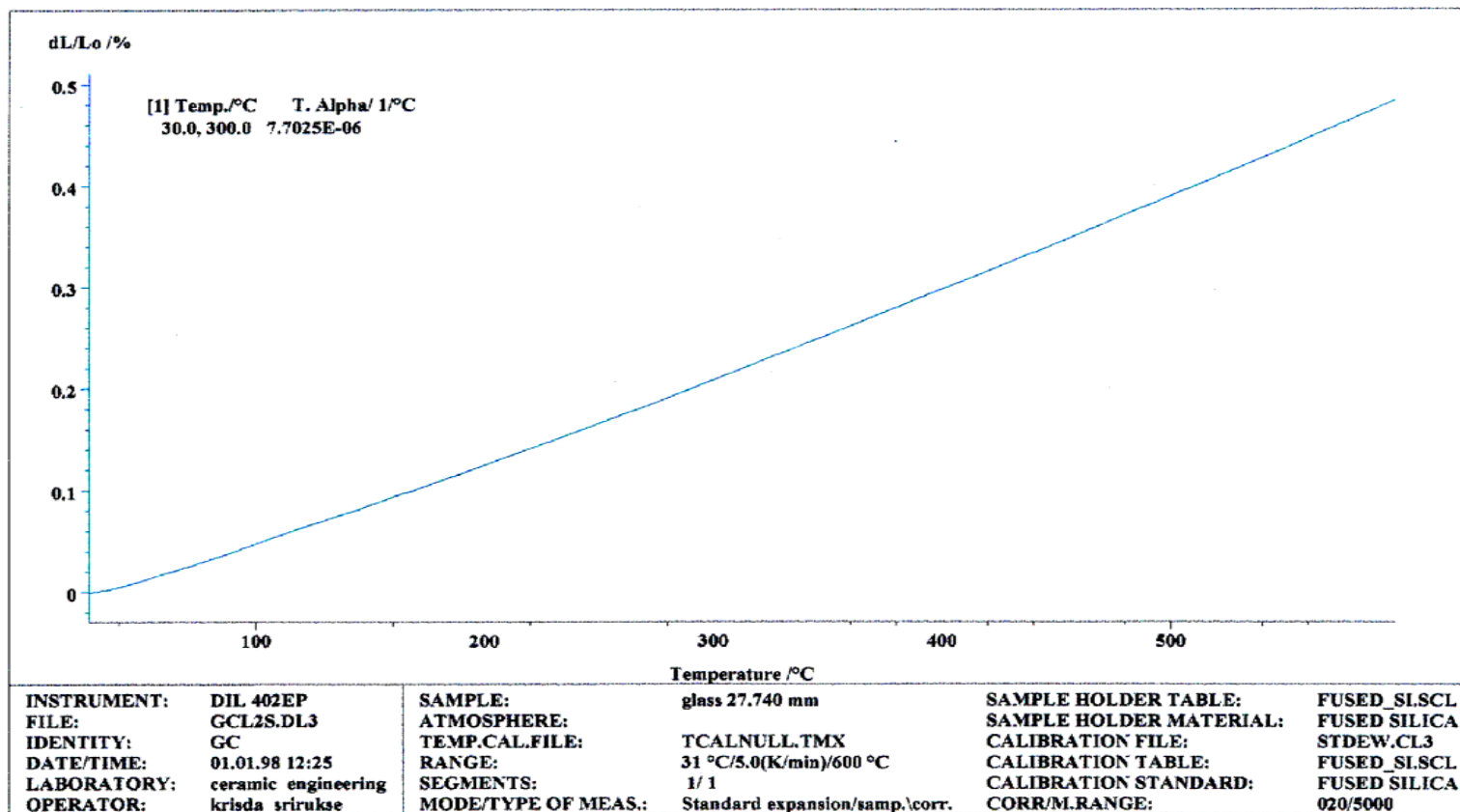
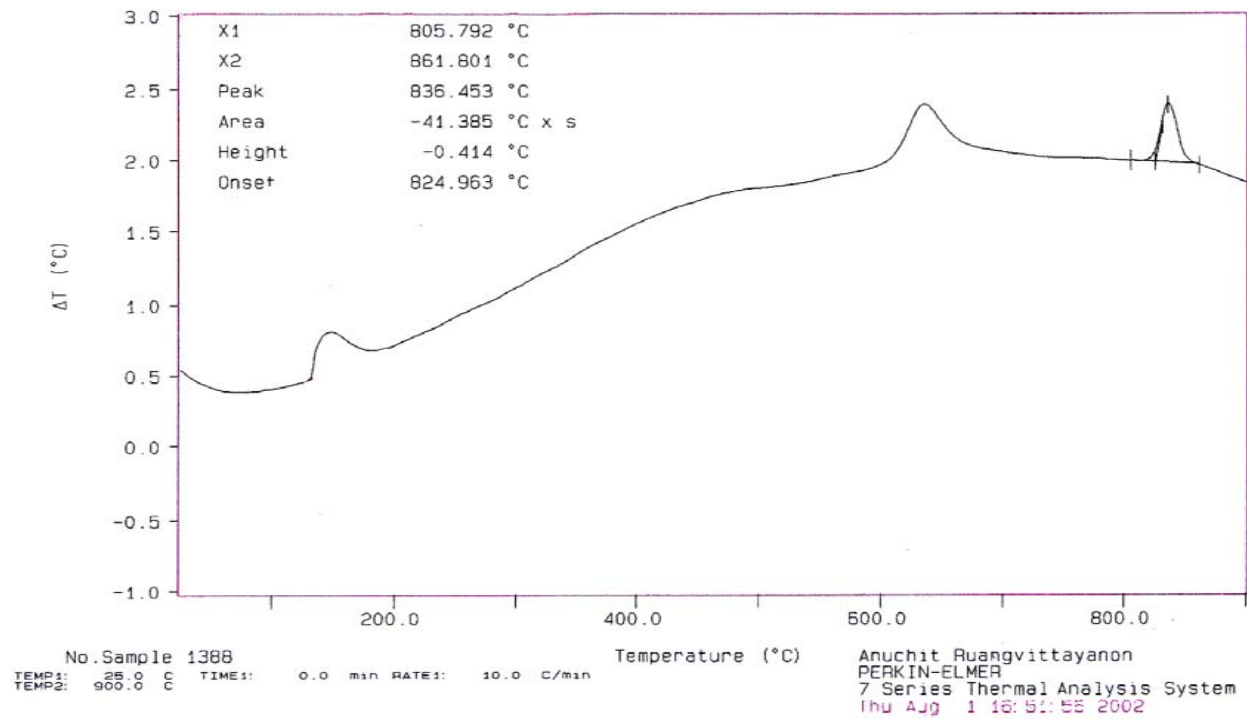


Figure G1 Thermal expansion trace report of  $\text{Li}_2\text{O-SiO}_2$  glass using Netsch 402EP at a heating rate of  $5^{\circ}\text{C}/\text{min}$



**Figure G2** Thermal expansion analysis trace of Li<sub>2</sub>O-SiO<sub>2</sub> transparent glass-ceramics using Netsch 402EP at a heating rate of 5°C/min

Curve 1: DTA in DTA Mode  
File info: PT1388 Thu Aug 1 16:34:51 2002  
Sample Weight: 13.370 mg  
LS3



**Figure G3** Differential thermal analysis trace of  $\text{Li}_2\text{O-SiO}_2$  glass using a Perkin-Elmer DTA-7 at a heating rate of  $10^\circ\text{C}/\text{min}$ .

**Table G1** Density and volume report of Li<sub>2</sub>O-SiO<sub>2</sub> glass-ceramics (500°C-15h,700°C -10h) by He-gas substitution method using Accupyc (Micrometrics).

Accupyc 1330 V2.04M Serial Number: 0 Density and Volume Report					
Sample ID: 0001			Started: 30/01/06 17:19:13		
Sample Weight: 2.5953g			Completed: 30/01/06 17:39:45		
Temperature: 30.7 C			Equilibration Rate: 0.0050		
Number of Purges: 30 psig/min			Expansion Volume: 75.0173 cm <sup>3</sup>		
Cell Volume: 16.5551 cm <sup>3</sup>			Calibration Factor: 1.000738		
Chamber Insert: 10 cm <sup>3</sup>					
Run#	Volume cm <sup>3</sup>	Deviation cm <sup>3</sup>	Density g/cm <sup>3</sup>	Deviation g/cm <sup>3</sup>	Elapsed Time (h:m:s)
1	1.0904	-0.0006	2.3801	0.0014	0:10:23
2	1.0910	-0.0001	2.3789	0.0002	0:11:25
3	1.0907	-0.0004	2.3795	0.0008	0:12:28
4	1.0915	0.0005	2.3777	-0.0010	0:13:34
5	1.0905	-0.0006	2.3800	0.0013	0:14:42
6	1.0909	-0.0002	2.3790	0.0004	0:15:49
7	1.0913	0.0003	2.3781	-0.0006	0:16:56
8	1.0916	0.0006	2.3774	-0.0012	0:18:04
9	1.0916	0.0005	2.3776	-0.0011	0:19:16
10	1.0911	0.0001	2.3785	-0.0002	0:20:24
Average Volume: 1.0911 cm <sup>3</sup>			Standard Deviation: 0.0004 cm <sup>3</sup>		
Average Density: 2.3784 cm <sup>3</sup>			Standard Deviation: 0.0010 g/cm <sup>3</sup>		

**Table G2** Density and volume report of Li<sub>2</sub>O-SiO<sub>2</sub> glass by He-gas substitution method using Accupyc (Micrometrics).

Accupyc 1330 V2.04M Serial Number: 0 Density and Volume Report					
Sample ID: 0000			Started: 30/01/06 11:1-06:15		
Sample Weight: 5.7356g			Completed: 30/01/06 11:24:48		
Temperature: 24.6 C			Equilibration Rate: 0.0050 psig/min		
Number of Purges: 30			Expansion Volume: 75.0173 cm <sup>3</sup>		
Cell Volume: 16.5551 cm <sup>3</sup>			Calibration Factor: 0.999495		
Chamber Insert: 10 cm <sup>3</sup>					
Run#	Volume cm <sup>3</sup>	Deviation cm <sup>3</sup>	Density g/cm <sup>3</sup>	Deviation g/cm <sup>3</sup>	Elapsed Time (h:m:s)
1	2.4750	0.0003	2.3174	-0.0003	0:09:44
2	2.4742	-0.0005	2.3182	0.0005	0:10:41
3	2.4743	-0.0004	2.3180	0.0003	0:11:41
4	2.4758	0.0011	2.3166	-0.0011	0:12:37
5	2.4761	0.0014	2.3164	-0.0013	0:13:33
6	2.4764	0.0017	2.3161	-0.0016	0:14:34
7	2.4736	-0.0011	2.3188	0.0011	0:15:32
8	2.4741	-0.0005	2.3182	0.0005	0:16:28
9	2.4729	-0.0018	2.3193	0.0016	0:17:27
10	2.4745	-0.0002	2.3179	0.0002	0:18:25
Average Volume: 1.0911 cm <sup>3</sup>			Standard Deviation: 0.0004 cm <sup>3</sup>		
Average Density: 2.3784 cm <sup>3</sup>			Standard Deviation: 0.0010 g/cm <sup>3</sup>		

## **BIOGRAPHY**

Mr. Chokchai Yatongchai was born on April 5, 1978 in Nakhon Panom, Thailand. He earned Bachelor's Degree in Ceramic Engineering from Suranaree University of Technology (SUT) in 2001. After graduation, he worked for Bangkok Sengthai Refractory & Monolithic Co., Ltd in the position of Production Engineer for 3 years. He continued his Master's Degree in Ceramic Engineering at School of Ceramic Engineering, Institute of Engineering at Suranaree University of Technology in 2004. During his Master's Degree study, he presented a paper entitled "Strengthening and Amorphization of  $\text{Li}_2\text{O}\cdot\text{SiO}_2$  Transparent Glass-ceramics By Ion Exchange" in the 46<sup>th</sup> Fall Meeting on Glass and Photonics Materials, University of Shiga-Prefecture, Hikone-City, Japan. He published a paper entitled "Strengthening of  $\text{Li}_2\text{O}\cdot 2\text{SiO}_2$  Transparent Glass-Ceramics By Ion Exchange" in Journal of the Ceramic Society of Japan, Vol.114, March 2006.